# The influence of mental stress on the musculoskeletal human back during static posture and trunk motion

Dissertation
zur Erlangung des Doktorgrades
der Humanwissenschaften
(Dr. sc. hum.)

der
Fakultät für Medizin
der Universität Regensburg

vorgelegt von
Franz Süß
aus
Wald

im Jahr
2021

# The influence of mental stress on the musculoskeletal human back during static posture and trunk motion

Dissertation
zur Erlangung des Doktorgrades
der Humanwissenschaften
(Dr. sc. hum.)

der
Fakultät für Medizin
der Universität Regensburg

vorgelegt von
Franz Süß
aus
Wald

im Jahr
2021

| | |
|---|---|
| Dekan: | Prof. Dr. Dirk Hellwig |
| Betreuer: | Prof. Dr.-Ing. Dendorfer, Sebastian |
| Tag der mündlichen Prüfung: | 17.06.2021 |

# Abstract

The investigation of the influence of mental stress on muscle recruitment of the back and its effect on the intervertebral discs was the main focus of this work. Furthermore, the goal was to develop algorithms to use mental stress as an input parameter in musculoskeletal simulation models.

In the first step, a study was designed to investigate the influence of emotional and cognitive stress without kinetic influencing factors during sitting. At the muscular level, emotional stress was found to affect the upper back, while cognitive stress elicited higher muscle activity in the upper and lower back. Using a newly developed algorithm to apply back muscle recruitment changes to static inverse kinematic simulation models, load increases at the discs of up to 189 N on average and up to 907 N at peak were found.Based on the results of the first study, a second dynamic study was designed and conducted. In this case, the focus was on the cognitive stressor and the lower back. Using a dynamometer, subject-specific loads were applied during extension and flexion of the upper back. In contrast to the first study, in the upper back, only the right m. trapezius pars descendens showed a load-induced difference in muscle activity, but the lower back did. To investigate the effects of muscle tone increase in detail, the algorithm developed in the first study was extended to the dynamic case. The use of simulation models allowed the inference of the effects of the purely stress-induced tone increase. For this purpose, the kinetic and muscular effects were isolated and simulated. The study revealed a stress increase of 47% of the body weight in the L4L5 disc. The final numerical study focused on the general application of muscle activities to inverse kinematic simulation models. This was based on the novel simulation algorithm used in study two and the measured muscle activities. The simulation of the measured muscle activities formed the link between reality and simulation. To simulate the activities, neural networks and gradient boosting regression algorithms were investigated. The latter were found to be better suited to represent the data. However, the data is too small for a detailed statement, especially for loads below 100%.

The results of this work can help to better assess the musculoskeletal effects of psychological stress on the musculoskeletal system and, if necessary, to develop ergonomic prevention strategies. By recognizing stress-related kinematic difference, as well as subsequent prompting of trunk movement, could help prevent long-term effects. When examining any situation, the combination of machine learning and musculoskeletal simulation tools can help examine and minimize the effects of psychological stress.

# Kurzfassung

Die Untersuchung des Einflusses von mentalem Stress auf die Muskelrekrutierung des Rückens und dessen Auswirkung auf die Bandscheiben war der Schwerpunkt dieser Arbeit. Des Weiteren war es das Ziel, Algorithmen zu entwickeln, um die mentale Belastung als Eingabeparameter in muskuloskelettalen Simulationsmodellen zu nutzen.

Im ersten Schritt wurde eine Studie konzipiert, um den Einfluss von emotionalem und kognitivem Stress ohne kinetische Einflussfaktoren beim Sitzen zu untersuchen. Auf muskulärer Ebene wurde festgestellt, dass emotionaler Stress den oberen Rücken beeinflusste, während kognitiver Stress höhere Muskelaktivität im oberen und unteren Rücken auslöste. Unter Verwendung eines neu entwickelten Algorithmus zur Anwendung von Rekrutierungsänderungen der Rückenmuskulatur auf statische inverse kinematische Simulationsmodelle wurden Belastungserhöhungen an den Bandscheiben von bis zu 189 N im Mittel und bis zu 907 N in der Spitze gefunden.

Basierend auf den Ergebnissen der ersten Studie wurde eine zweite dynamische Studie konzipiert und durchgeführt. In diesem Fall lag der Fokus auf dem kognitiven Stressor und dem unteren Rücken. Mit Hilfe eines Dynamometers wurden subjektspezifische Belastungen während der Extension und Flexion des Oberkörpers aufgebracht. Im Gegensatz zur ersten Studie konnte im oberen Rücken, nur im rechten m. trapezius pars descendens ein Lastfall bedingter Unterschied in der Muskelaktivität festgestellt werden, wohl aber im unteren Rücken. Um die Auswirkungen der Muskeltonuserhöhung im Detail zu untersuchen, wurde der in der ersten Studie entwickelte Algorithmus auf den dynamischen Fall erweitert. Die Verwendung von Simulationsmodellen erlaubte den Rückschluss auf die Auswirkungen der rein stressinduzierten Tonuserhöhung. Hierfür wurden die kinetischen und muskulären Effekte isoliert und simuliert. Die Studie ergab eine Belastungserhöhung von 47 % des Körpergewichts in der L4L5 Bandscheibe.

Die abschließende numerische Studie konzentrierte sich auf die allgemeine Anwendung von Muskelaktivitäten auf inverse kinematische Simulationsmodelle. Grundlage dafür waren der neuartige Simulationsalgorithmus, der in Studie zwei verwendet wurde, und die gemessenen Muskelaktivitäten. Die Simulation der gemessenen Muskelaktivitäten bildete das Bindeglied zwischen Realität und Simulation. Um die Aktivitäten zu simulieren, wurden neuronale Netze und Gradient-Boosting-Regressionsalgorithmen untersucht. Es zeigte sich, dass letztere besser

geeignet sind, die Daten abzubilden. Für eine detaillierte Aussage, insbesondere für Belastungen unter 100 %, ist die Datenlage jedoch zu klein.

Die Ergebnisse dieser Arbeit können helfen, die muskuloskelettalen Auswirkungen psychischer Belastungen auf den Bewegungsapparat besser einzuschätzen und ggf. ergonomische Präventionsstrategien zu entwickeln. Durch das Erkennen stressbedingter kinematischer Unterschied sowie die darauffolgende Aufforderung zur Rumpfbewegung könnte helfen, langfristige Auswirkungen zu vermeiden. Bei der Untersuchung beliebiger Situationen, kann die Kombination aus maschinellem Lernen und muskuloskelettalen Simulationswerkzeugen helfen, die Auswirkungen psychischer Belastungen zu untersuchen und zu minimieren.

# Abbreviations:

| | |
|---|---|
| ACC | Acceleration |
| AP | Anterior-Posterior |
| APF | Anterior-Posterior Force |
| BW | Body Weight |
| CC | Contractile Component |
| CC | Cranial-Caudal |
| CCF | Cranial-Caudal Force |
| CNS | Central Nervous System |
| COS | Cognitive Stress |
| Dir | Direction |
| DNN | Deep Neural Networks |
| EMG | Electromyography |
| EMS | Emotional Stress |
| IZ | Innervation Zone |
| KMM | Kinetic Musculoskeletal Model |
| LDLJ | Log Dimensional Jerk |
| MA | Muscle Activity |
| MAV | Mean Absolute Value |
| ML | Medio-Lateral |
| MRM | Muscle Recruitment Model |
| MSJ | Mean Squared Jerk |
| MTU | Muscle Tendon Unit |
| MU | Motor Unit |
| MUAP | Motor Unit Action Potential |
| MVC | Maximum Voluntary Contraction |
| NIOSH | National Institute for Occupational Safety and Health |
| NN | Neural Network |
| PEC | Parallel-Elastic Element |
| ReLU | Rectified Linear Unit |
| RMS | Root Mean Square |
| ROM | Range of Motion |
| SEC | Series-Elastic Element |
| TNN | TensorFlow Neural Network |
| VEL | Velocity |

# 1. Introduction

In recent decades, working conditions have changed due to a greater emphasis on cognitive components, multitasking and the permanent processing of incoming information. In addition, in many Western countries, we are dealing with an aging population whose resistance to psychological stress and physical strain is often lower.

Recent data on absenteeism in Germany show the importance of musculoskeletal and psychological problems, which are the two most important factors for incapacity to work. Musculoskeletal disorders are responsible for around 23% of all absences. Mental health problems have increased in recent years and were responsible for around 17% of sick days in 2016 (DAK, 2017). In addition, almost all industries report an increase in stress levels in recent years. Statistics from 2012 show an increase of 45% stress and a quantitative overload of 17% for the manufacturing sector (BAUA, 2017), indicating a growing need for interventions. Therefore, stress has become an important issue in recent decades and is obviously having an increasing impact on the lives of individuals and society (Sharma and Gedeon, 2012). Stress can affect the human body in various ways, leading to a higher risk of cardiovascular disease (Teufel, 2018), pain (Haukkal et al., 2011) and having negative effects on musculoskeletal loading (Taib and Yun, 2014). Among musculoskeletal disorders, neck and lower back pain have been identified as major causes of disability and an urgent need for further research has been defined (Hoy et al., 2010a; Hoy et al., 2010b). Several literature reviews examined the main causes of back pain and identified extensive physical strain and demanding spinal positions during work, such as bending or twisting, as well as psychological stress (SBU Yellow Report no 227, 2014; Schneider et al., 2006). In addition, other psychological influencing factors, such as the individual's personality, were found to affect the stress response in the shoulder region and contribute to the medical disorder (Nimbarte, 2014).

In particular, the influence of psychological stress on trapezius muscles and thus a relationship between psychological and musculoskeletal parameters have been the subject of a number of studies. Typically, electromyography (EMG) measurements provide a tool to explore the physical response.

In a study by Larsson et al. (Larsson et al., 1995) the experimental EMG setup was extended with vital signs during upright sitting with application of a static load to the subject. They found an increase in muscle tension with a concomitant increase in blood flow and heart rate at a lower skin temperature. Assessment of the mean power frequency allowed them to attribute their findings to the load and rule out possible fatigue in the subjects. Shahidi et.al (Shahidi et al., 2013) investigated the relationship of muscle tension in combination with cervical posture, low and high stress levels during sedentary office work. Their study identified the trapezius descendens as the muscle with a significant increase in muscle activity independent of factors such as posture or fatigue. The research by Roman-Liu et al. (Roman-Liu et al., 2013) examined different types of mental tasks while sitting in an office chair. They were able to show effects on vital signs such as heart rate, respiratory rate, as well as muscle recruitment in the shoulder-arm group. Their results revealed a stress level dependent activity level in the shoulder and arm, but not in the forearm.

While previous studies focused primarily on a reduced laboratory setup, Mork and Westgaard (Mork and Westgaard, 2007) focused specifically on computer work and recorded trapezius muscle activity hourly during a workday in a seated position. They were unable to observe any evidence of different activation patterns due to high versus low load or relate arm elevation to trapezius muscle activation. This basic research question of how computer work is affected by stress was extended by Taib et al. (Taib et al., 2016) to include mobile computing devices. In this study, muscles at the shoulder, neck, and forearm were recorded while working with mobile devices and desktop computers in a seated position They found a correlation between mental load and trapezius activity as a function of load level, increasing with load level. In addition, the device itself affected muscle response. Mobile devices reduced the effect compared to the more ergonomic environment provided by a desktop computer. Other related research in real work environments has been conducted among supermarket cashiers. Lundberg et al. (Lundberg et al., 1999) examined muscle tension during the workday, while Rissen et al. examined stress due to job rotation (Rissén et al., 2002). In the latter case, EMG measurements were performed on the trapezius before and after job rotation. Analysis of the results showed a significant decrease on the non-dominant side of the participants after the subjects regularly changed their task area. In a follow-up study Lundberg et al. (Lundberg et al., 2002) examined the effect of psychological stress at the

motor unit level in more detail. Their results suggest that stress keeps low-threshold motor units active and thus produces higher trapezius activity.

Despite interest in the association of psychological stress and upper back muscle, recruitment changes in the low back have not been the focus of many research studies and have mostly been associated with back pain. Attention-demanding tasks (visually presented alphanumeric and graphic information and a response by pressing two keys with the right hand) were used by Waersted and Westgaard (Waersted and Westgaard, 1996) to determine if there were patterns of activation in different regions. This study included 20 different muscle groups, including activities in the upper and lower back including trapezius and erector spinae. They were able to show that the upper and lower trapezius responded with significantly higher activity. In addition, higher expression was found on the right side. Although almost all subjects were right-hand dominant, their results suggest that this finding is independent of the type of keystroke. Additional experiments in which both hands were used to press the feedback keys showed similar results. For all other muscle groups, the inter-individual variation was rather high and not significant. Flor et al. (Flor et al., 1985) chose a setup with chronic back pain patients in a static sitting position. Mental arithmetic and recitation of the alphabet provided stress and a psychophysiological response in the lumbar spine muscles. Statistical analysis showed a significant difference in activity compared to the healthy control group. The result at return to baseline measurement was similar. Other research groups have been able to show higher lumbar muscle activity in back pain patients with slower recovery to baseline when exposed to emotional stress such as anger or sadness (Burns, 2006). This result may differ from the findings of Flor et al. (Flor et al., 1985; Glombiewski et al., 2008) but considering that they used a cognitive stressor, this could indicate a stress-related response depending on the stressor type. Although the additional muscle activity generates additional loads on biomechanical structures, the mechanical effects have not been studied in detail. By using a combination of experimental and computational models, Chany et al. have shown that the loading on the lumbar spine during lifting tasks also depends on the personality of the subject (Chany et al., 2006). The contribution of workplace factors to lumbar spine strain was studied by Davis and Marras (Davis et al., 2002a; Davis and Marras, 2003). They found a large contribution of job-related stress and personality on lumbar spine strain.

However, the majority of studies have focused on the upper back muscle groups with little, if any, physical loading. The resulting spinal forces in the cervical spine have not been described in any of the previous publications. Furthermore, in pain-free subjects, little is known about the influence of stress on the strain on the entire back musculature and the resulting spinal loads. This includes tasks with and without external loads. Furthermore, multiple stressors, ranging from emotional to cognitive stressors, affect humans, and their respective influence on musculoskeletal strain has not been studied in detail.

## 1.1. Objectives of the thesis

The aim of this work is to determine the influence of short-term emotional and cognitive stressors on the activation pattern of the back muscles. In addition, spinal load changes due to altered muscle loading and kinetic changes in human movement will be determined.

This leads to several research hypotheses:

1. Different types of stressors affect back muscle recruitment differently.
2. Mental stress causes muscle tension and generates additional spinal disc loads.
3. Mental stress in combination with trunk motion is changing muscle recruitment and produces additional load in the lumbar spine.
4. The use of state-of-the-art regression models allows the introduction of mental stress into musculoskeletal simulation models.

## 1.2. Outline of this thesis

The studies designed in the first and second work packages investigate how different types of psychological stress influence muscle recruitment. In order to eliminate other factors that influence muscle recruitment as much as possible, an experimental design was chosen that involves almost no physical load or motion. This allows a basic insight into how recruitment

changes and serves to investigate hypothesis one and two. With the results of the first study, a new protocol was developed. This new setup is able to define and measure the boundary conditions acting on the human body during a very simple movement. The third part of this work sheds light on the relationships and thus tests hypotheses two and three. Hypothesis four is the defining factor in the final work package. It focuses on the development of a novel algorithm to extend musculoskeletal simulation models to simulate mental stress and its magnitude.

## 1.3. Mental stress

In general, psychological stress is the reaction to harmful situations and describes the strain or demand to which every person is exposed. This can trigger both positive and negative reactions, which Selye (Selye, 1975) divides between eustress and distress . Eustress describes a positive feeling resulting from demands and pressures that do not overwhelm the person. The person is able to complete the work or requirements successfully, with enthusiasm, joy, and excitement within a given time frame. This contrasts with distress, which occurs when the personal coping strategy is not sufficient to overcome the challenges. While positive stress helps to accomplish the tasks at hand, negative stress contradicts performance and even leads to negative psychological and physical reactions. Thus, stress affects individual performance, yet prolonged eustress, which normally helps to achieve certain goals, can lead to distress. Figure 1.1 (Godin and Hansen, 2015) illustrates the chain of reactions of how performance is affected by the level of stress.

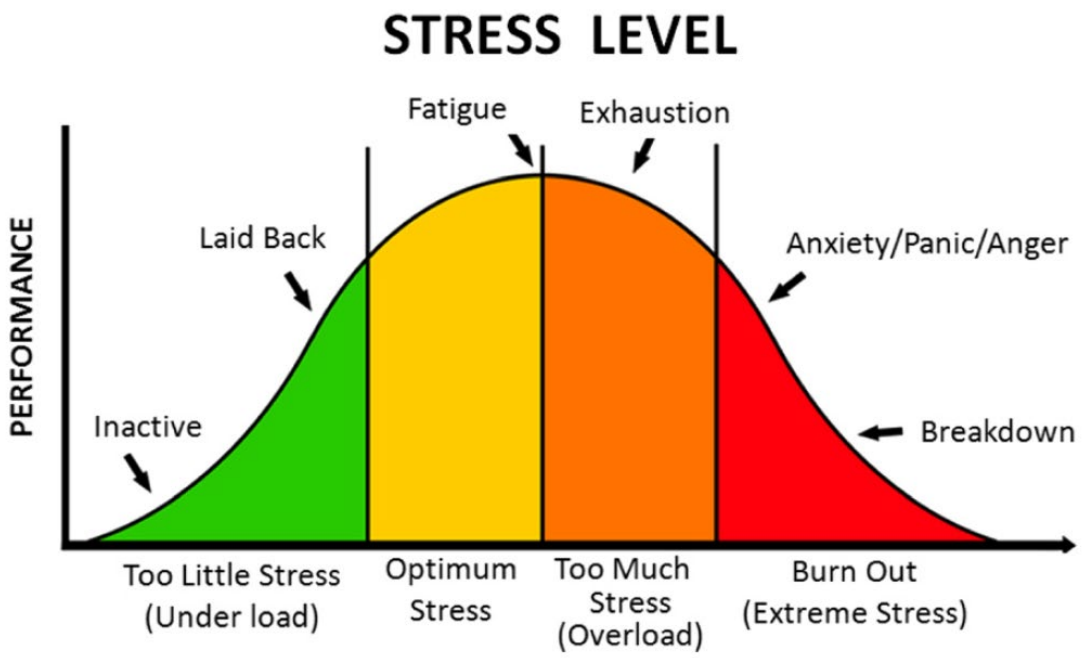


**Figure 1.1:** Human performance dependent on stress level (adapted from Godin and Hansen, 2015)). In case of a low and moderate exposure, it can enhance the human capacity but stress overload leads to mental issues like exhaustion or "Burn Out".

Prolonged exposure to either situation can lead to chronic stress. However, long-term stress can lead to burnout or an increased likelihood of a suppressed immune system and thus greater susceptibility to infectious diseases. Short-term exposure to negative stress also has physical consequences. Depending on the category, the cause and symptoms can vary. Three psychological types of stress (Lazarus and Folkman, 1984) are distinguished:

- **Perceptual stress**: beliefs, roles, stories, attitudes, worldview
- **Emotional stress**: resentments, fears, frustration, sadness, anger, grief/bereavement
- **Cognitive stress**: information overload, accelerated sense of time, worry, guilt, shame, jealousy, resistance, attachments, self-criticism, self-loathing, unworkable perfectionism, anxiety, panic attacks, not feeling like yourself, not feeling like things are real, and a sense of being out of control/not being in control

The physical reactions follow the "fight or flight response" stress theory first proposed by Landis (Landis, 1930). Here, the sympathetic nervous system prepares the subject for a possible attack. This includes the release of hormones such as testosterone, cortisol, and

estrogen, as well as dopamine and serotonin (Lovallo and Thomas, 2000). The release of these substances leads to increased muscle tension. (Selye, 1956)

On the physiological level Lundberg et al. (Lundberg et al., 2002) studied their effects in more detail. They showed a higher number of activated motor units and a higher firing rate in combination with other physiological parameters such as respiratory rate. In a follow-up study (Lundberg, 2002) ), they expanded their protocol to include measurements of blood pressure, heart rate, and catecholamine. They concluded that physical and psychosocial working conditions contribute to the development of work-related upper extremity disorders.

## 1.4. Muscle physiology

This thesis deals with the influence of psychological stress on the human musculoskeletal system. The focus is on the skeletal musculature. Other types of muscles found in the human body, such as smooth muscle, which is responsible for pumping blood in hollow organs and blood vessels, and the heart as cardiac muscle (Schmidt et al., 2006), are not addressed in this work. According to Brandes et.al. (Brandes et al., 2019), skeletal muscles are responsible for locomotion in all multicellular organisms. Skeletal muscles are divided into two groups: extensors and flexors, which have opposite functionality during movement. Whenever the flexor is active, the extensor relaxes to allow movement. Furthermore, he describes the associated processes to perform muscle contractions. The structure of each muscle defines its individual physical properties. For example, the force it can generate depends primarily on fiber length and contraction velocity. In addition, the fiber arrangement, which is defined by the angle between the fibers and the action line, has a major influence. This angle is usually no more than 15 degrees. A pennate muscle consists mainly of non-parallel fiber orientations and generally favors force over a range of motion (Figure 1.2).

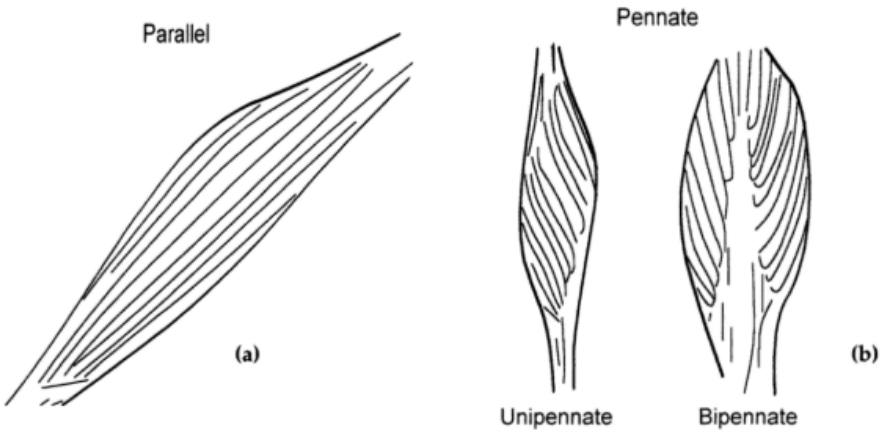


**Figure 1.2:** Illustration of pennation angles (adapted from Knudson, 2003 ). The fiber arrangement influences the range of motion and force. A muscle with non-parallel fiber orientations and in general, favors force a over range of motion

They are the only muscles that allow conscious muscle control through the somatic nervous system. The signals travel through α-motor neurons in the spinal cord and connect the brain to each muscle. They exit the spinal cord at the anterior side. In combination with the connected muscle fibers, they form a motor unit (MU). Innervation occurs through a synapse called the end plate and the individual motor axons that connect different fibers (Dale Purves et al., 2001). A MU can connect up to 100 fibers and controls muscle force with a typical latency of 10-15 milliseconds (Figure 1.3).

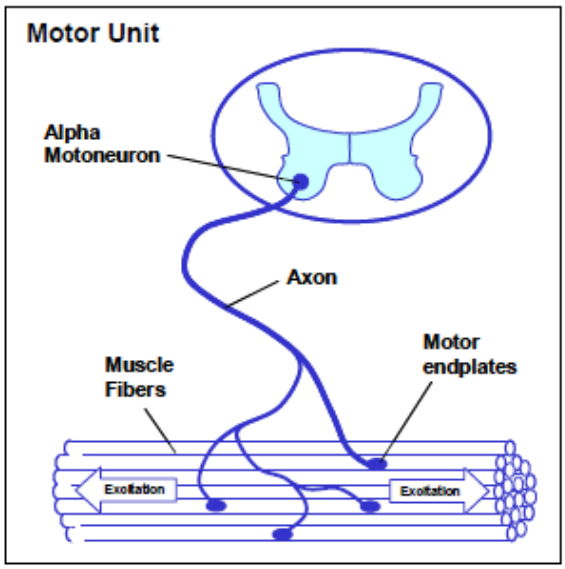


**Figure 1.3:** Illustration of a motor unit (adapted from Dale Purves et al., 2001). A motor unit connects up to 100 muscle fibers with the spinal cord using alpha motor neurons.

At the fiber level, it is composed of myofibrils and surrounded by sarcoplasmic reticulum. The intercellular fluid contains mitochondria as energy producers and glycogen granules. The proteins myosin and actin, linked by titin, form the kinetic complex for force generation. Troponin and tropomyosin act as regulatory proteins in muscle contraction. Collectively, they account for about three-quarters of the protein in a single muscle. Muscle contraction occurs because of a process called the "ATP cross-bridge cycle," discovered by Lymn and Tayler (Lymn and Taylor, 1971) and based on the sliding filament theory established by Huxley and Handson (HUXLEY and NIEDERGERKE, 1954). ATP is the abbreviation for the energy carrier adenosine triphosphate, a nucleotide molecule (Knowles, 1980) produced by mitochondria. The cross-bridge cycle, describes the kinetic protein interaction that increases the overlap of thin and thick filaments. Troponin and actin are located on the thin filament, their counterpart myosin on the thick filament. Muscle contractions begin with a sufficient potential at the end plates that opens ion channels embedded in the sarcolemma, causing sodium Na+ ions to flow into the interior of the cell and potassium K+ ions to be withdrawn to the exterior(Hopkins, 2006). This depolarization shifts the action potential (AP) from the equilibrium potential at the cell membranes of muscle fibers from about -80mV to 30mV. The resting potential is immediately restored, with ion pumps, which are also embedded in the cell membrane, obtaining their energy from the hydrolysis of ATP (Gadsby, 2009). During this depolarization-repolarization process, there is an increase in Ca2+ concentration in the sarcoplasm, leading to muscle contraction (Konrad, 2005; Toyoshima, 2007). This increased Ca2+ level binds to troponin, causing a conformational change and moving tropomyosin away from the thin filament. This results in an opening of the myosin binding site on actin. This unlocking mechanism allows myosin to form a cross-bridge and displace the actin filament by 5-10nm. The binding of ATP to the myosin head, in which it is hydrolyzed to adenosine diphosphate (ADP) and organic phosphate, provides energy for movement. In skeletal muscle, this cycle repeats at 10 - 100Hz. By lowering the Ca2+ concentration in the sarcoplasm, tropomyosin again blocks the binding site and muscle contraction stops. Starting from the end plate, depolarization proceeds through the fibers at a rate of 3-5m/s (Brandes et al., 2019).

Depending on myosin binding type, muscle fibers are divided into three categories. Type I fibers are both slow-moving and fatigue resistant, and are most active when the muscle is under static load. Faster-moving type IIA fibers have a slightly higher fatigue response than

type I, but a much lower fatigue response than fast-moving type IIX. With the accompanying increase in force in faster fiber types, the recruitment cascades from slow to fast moving fibers begin (Elwood Henneman and Lorne M. Mendell, 2011)

## 1.5. Electromyography

EMG provides a noninvasive method for quantifying muscle energy and activity (Cram et al., 1998). As described in the introduction, EMG measurements are often used to determine the level of muscle activity. This is possible because the activation process of the MU generates an action potential (MUAP) (chapter 1.4). Two methods are commonly used to measure this MUAP voltage. By means of surface electrodes on the skin or by needle electrodes which are pricked into the muscle. Because each MU emits a signal during contraction, the surface measurement represents a superimposed signal emitted from each MU. Surface EMG represents a non-invasive method and allows non-medical personnel to record muscle activity at low risk and are therefore used in this study.

Due to the distance between the signal source and the sensor, the signal amplitude depends on the type of tissue between the electrodes and the MU as well as the muscle structure. Increased temperature, a fat layer between skin and muscle or sweating decrease the signal amplitude and frequency (Freund, 1983). These parameters vary not only between people but also between skin sites. Therefore, different procedures and methods are necessary to compare surface EMG measurements between subjects, but also each time a sensor is placed on a specific muscle (Basmajian, 1962).

### 1.5.1. Artifacts

In addition to the considerations of sensor placement and skin contact, Konrad (Konrad, 2005) presents several other aspects that must be considered or of which one should be aware when working with EMG. Artifacts describe the change in an EMG signal due to interference. The most relevant for this work are:

- **Cross Talk**

All active muscle fibers emit and conduct an electrical field through the tissue of nearby muscles to the measuring site. They can all contribute to a specific signal associated with the measured muscle. This is possible because the signal is a superposition of all the MUAP of the individual fibers, not the individual muscle. This results in a muscle activity signal composed of all the potentials around the deduction site. Several studies (Barr et al., 2010; Luca and Merletti, 1988; Solomonow et al., 1994) investigated the contribution of adjacent muscles using needle and surface EMG. They all conclude that surface EMG signals should be interpreted cautiously, as the results may correspond not only to the specifically measured muscles but also to all adjacent muscles. In addition, appropriate electrode size, inter-electrode spacing, and precise sensor placement are necessary to minimize this type of artifact (Solomonow et al., 1994).

- **Motion artifacts**

Motion artifacts are closely related to the skin-electrode interface due to skin deformation, electrode contact pressure, and skin type and condition (Roy et al., 2007) Muscle movements and the associated change in their geometry are also not negligible (Luca et al., 2010). This change affects the distance between the MU and the electrode, which significantly alters the measured muscle activity (Shankar et al., 1989). Mesin et.al. (Mesin et al., 2009) use simulation models to determine the best sensor position and promote a position between the axon innervation zone (IZ) and the tendon, with no electrode moving across the IZ throughout the range of motion. These results do not represent the majority of research studies in his literature review, where most authors advocate a position on the most prominent bulge of the muscle belly, as reported by Luca et.al. (Luca, 1997). In general, the exact sensor position should be subject-specific (Rainoldi et al., 2000).

### 1.5.2. EMG processing

Due to the stochastic nature of the EMG signal, the raw signal alternates between negative and positive peaks. Figure 1.4 shows an example raw EMG signal including the derived muscle activity.

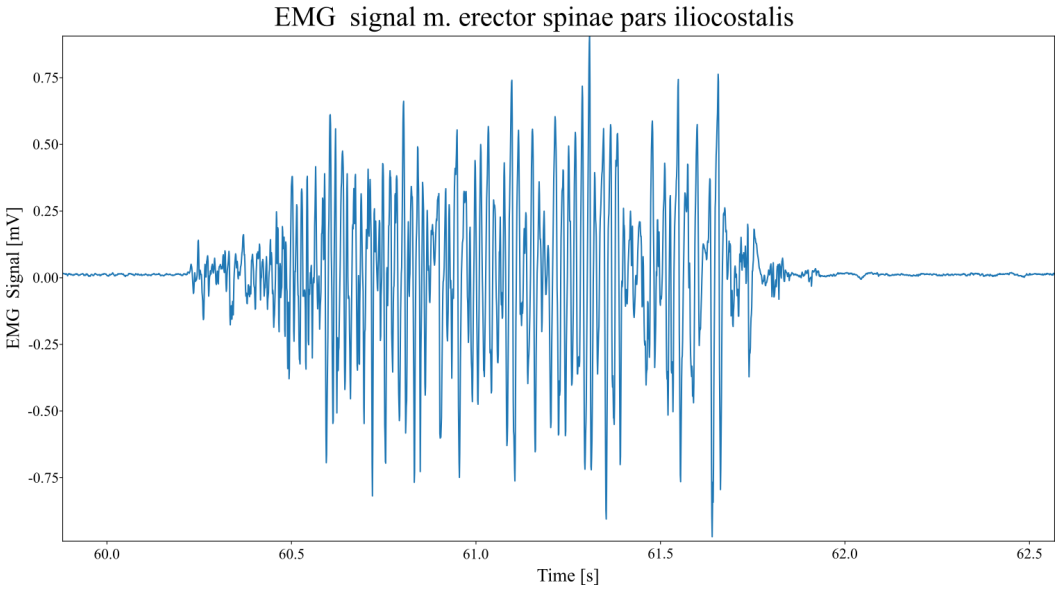


**Figure 1.4:** The figure depicts a raw EMG signal. The MUAP consists of positive and negative voltage proportion. In case the muscle tension growts, the signal magnitude increases and declines when it returns to the relaxed stated.

In time domain EMG processing, two different methods are commonly used to characterize the respective muscle activity. The mean absolute value (MAV) (1.1) represents the area under the signal. represents the area under the signal. The second method calculates the signal power by the root mean square (RMS) value (1.2). In contrast to the MAV value, it represents a physical quantity and is generally preferred, but both values characterize an adequate representation of the respective muscle activation (Luca, 1997; Luca and van Dyk, 1975).

$$MAV = \frac{1}{N}\sum_{k=1}^{N}|x_k| \tag{1.1}$$

$$RMS = \sqrt{\frac{1}{N}\sum_{i=1}^{N}x_i^2} \tag{1.2}$$

By using a sliding window operation (1.3) for convolution, the temporal resolution is preserved during a movement. Window sizes and their constant overlap influence the signal accuracy and smoothness. Konrad (Konrad, 2005) suggests values depending on the underlying task velocity. The range of values starts at the low end of 20ms for fast exercises

such as a sprint, reflex studies, etc., and 500ms for slow or static movements that occur, for example, in a sitting position.

$$x_i = \sum_{n=i}^{N=i+m} RMS(x_n) \tag{1.3}$$

*with:*
$m = Window\ size$
$i = 1..Sample\ size$

### 1.5.3. EMG normalization

Normalization is required to allow comparison of EMG data between subjects, different muscles, and even the signal from a single sensor if it has been removed and reattached at a specific location (Basmajian, 1962). EMG normalization is achieved by dividing the sensor signal by a reference value and was first introduced by Eberhart et al. (EBERHART, 1954). In general, it is a linear transformation of amplitude, with zero mapped to zero and the reference value mapped to one It is often defined as a 0-100% muscle activation scale. The determination of the normalization quotient should meet a number of requirements: Measurement of the same muscle, use of the same electrode configuration, and repeatability should allow comparison between muscles and subjects. Normalization changes the signal magnitude and affects the interpretability of the signal. Therefore, the choice of normalization method is critical (Burden, 2010). Several normalization methods have been established and are widely used in applications or research with EMG.

- **No normalization**

This type of normalization provides limited insight from a time domain perspective, but may be the only method needed or available for a particular population, e.g., individuals with medical conditions such as back pain, myalgia, etc. If timing between different muscle groups is of interest, this can be a useful tool (Di Fabio, 1987; Hodges and Richardson, 1996). The main uses of non-normalized signals are frequency domain algorithms. Methods such as wavelet analysis or power density analysis are used to analyze muscle at the fiber level (Chapter 1.4). This research focuses on general recruitment changes and the corresponding

musculoskeletal loading changes of the spine. Therefore, frequency methods are not addressed in this thesis.

- **Mean or maximum peak during the task.**

In-task normalization uses either the peak or mean value obtained during the activity under study. This method was one of the first methods used to examine patterns in muscle activation in a variety of research applications, such as gait analysis (EBERHART, 1954; Winter and Yack, 1987; Yang and Winter, 1984) or sports science (Trevithick et al., 2007). This technique has been the focus of several studies and the use of the mean value has been identified as a valid tool to reduce subject-specific variability (Chapman et al., 2010; Knutson et al., 1994; Winter and Yack, 1987; Yang and Winter, 1984). Consideration of biological aspects is important to generate data that are comparable between subjects. Each individual varies in terms of height, weight, fitness level, and effort an individual must exert during an activity. Therefore, the amount of muscle activity may be lower or higher compared to others. Nevertheless, this method is a useful strategy when exploring recruitment patterns (Bolgla and Uhl, 2007; Morris et al., 1998). This method allows normalization by values obtained during exercises that a subject can perform. This allows comparison of groups with pain or limitations. This may be the case, for example, in patients with musculoskeletal disorders or in the elderly.

- **Maximum voluntary contraction**

Maximum voluntary contraction (MVC) is the most comprehensive method for EMG normalization. It allows comparison of individuals, muscles, and activities and includes a separate measurement to obtain maximal muscle activation. During an isometric contraction, the participant maximally activates the muscle in its optimal line of action. Both requirements already reveal possible causes of signal inconsistency and variability. The necessary externally applied static resistance does not always have the same orientation for all subjects because they differ in anthropometry and physiology. The ability of self-motivation during the test may influence the reference value and provides a significant contribution to signal interpretation (Hald and Bottjen, 1987; Peacock et al., 1981). This can lead to either underestimation or muscle activities higher than 100%. Konrad (Konrad, 2005) suggests body postures including fixations and force direction to determine MVC values for specific muscle

groups (Figure 1.5, Figure 1.6). In addition, he presents procedures that provide a structured, deterministic way to obtain a reliable reference value. First, the subject is immobilized in an isometric testing apparatus. Then, the subject increases the force to the maximum in 3-5 sec, maintains the maximum force after a slow decrease in 3-5 sec for another 5 sec, and repeats the exercise after a rest of at least 30 sec to avoid fatigue ++or discomfort.

| Muscle group | Exercise | Comments |
|---|---|---|
| Forearm flexors / extensors |  | Select a seated or kneeling position (in front of a bench) and arrange a stable forearm support. Manual resistance, barbells or cable/belts can be used. Consider using the latissimus d. and pectoralis major MVC test as a control exercise |
| Biceps Brachii |  | A valid biceps b. MVC needs a very stable elbow and trunk fixation. This can best be arranged in a seated or kneeling position (in front of a bench). Consider using the latissimus d. MVC-test as a control exercise. |
| Triceps Brachii |  | Same instruction as biceps b.! Consider using the pectoralis major MVC-test as a control exercise. |
| Deltoideus |  | Select a seated position, if possible with fixated back. Fixate near the arms near the 90° position. The bilateral contractions guarantee a balanced force distribution for the trunk. The abduction works best for the pars acromialis of the deltoid muscle. Consider a flexion/extension position for the pars clavicularis. |
| Trapezius p. descendens | 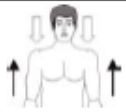 | The MVC test can be performed with one side only. A static resistance can be arranged by manually fixating the arm or arrange a large enough load to press the shoulder down (difficult). |
| Pectoralis major |  | Numerous test positions can be used! However, all of them need a very good shoulder/back resistance. The prone lying position would best be performed with a (fixated) long bar. The push up may work as an easy to arrange alternative. Both positions should be performed in 90° elbow position. |
| Infraspinatus | 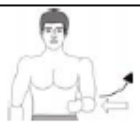 | Being the most important outward rotator of the shoulder cuff, any related outward rotation may work. Good results are achieved with uni- or bilateral manual resistance against the forearm |
| Trapezius p. trans. / Rhomboideus | 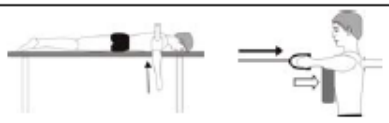 | The horizontal abduction best addresses the shoulder stabilization muscles. In the prone laying position a barbell or bilateral manual resistance can be used. The seated position requires a good breast fixation and a cable or machine resistance (rowing machines). |
| Latissimus/Trapezius p. ascendence | 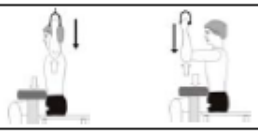 | The simulation of a pull-up addresses the highest latissimus innervation. Consider/check a frontal and a lateral arm position at 90° elbow flexion. You may find MVCs for the biceps and the lower trapezius also. |

**Figure 1.5:** Upper body maximum voluntary contraction exercises. Arrows indicate support positions and force directions (adapted from Konrad, 2005).

| Muscle group | Exercise | Comments |
|---|---|---|
| Rectus abdominis<br>Obliquus internus abdominis |  | A valid MVC test for the abdominals is difficult to arrange. Sit-up styled movements with very good leg fixation (!) work best. Let the spine flex by around 30° and use a belt or manual fixation for that position. The obliques may fire higher when an additional trunk rotation is added to the flexion |
| Obliquus externus abdominis | 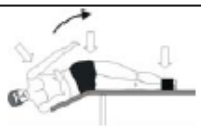 | This MVC test needs good coordinative skill. A side laying position with leg and hip fixation is a good start position. Let the subject flex up and fixate early in the flexion position. An important check exercise is the MVC test for the rectus abdominis |
| Erector spinae / Multifidii |  | The prone laying position on a bench is a very productive MVC test position. Because all back muscles are facilitated within a muscle chain, MVCs for the erector spinae, the gluteus and the hamstrings can be found here. A check exercise is the isolated back extension at a machine |
| Glutaeus maximus | 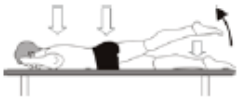 | A control exercise for the gluteus maximus muscle! It should be performed both in extended and flexed knee position with slightly outward rotated legs. The hyperextension position (~20°) is important. |
| Glutaeus medius |  | The hip abduction can be performed in fixated side laying position or supine position. Some subjects show higher EMGs in standing position |
| Mm. adductores |  | A big and stiff roll cushion is pressed between the flexed legs |
| Rectus femoris |  | An easy and beneficial exercise for all quadriceps muscles! A single leg knee extension between 90 and 70° knee flexion position is performed |
| Mm ischiocrurales | 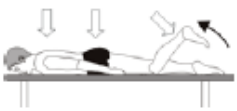 | Isolated test for the hamstrings. Arrange a very good fixation of the hip (belt/heavy person) and perform a unilateral knee flexion at ~ 20-30° knee flexion. An important check exercise is the prone laying MVC test for the erector spinae |
| Gastrocnemius |  | Being one of the strongest human muscles, the triceps surae group needs very rigid (machine) resistance against the fixated hip. Perform an unilateral plantar flexion at 90° ankle position |
| Soleus |  | This is an important check exercise for the soleus muscle because the gastrocnemius is at a difficult work position. Perform a unilateral plantar flexion. A very rigid fixation of the knee is needed due to high forces |
| Tibialis anterior |  | The tibialis anterior usually can be fixated by manual resistance, work unilateral |

**Figure 1.6:** Lower body maximum voluntary contraction exercises. Arrows indicate support positions and force directions (adapted from Konrad, 2005).

## 1.6. Muscle stress relationship

As described in chapter 1.3 mental stress prepares the body for a fight or flight situation. This reaction increases blood flow, respiration and muscle energy. On the cardio-vascular side, blood thickens to prevent excessive bleeding in the event of injury. Additionally, the release of endorphins suppresses the effects of pain or injury. Increased muscle tension is necessary to prepare for rapid intervention such as attack, defense, or change in posture. The stress system controls this response, is located in the central part of the hypothalamus and brainstem, and is part of the central nervous system (CNS). In peripheral organs, stress is responsible for the lack of homeostasis. It also affects the balance of interconnected neuroendocrine, cellular, and molecular infrastructure (Chrousos, 2009; Constantine Tsigos et al., 2016). Stressful situations increase muscle activity only for a short period of time and are the subject of investigation in this thesis.

Nonetheless, a high prevalence of short-term stress can lead to persistent psychological distress that causes the development of non-acute muscle fiber dysfunction. Several theories have been proposed to explain these effects. The widely accepted energy crisis model is formulated by Simons and Travell (Simons and Travell, 1981). In this model, energy consumption exceeds the level provided, resulting in prolonged actin-myosin coupling The result is a decrease in blood flow and a lack of supply to the muscle due to a reduction in the ATP process. Finally, the Ca2+ level can no longer be completely lowered, leading to increased muscle tone (Chapter 1.4).

While the energy crisis model focuses on the molecular level, the Cinderella hypothesis (Kadefors et al., 1999) uses the level of motor units to describe dysfunction and is based on the findings of Hägg(Hägg), Henneman (Henneman et al., 1965) and Henriksson (Henriksson, KG, 1988). It is based on a recruitment cascade of muscle fibers. Initially, type I muscle fibers are triggered and remain active throughout the contraction, whereas faster types are recruited only when needed. This low-threshold long-term activation leads to irreversible degenerative processes that result in pain.

Several studies have already shown that psychological stress leads to tension in the trapezius muscle. Table 1.1 gives a small overview of studies by other research groups whose results

show a much higher response in the context of work. The relationship between stress and muscle physiology has also been the focus of researchers. Wærstedet al. (M. Wærsted et al., 1996) conducted a study linking an attention-intensive task to prolonged activation of type I fibers, supporting the Cinderella hypothesis as a possible cause of chronic shoulder and neck pain.

| Study | Load | Trapezius response |
|---|---|---|
| (Larsson et al., 1995) | static | 20% increase |
| (Leyman et al., 2004) | Dual Task type writing | 67% right<br>8% right |
| (Rissén et al., 2002) | Work | Right 102%<br>Left 123% |
| (Lundberg et al., 1999) | Cashier Work | Left 110%<br>Right 87% |
| (Lundberg et al., 2002) | Mental arithmetic | 9% |
| (Mork and Westgaard, 2007) | Seated | Dominant 1.6%<br>Non-Dominant 0.8% |

**Table 1.1:** Overview of various studies investigating trapezius activity during stress with light or non-work load

## 1.7. Musculoskeletal modeling systems

Musculoskeletal simulation provides an effective way to investigate internal loads on the human body in silica. Otherwise, the usage of sensor implants or prostheses with applied measurement gauges is necessary. Even if this is possible, for example the in case of a total joint endoplasmic, in other areas like ergonomics, sports or pre-operation planning this is not a possible solution. Therefore, this kind of simulation model is an indispensable tool to gain insight into the human body. In general, a rigid body system formulates the musculoskeletal

correlations of the human body. The following differential equation (1.4) describes this system in general. (Pandy, 2001)

$$M(q)\ddot{q} + C(q)\dot{q}^2 + G(q) + R(q)F^{MT} + E(q,\dot{q}\,) = 0 \tag{1.4}$$

*With:*

$q, \dot{q}, \ddot{q}$ *generalized coordinates, velocities, acceleration*

$M(q)\ddot{q}$ *Internal forces and torques*

$M(q)$ *System mass matrix*

$C(q)\dot{q}^2$ *Centrifugal, Coriolis forces and torques*

$R(q)F^{MT}$ *muscle tendon torques*

$R(q)$ *Matrix of muscle moment arms*

$F^{MT}$ *Muscle tendon forces*

$G(q)$ *Gravitational forces and torques*

$E(q,\dot{q}\,)$ *vector of external forces and torques to the human body*

EMG-driven forward dynamic and inverse dynamic approaches have been established and successfully used in the last decades. Common to all of them is the need to know material-specific properties of muscles and tendons (Chapter 1.4). Furthermore, the integration of human kinematics and kinetics into the model is essential to model the interaction with the environment and to include force boundary conditions. Different models differ in how body motion is determined. In forward dynamic simulation, algorithms determine the best way for applied forces to execute a given motion. The forces are derived from muscle activations, the estimation of which is based on EMG measurements and thus takes into account individual patterns of muscle recruitment. Inverse dynamics reverses this approach. Using the known motion, the necessary forces and moments are calculated to perform the motion. Figure 1.7 illustrates both simulation procedures.

**Forward Dynamics:**

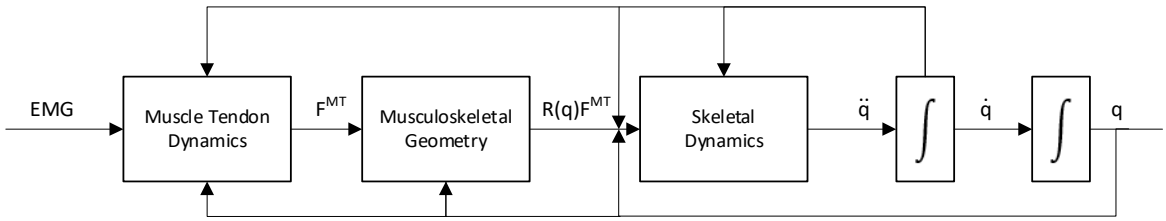


**Inverse Dynamics:**

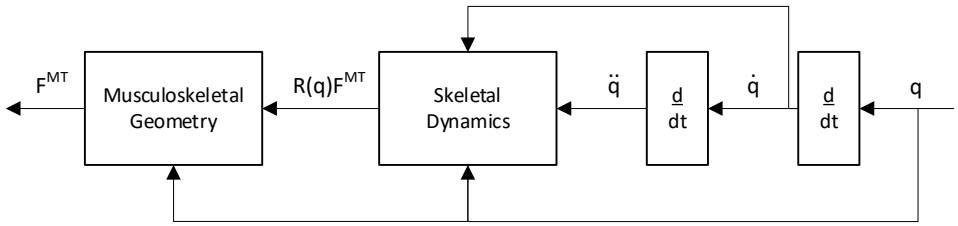


*with:*

$q, \dot{q}, \ddot{q}$ *generalized coordinates, velocities, acceleration*

$R(q)F^{MT}$ *muscle tendon torques*

$R(q)$ *Matrix of muscle moment arms*

$F^{MT}$ *Muscle tendon forces*

*EMG Electromyography signal*

**Figure 1.7:** Workflow of forward and inverse dynamic models. Forward dynamic models use EMG data to simulate the resulting motion. Inverse dynamic choses the opposite approach by using kinematic data to compute the muscle forces. (adapted from Pandy, 2001)

Since the number of muscles and their direction of action do not coincide with each degree of joint freedom, the human body is an over determined system. Nonlinear optimization algorithms solve the resulting system of equations. The complexity of the forward dynamic model is quite high. To calculate the muscle and joint forces, the optimization problem includes the entire motion cycle. In contrast, the inverse dynamic problem includes individual time steps along with the motion (Pandy, 2001).

Forward EMG-driven simulation models derive the required muscle forces from EMG measurements. A muscle force-activity model derives the necessary correlation. This

approach has been used in several musculoskeletal loading models such as ankle (Hof and van den Berg, 1981), knee (Lloyd and Besier, 2003; Piazza, 2006; Piazza and Delp, 1996) or lower back (Granata and Marras, 1993; McGill, 1992; McGill and Norman, 1986; Nussbaum and Chaffin, 1998). Fundamental to all models is muscle activation and force calculation for the measured muscles. Therefore, a correct system model of the muscle-tendon unit (MTU) is essential (Figure 1.8). A common approach is the three-element Hill model, which has been extended to include an element representing the tendon (1938) (Figure 1.8). The force, length, and velocity properties are modeled using a contractile component (CC), active stiffness is included with a serial elastic element (SEC), while the passive component includes a parallel elastic element (PEC) (Miller, 2018).

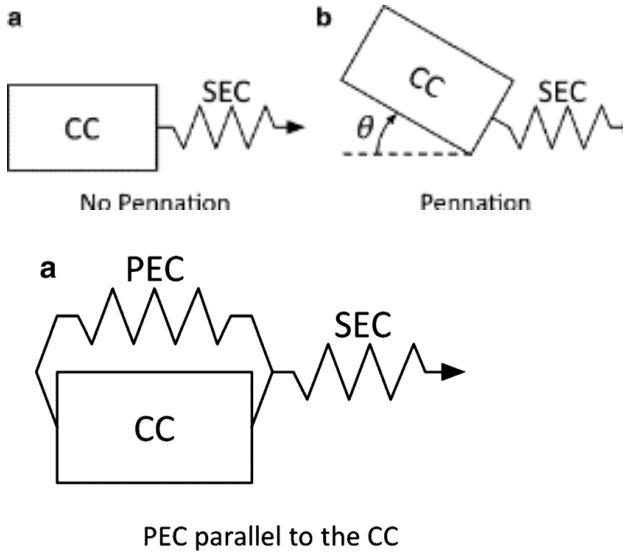


**Figure 1.8:** Models of muscle tendon units. The muscle models including pennation angle θ, series-elastic (SEC), parallel elastic(PEC) and contractile components(CC) (adapted from Miller, 2018)

The muscle force generated depends on the fiber pennation angle (θ) and the forces generated by the CC and PEC elements (1.5).

$$(FCC + FPEC)\cos(\theta) = FSEC \tag{1.5}$$

In addition to the pennantion angle, the use of other muscle-specific parameters influences the forces and serves to adapt the modeled system to the physiological properties. Sovil et.al. (Scovil and Ronsky, 2006; Umberger et al., 2003) identified the following parameters as the most dominant:

1. Optimal fiber length (Lo)
2. Fiber pennation angle (θ)
3. Physiological cross-sectional area (PCSA)
4. Unloaded tendon length (Lu)
5. Fraction of "fast-twitch" fibers (FT)

In case of quasi-static or slow motion the correlation of the mean rectified EMG signal the correlation between force and muscle activation can be described as linear (1.6) (Hof, 1984).

$$F = g1 * E + const \tag{1.6}$$

with:

E: EMG Signal

g1: gain factor

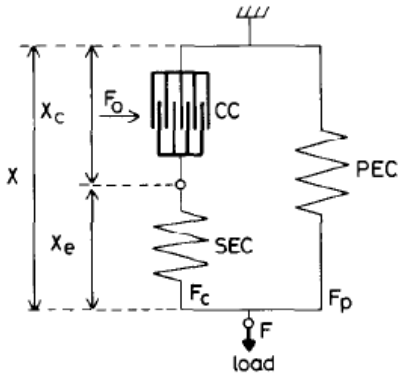


**Figure 1.9:** Illustration of a hill type muscle model including the normalized muscle length and CC, SEC and PEC forces (adapted from Hof, 1984).

Despite the rather simple correlation, the determination of g1 can be quite complex. The procedure includes an experimental design, which allows the isometric measurement of the muscle in a rigid setup like a dynamometer. In case of a dynamic contraction, the knowledge of the current muscle length is needed as well as the EMG signal E(t). The Hill model defines

the base model of the force EMG correlation. The CC and SEC element define the active muscle part. The normalized muscle length is defined by:

$$x = \frac{l}{l_0} \tag{1.7}$$

with l the current length and l_0 a normalization length at a standardized position. Due to the parallel configuration, the muscle force is defined by:

$$F = F_c + F_p \tag{1.8}$$

The PEC represents the muscle tendons and joint ligaments. In the case of an inactive muscle, it can be described by the exponential function, which is highest at the muscle length extremes:

$$F_p(x) = F_p e^{p(x-1)} \tag{1.9}$$

The active force produced by the active element depends on whether there is an isometric or dynamic case. In the case of an isometric load, the force is length-dependent and proportional:

$$F_c = f(x_c)F_0 \ (x_c \ constant) \tag{1.10}$$

with f(xc) €[0,1] either parabolic (Woittiez et al., 1983) or Gaussian curve (Hatze, 1981)

For a dynamic movement, a force-velocity relation must be considered and a shortening velocity defined by:

$$v_c = -\frac{dx_c}{dt} \tag{1.11}$$

It results in an extended force equation by included in the Hill equation:

$$F_c = \frac{F_{0\left(f(x_c)-\frac{nv_c}{b}\right)}}{1+\frac{v_c}{b}} \ with \ f_c \leq (1+c)F_0 f(x_c) \tag{1.12}$$

with:

n and b used as calibration factors.

b velocity decrease

n overall concave curve shape.

According to the definition of the Hill equation, the rectified EMG signal is directly proportional to the force F0, confirmed by Bigland et.al. (BIGLAND and LIPPOLD, 1954)

$$F_0 = gE\ (quasi - static) \tag{1.13}$$

In the case of dynamic motion, equation (1.13) holds for an increasing EMG signal E(t) and $F_0(t) = g*E(t)$. When a relative maximum occurs, this value is held for a certain time and then decreases exponentially. For a more detailed description of the timing and force decay, I refer to Hof (Hof, 1984).

EMG data partially introduce muscle recruitment in forward EMG-driven models. In the case of an inverse dynamic approach, muscle recruitment must be implemented in the simulation model itself and mimics the central nervous system (CNS).

In this work, the simulation software AnyBody Modeling System™ by Anybody Technology A/S used and its approach is discussed. (Damsgaard et al., 2006). In contrast to forward dynamic models the muscle recruitment by the CNS is simulated here. This is achieved by nonlinear optimization with a suitable target function. In general, optimization problems can be described in the form:

$$\begin{aligned} &Minimize\ \ G\left(f^{(M)}\right) \\ &Subject\ to\ Cf = d \\ &0 \le f_i^M \le N_i, i \in \{1, \dots, n^{(M)}\} \end{aligned} \tag{1.14}$$

*with:*

*G: objective function representing the CNS*

*f(M): Muscle forces*

The function G(x) represents the objective function and formulates the CNS recruitment strategy, where f(m) describes all unknown muscle and joint reaction forces. Expression d represents additional constraints and contains external and inertial forces. Matrix C contains the unknown forces demanding equilibrium with the external loads.

Three approaches to describing the objective function G have been established, with polynomial form often used (Bean et al., 1988):

$$G(f^{(M)}) = \sum_{i=1}^{n^{(M)}} \left( \frac{f_i^{(M)}}{N_i} \right)^p \tag{1.15}$$

$N_i$ describes a normalization function, such as the modified Hill model introduced by Zajac (1989) or constants such as maximum muscle force, which represent a numerical model of physiological muscle. The resulting normalized muscle forces express muscle activity. The power value p has been the subject of numerous studies (Crowninshield and Brand, 1981; Herzog, 1987; Pedotti et al., 1978; Röhrle et al., 1984). The value represents a trade-off between a decrease in numerical stability and a more physiologically meaningful recruitment of muscles at a higher p value. A value of one only favors the recruitment of a stronger muscle, which does not correspond to reality. In general, the CNS favors load sharing. At higher values, optimization converges to a more realistic recruitment pattern where fatigue is postponed (Rasmussen et al., 2001). In this work, a p value of three is used. Pandy et al. showed that both approaches can produce the same results (Pandy, 2001).

## 1.8. ML Gradient boost tree, neural network

Regression models describe the correlation between one or more independent feature variables and a dependent outcome variable. Depending on the underlying data, the correlation is described as either a nonlinear or linear problem. In the latter correlation, a hyperplane is fitted to the data to minimize residual using a least squares method (Fahrmeir et al., 2009). If the linear function inadequately describes the relationship between outcome and feature, the problem is nonlinear. In this case, the regression hyperplane is changed to a nonlinear function that best fits the data.

In recent years, supervised machine learning algorithms have emerged in the field of regression for prediction and forecasting. In this work, the two most common approaches are used to predict the response of unstressed and stressed muscle activity. In particular, neural networks (NN) and gradient reinforcement methods provide a tool to address a wide range of problems, from linear to nonlinear models.

### 1.8.1. Gradient boosted regression trees

Gradient Boosted traces its origins to the work of Jerome E. Friedman (2001) and Mason et.al. (Mason et al.). In particular, Friedman's work is the basis for the Python library of XGBoost (2020c; Chen and Guestrin) used in this study. This chapter outlines the algorithm; for details, I refer the reader to Chen et.al. (Chen and Guestrin) as the author of this algorithm and implementation. Boosting describes the basic method of this algorithm, which builds trees sequentially to reduce the residual of the previous tree (Figure 1.10). First, an initial prediction is made using the mean initial value for the data sets. Based on this best estimate, residuals between the real values and the estimate are calculated, resulting in pseudo-residuals. Now the feature values are used to predict these residuals. To do this, a feature is selected as the root leaf and the dataset is split into two clusters. In the following, new leaves are selected for the next feature, which again splits the dataset. Depending on the maximum allowed levels, the feature nodes are followed by the residual. If the branch selects more than one residual, the middle residual represents the error. The initial guess and tree are then used to make a prediction and generate new residuals by comparing the output to the original dataset. The difference represents the new pseudo-residuals for a new boosted tree. This process repeats until either the maximum number of trees is reached or there is no change in accuracy. To perform a prediction, the results of each tree are added in the same order in which the tree structure was built, providing the corresponding output value.

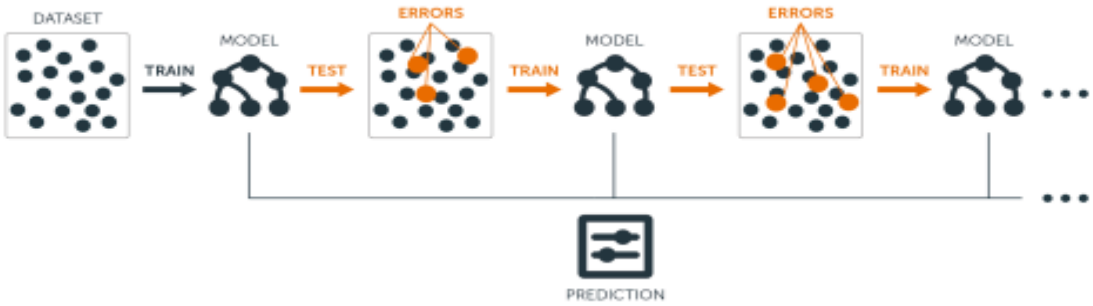


**Figure 1.10:** Workflow of training a gradient boosted regression tree and predict the provided dataset. The prediction error is used to train a new tree to increase the overall model accuracy. (adapted from Chen and Guestrin)

### 1.8.2. Deep neural network regression

Artificial neural networks mimic the human brain with its neurons and axons. Like the brain, the network contains several interconnected layers. Feature values are represented in the input layer, while result variables are represented in the output layer. The number of neurons depends on the number of features and result variables. While the outer layers depend on the number of variables, the connection layers or hidden layers depend on the regression problem and scale with it. A very simple network with only one hidden layer is only capable of modeling linear regression models. Adding more layers increases the complexity, but thus enables the modeling of nonlinear relationships.

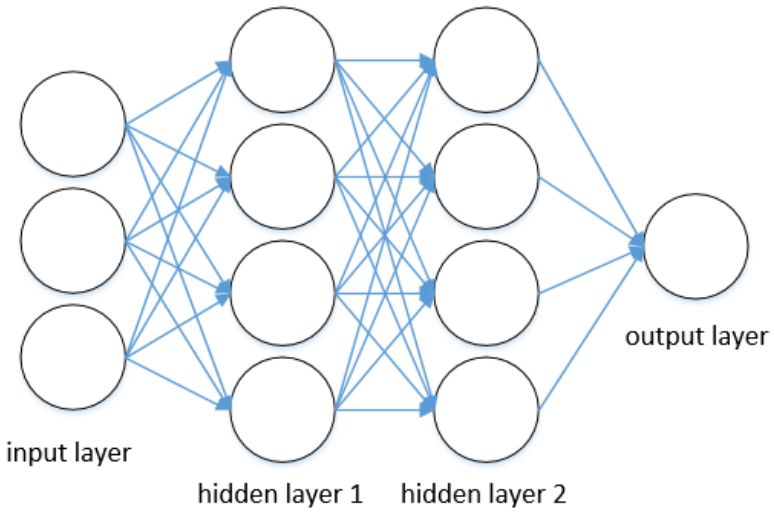


**Figure 1.11:** Simple neural network with three input neurons. The single neuron in the output layer is connected to the input with two hidden layers containing four neurons each.

In detail, each neuron consists of multiple inputs and one output connected with an activation function and a bias. The number of inputs depends on the number of features in the case of the first hidden layer or the number of neurons in the previous layer, since all neurons are connected to each previous one. All inputs are combined by summation and passed to an activation function (Figure 1.13). Various functions are discussed in the literature, depending on the underlying physical data. Figure 1.12 gives a graphical overview of activation functions In practice, it has been found that the rectified linear unit (ReLU) function (*1.16*) fit is best suited for regression.

$$f(x) = \begin{cases} 0 \; for \; x \leq 0 \\ x \; for \; x > 0 \end{cases} \tag{1.16}$$

Although non-differentiable, its simplicity and computational speed outweigh this drawback in the necessary nonlinear optimization used during back-propagation training. During training, sample data are available at the input and output neurons. Then, nonlinear optimization is used to adjust the weights and bias (*1.17*) of each neuron to fit the sample data.

$$Minimize \; f(b + \sum_{i=1}^{n} x_i * w_i) \tag{1.17}$$

*With:*

*$w_i$: Input weight.*

*b: neuron bias*

*f(x): Activation function*

For training, the data is split into batches and epochs to train the network. This procedure is intended to prevent overfitting and underfitting of the neural network. Overfitting describes a network that maps the training data too well and consequently produces inaccurate results for new input data. Underfitting means that not enough training data is available and the network is not sufficiently trained.

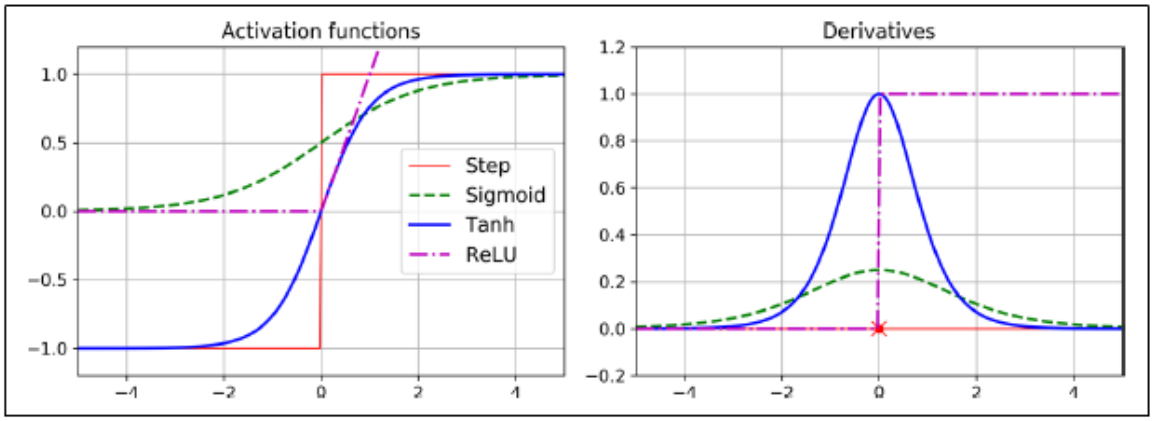


*Figure 10-8. Activation functions and their derivatives*

**Figure 1.12:** Deep neural network activation functions and their derivatives (adapted from Géron, 2019)

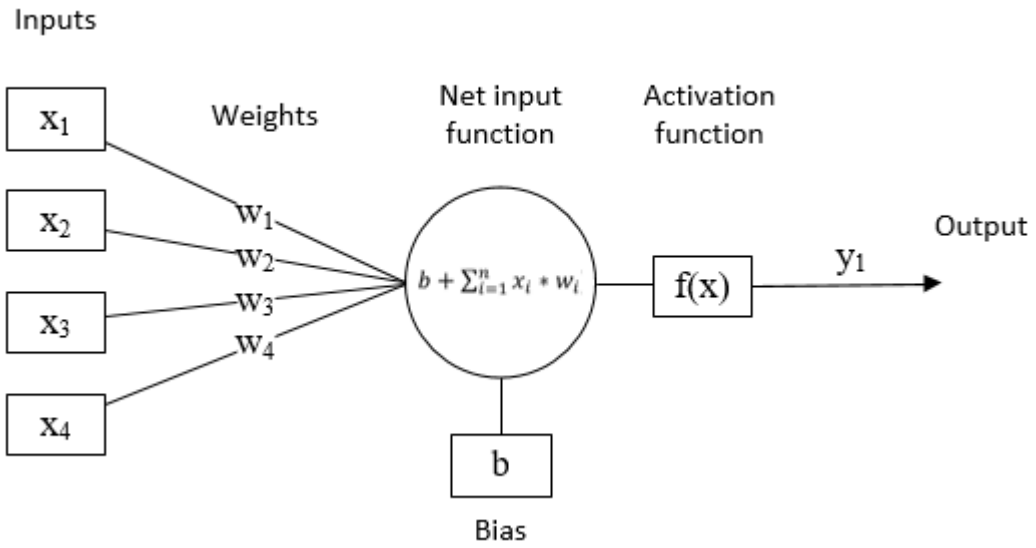


**Figure 1.13:** Graphical representation or a single neuron with four inputs, bias and activation function.

While the weights and biases of the neurons are trained during the optimization procedure, the number of epochs, the batch size, the activation function, the learning rate, the number of layers, and the number of neurons in each layer must be fixed and cannot be changed during

training. These parameters are referred to as hyperparameters and are critical to the accuracy of the NN. Despite a large number of empirical values in the literature, it is recommended to search for the most appropriate values in upstream steps. In this work, two methods are used to find optimal values. To find initial values for Bayesian optimization, a grid search in parameter space was performed. The result of Bayesian optimization parameterizes each training of the individual result values (Archetti and Candelieri, 2019; Géron, 2019).

### 1.8.3. Hyperparameter optimization

Hyperparameters, are model properties that cannot be learned during the training process (Taulli, 2019). These parameters control the training process and must be defined before the actual training. Therefore, they are closely related to the problem and affect the performance of any machine learning algorithm. Due to the diversity of these parameters, a simple definition is not possible. This results in the need to use optimization algorithms to determine the optimal values. Regardless of the machine learning method used, various search techniques exist. These vary from very deterministic approaches such as grid search or gradient-based methods to probabilistic methods such as random search or Bayesian optimization (Bergstra and Bengio, 2012). A third category is evolutionary or population-based methods. Deterministic models only fit scenarios with known gradient information or a limited number of parameters. Nevertheless, grid search is used to find initial values for the following hyperparameter optimization. Due to the complexity and size of the underlying models, the selection is reduced to probabilistic models that continuously contain information about the optimization progress. This is given by Bayesian and population optimization. (Rao and Rao, 2020)

In this case, a grid search evaluates the model at the system boundaries, which are defined by a full factual design. This involves a design where each minimum/maximum combination is tested for all features. This results in $2^n$ models that are tested and scored (Bergstra and Bengio, 2012) (Table 1.2). The model with the best score is used as the starting value for the following Bayesian optimization.

| Feature / Model | 1 | 2 | 3 | … | n | Score |
|---|---|---|---|---|---|---|
| 1 | - | - | - | - | - | $S_1$ |
| 2 | + | - | - | - | - | |
| … | | | | | | |
| $2^n$ | + | + | + | + | + | $S_n$ |

**Table 1.2:** Model overview with maximum and minimum features. – represents the minimum and + the maximum feature value. For every model n and feature combination a score $S_n$ is computed.

In general, optimization algorithms try to find a global minimum of an objective function. The Bayesian approach uses statistical methods to examine the feature space and find the optimal parameter set. A distribution of features describing the objective function f(x) is constructed (Rasmussen and Williams, 2008). This process depends on previous observations, improving the distribution as the number of observations increases. This information shifts the regions worth exploring and performs a best guess in that part of the distribution ("best guess") (Archetti and Candelieri, 2019) and therefor does not need to know the objective function.

## 1.9. Usage of musculoskeletal simulation models

For this work, musculoskeletal simulation models represent the only tool to study the current situation as well as to identify changes in human behavior with their environment. The use of these models requires the measurement of the motion and boundary conditions of the human body interacting with the surrounding. These models follow the laws of physics to establish a balance of forces and torques that results in a specific muscle activity capable of performing the measured task. Psychological stress directly affects muscle activity and even alters default

recruitment. This adds a psychological dimension to the simulation models. To extend the ability of the models to incorporate features such as mental stress, muscle recruitment needs to be adjusted and extended. Therefore, to gain a more detailed insight into how stress affects the system (MSC) in arbitrary situations, an extension of the standard muscle recruitment is presented in this work.

# 2. Experimental study to investigate static sitting

## 2.1. Introduction

During daily life, humans are exposed to both emotional and cognitive stress resulting from a high workload (Grandey, 2000). In contrast, the musculoskeletal effects on the trapezius and lumbar back muscles, respectively, have been commonly studied (Chapter 1). Hypothesis one states that the two types of stressors affect the recruitment of the back muscles differently. To gain general insight into how recruitment differs, a study was conducted without additional physical loading. Using musculoskeletal simulation, hypothesis two is examined to gain information on how and to what magnitude mental tension produces spinal loading. Figure 2.1 shows the general study procedure.

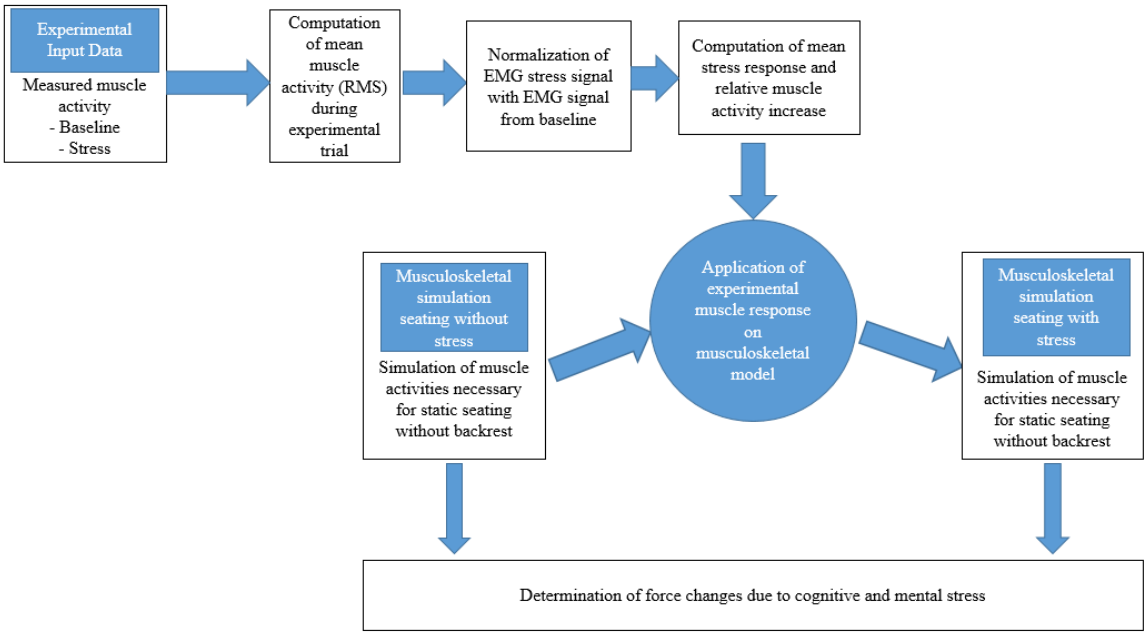


**Figure 2.1:** General study workflow. The experimental EMG data is process to compute the relative change in muscle activity. This data is transferred to simulation models, which result in the determination of spinal load changes because of mental stress.

## 2.2. Methods

In this study, 35 subjects registered to participate. The group included 14 female and 21 male participants. Their mean age was 22.8±2.4 and weight was 72±13.9 kg with a mean height of 176±10 cm. None of the subjects had a history of back pain or mental illness. A psychologist examined all study participants to exclude individuals with acute psychological distress. To comply with the individual's right to privacy, subjects who did not meet the mental health requirements were not treated separately in the experiment. In this case, the data should remain unused in the data processing part. All subjects passed the mental examination and no data were excluded from the analysis. The local ethics committee approved this study and procedure.

Before the experiment, the supervisor instructed each person about the general procedure and explained the questionnaire to assess personal stress level. After that, anthropometric measurements took place, especially weight, height and the sensor application on the back muscles.

As described in chapter 1.5, correct sensor placement and appropriate skin-electrode interface is essential for recording a high-quality EMG signal. In this thesis, electrode placement and skin preparation follows Criswell et al. (Criswell, 2010) and the European project "Surface Electromyography for the Non-Invasive Assessment of Muscles" (SENIAM) (2004). Table 2.1 shows the muscle groups and their sensor location in relation to landmarks. In addition, the use of the functional tests helped to locate the muscle belly. The EMG sensor design used by the manufacturer limits crosstalk due to the electrode size and the pre-installed filter mechanism (Luca et al., 2012).

| Muscle | Location | Function |
|---|---|---|
| m. erector spinae (lower m. multifidi) | Palpate the iliac crest, electrodes 2cm apart, approx. 2cm from the spine parallel to the spine over the muscle mass. Iliac crest may be used to determine the L3 vertebra. Electrodes best placed while patient is in a slight forward flexion | Forward flexion and return to midline of the torso |
| erector spinae pars longissimus | To find T12 have the patient flex forward and palpate where the lowest rib joins the spine, going laterally from the spine approx. 3cm the electrodes are placed 3cm apart, so that they can run parallel to the spine over the fleshy muscle mass. Electrodes are best placed while subject leaning forward | Prone extension, return from forward flexion of the trunk |
| m. erector spinae pars iliocostalis | The electrodes need to be placed 1 finger width medial from the line from the posterior spina iliaca superior to the lowest point of the lower rib, at the level of L2, in the direction of the line between the posterior spina iliaca superior and lowest point of the lower rib. | Lifting the trunk from a prone position |
| m. trapezius ascendens | Palpate the intersacapular region. Have the patient retract and depress the scapula and then flex the arm to at least 90°. Palpate the inferior medial border of the scapula for the muscle mass that emerges. Place the | Abduction of arms; retraction of the shoulder back and down at a 45° angle |

| | | |
|---|---|---|
| | electrodes on an oblique angle, approx. 5cm down from the scapula spine. The electrodes are placed next to the medial edge of the scapula at a 55° oblique angle, approx. at the level of T8 | |
| m. trapezius pars transversa | Locate the medial boarder of the spine of the scapula. Electrodes are placed horizontally, 2cm apart, next to the root, at level of T3 | Retract the scapula and abduct the arms through the full ROM |
| m. trapezius pars descendens | Along the ridge of the shoulder, slightly lateral about one half the distance between the cervical spine at C7 and the acromion. Palpate the muscle mass and place the electrodes over the muscle belly parallel to the muscle fibers | Shoulder elevation/shrug, lateral bending of the head |

**Table 2.1:** Overview of the measured EMG sensor. The description provides the method to identify the correct sensor location and muscle function.

All participants sat on an office chair in a standardized position to reduce physical load. This position required a 90-degree bend in the knee joint and an upright upper body, but not supported by the backrest. The hands were placed palm up on the thigh (Figure 2.3). The subject remained static in this position and was guided by the supervisor before and during the experiment. Changes in the recruitment of the back muscles were determined by measuring 12 muscle groups. Pre-amplified EMG Delsys Trigno IM sensors (Delsys Inc., Wellesly MA, USA) were placed on the m. multifidi, erector spinae pars longissimus, m. erector spinae pars iliocostalis, m. trapezius ascendens, m. trapezius pars transversa and m. trapezius pars descendens (Figure 2.2). The placement itself followed positioning in relation to specific landmarks provided by SENIAM and Criswell et al. (2004; Criswell, 2010).

| Muscle | EMG ID | |
|---|---|---|
| m. trapezius pars descendens | 1 | 2 |
| m. trapezius pars transversa | 3 | 4 |
| m. trapezius ascendens | 5 | 6 |
| erector spinae pars longissimus | 7 | 8 |
| m. erector spinae pars iliocostalis | 9 | 10 |
| m. multifidi | 11 | 12 |

**Table 2.2:** EMG Sensor ID attached to a specific back muscle group. Even IDs are placed on the left side

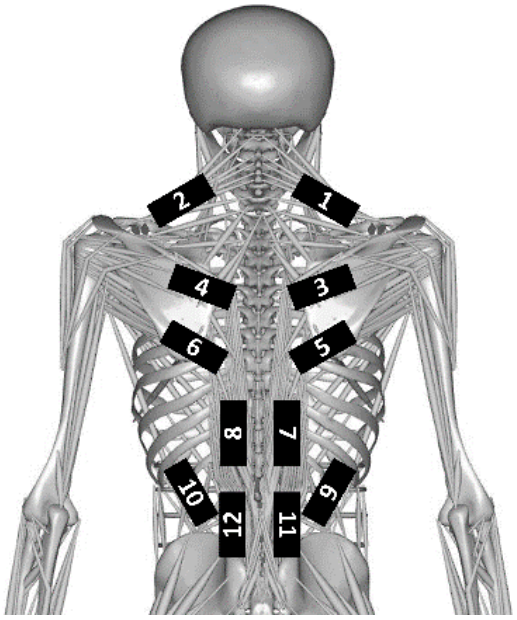


**Figure 2.2:** EMG Sensor ID and located muscle group on the back. Even numbers are on the left side starting at the top.

Treatment of all sensor locations with alcohol reduced effects caused by oily skin, and if necessary, local shaving was performed. The sampling rate of the recorded EMG signals was 1111 Hz and was bandpass filtered with a cutoff frequency of 20 Hz and 450 Hz. This setup corresponds to that of De Luca et al. (Luca, 1997).

Three different stressors were applied during the experiment. Their selection met the following criteria: They simulate demands that occur during a typical workday and can be divided into two groups: emotional and cognitive. Under laboratory conditions, all of these stressors exert psychological stress. Their individual effects have been investigated and validated in several studies (Reinhardt et al., 2012). Emotional stress (EMS) is expected to elicit a lower musculoskeletal response. Therefore, two stressors from this category were applied in the experiment. A cognitive stressor was used to simulate a high workload typical of the workplace. The procedure itself followed the Mannheim Multicomponent Stress Test (MMST) (Kolotylova et al., 2010), and the EMS consisted of a standardized anger-inducing movie clip (EMS movie) (Gross and Levenson, 1995) and the recall of a personally relevant

anger situation (EMS recall) (Coan and Allen, 2007). The paced auditory serial addition task (PASAT)(Lejuez et al., 2003) was used to model COS. The efficacy of the stressors was assessed with questionnaires. A two-dimensional affect grid (Russel et al., 1989) monitored both EMS. The subject placed a mark on a 9x9 grid to indicate their current mood before and after emotional arousal. The grid axes represent happiness - displeasure and arousal - sleepiness. Both axes range from one (not at all) to nine (extremely). The National Aeronautics and Space Administration Task Load Index (NASA- TLX) (Hart and Staveland, 1988) assessed the COS. It includes six subscales: mental strain, physical strain, time strain, overall performance, frustration, and effort. Workload itself is calculated by averaging the six subscales.

**Figure 2.3:** Participants were seated on a standard office chair. Knee and thorax flexion of approx. 90 degrees. The palms are facing upwards resting on the lap.

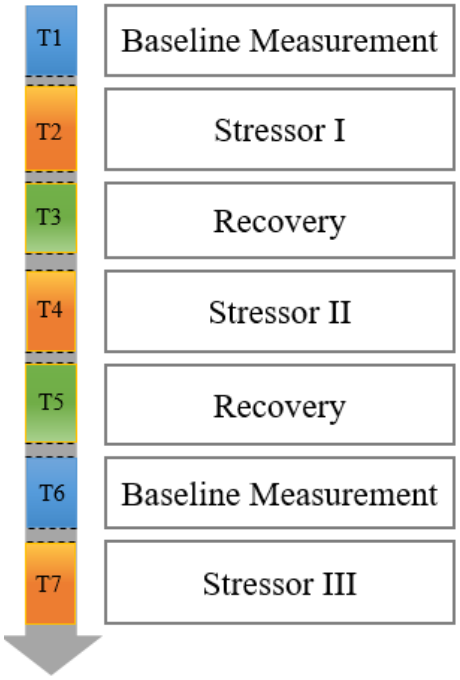


**Figure 2.4:** Experimental workflow T1–T7 mark the individual experimental sections. Stressors I–III represent the three stressors (COS, EMS (movie), EMS (recall)) in a randomized order.

To avoid bias in the data due to the order of the stressors, they were applied in a random order. Before each measurement, the subject was instructed to assume and maintain the upright position statically. A 120-second baseline measurement preceded the first and third stressors, followed by a 120-second relaxation period. These measurements were used for normalization and as a baseline for data processing. During the relaxation phase, the subject was able to use the backrest by leaning backward and otherwise maintaining the prescribed posture. The COS lasted 120 seconds and EMS (movie) 150 seconds, while the EMS (recall) lasted 90 seconds (Figure 2.4). The shorter time reflects the inability to maintain the recall for a longer period of time. After each load, the subject completed the questionnaires to assess the effectiveness of the stressor.

An RMS filter with a 500 millisecond non-overlapping sliding window processed all 12 EMG signals. These parameters follow Konrad's recommendations for static postures or slow movements (Konrad, 2005). Next, this subject-specific EMG signal was averaged and represents the mean muscle activation level for the specific trial or baseline measurement. In the following step, each EMG channel was normalized to the corresponding channel of the second baseline measurement. The second measurement was selected because this data contains changes in muscle activity due to tension or even possible fatigue. This normalization process yields the relative change in muscle activation due to the particular stressor at a subject-specific level. Taking the individual muscle changes and averaging them across all subjects yields the average stress response for the individual back muscle as well as the overall change in recruitment. This information is used to determine the effects on the spinal disc using musculoskeletal models.

COS is known to affect postural control in humans. Typically, these studies take place while the subject is standing on a device that measures the center of pressure like a force plate. Despite the difference in setup, an evaluation of the movement in this experiment provides information about any changes in controllability. This is necessary because the motion also generates muscle activity and thus affects the resulting lumbar disc forces. Motion was recorded using a VICON motion capture system with six cameras at a sampling rate of 200Hz. To monitor trunk motion, four markers were placed on the chair seat shell and one marker was placed at the level of the C7 disc. To apply the data to musculoskeletal models, the motion capture data is post-processed (Vicon Nexus 2.6.1). In a first step, the marker trajectory was

reconstructed following manual marker labeling. If gaps were present in the trajectory, they were reconstructed using rigid body gap filling for the seat pan marker, and spline interpolation was applied to the C7 marker data. In both cases, the maximum gap length allowed was less than 500 frames. The process ended with the export of c3d files. Basic kinematic properties are derived from these data. In a second step, a musculoskeletal model will be developed to investigate whether thoracic motion has a significant effect on the lumbar spine.

Cognitive stress is known to affect postural control. As the movement is observed, it contributes to any muscle activity recorded during the various experimental trials. First, the raw kinematic data is examined and later this information is used to identify if this motion contributes significantly to the disc stresses or if it can be neglected. Viewing the trajectory as a point distribution helps to examine the overall change in thoracic motion. The center of the point cloud provides a reference point for the motion (2.1). After moving the center to the origin (2.2), the coordinate axis divides the data into its medio-lateral (ML), anterior-posterior (AP), and cranial-caudal (CC) components. In addition to the mean, minimum (2.3), and maximum (2.4) value, the 95$^{th}$ percentile (2.5) magnitude of deflection was also determined to provide insight into the subject's range of motion.

$$COM_{Axis} = \frac{1}{N}\sum_{i=1}^{N} x_i^{Axis} \tag{2.1}$$

$$x_i^{Axis} = x_i^{Axis} - COM_{Axis} \tag{2.2}$$

$$x_{min}^{Axis} = \arg\min(x_i^{Axis}) \tag{2.3}$$

$$x_{max}^{Axis} = \arg\max(x_i^{Axis}) \tag{2.4}$$

$$x_{95\%}^{Axis} = (x_{(N*95\%)}^{Axis}) \tag{2.5}$$

with:

N: Number of points in trajectory

I: 1... Number of points N

Axis: Spatial x, y, z axis

The second and third derivatives of the trajectory give information about the acceleration (2.6) as well as jerk (2.7), which occur during the movement. For evaluation, the Euclidean norm of all three components is used in combination with the mean value as well as the RMS.

The jerk analysis is performed using the mean square jerk (MSJ) (2.8) and log dimensional jerk (LDLJ)(2.10) defined by Hogan et al. (Hogan, 1982, 1984; Hogan and Sternad, 2007, 2009).

$$Acc = \frac{dVel}{dt} \tag{2.6}$$

$$Jerk = \frac{dAcc}{dt} \tag{2.7}$$

*with:*

*Vel: Velocity*

*Acc: Acceleration*

$$MSJ = \frac{1}{t_2 - t_1} \int_{t_1}^{t_2} \frac{1}{2} \left| \frac{d^3 y}{dt^3} \right|^2 dt \tag{2.8}$$

*with:*

*MSJ: Mean squared jerk*

$$DLJ = -\frac{(t_2 - t_1)^5}{v_{peak}^2} \int_{t_1}^{t_2} \left| \frac{d^2 v(t)}{dt^2} \right|^2 dt \tag{2.9}$$

$$LDLJ = -\ln(|DLJ|) \tag{2.10}$$

*with:*

*DLJ: dimensional jerk*

*LDLJ: log dimensional jerk*

Typically, both methods help in assessing the progress of healing or disease progression after neurological conditions such as Parkinson's disease or stroke. They affect motor control abilities like mental stress and are therefore used in these studies to assess their use and differences between stressors.

As described in chapter 1.7, musculoskeletal simulation models are a well-established tool to determine non-measurable loads on internal human structures. In this work, the simulation software AnyBody Modeling SystemTM version 7.1 from Anybody Technology A/S was used. An algorithm with several steps was developed to calculate the musculoskeletal loading response. In the first step, the experimental setup was modeled in the simulation environment (Figure 2.6). Since no motion data were used, this results in a static, seated, whole-body model that includes frictional forces in the pelvis, thigh, and foot. The arms are oriented to replicate reality. The muscle activation determined during the stress trial , normalized with the baseline measurement, represents a response factor (RF) for the measured muscle group. Since we are interested in the general loading distribution, we do not simulate each individual, but rather the mean loading response across all participants. To obtain a more general prediction, the model configuration represents a European male of the 50th percentile with a weight of 75 kg and a height of 180 cm. As a first step, it is necessary to generate computational baseline data for the seating position. The simulation run performed determines the relaxed muscle activity (RMA) for each muscle and the joint forces to maintain this standard sitting position. From this, the muscle activity can be extracted and multiplied by the RF of the corresponding muscle group. This value generates a muscle activity boundary condition (MAB) (2.11) and extends the existing non-negative MA requirement (2.12) with a static MA condition ((2.13) (Figure 2.5).

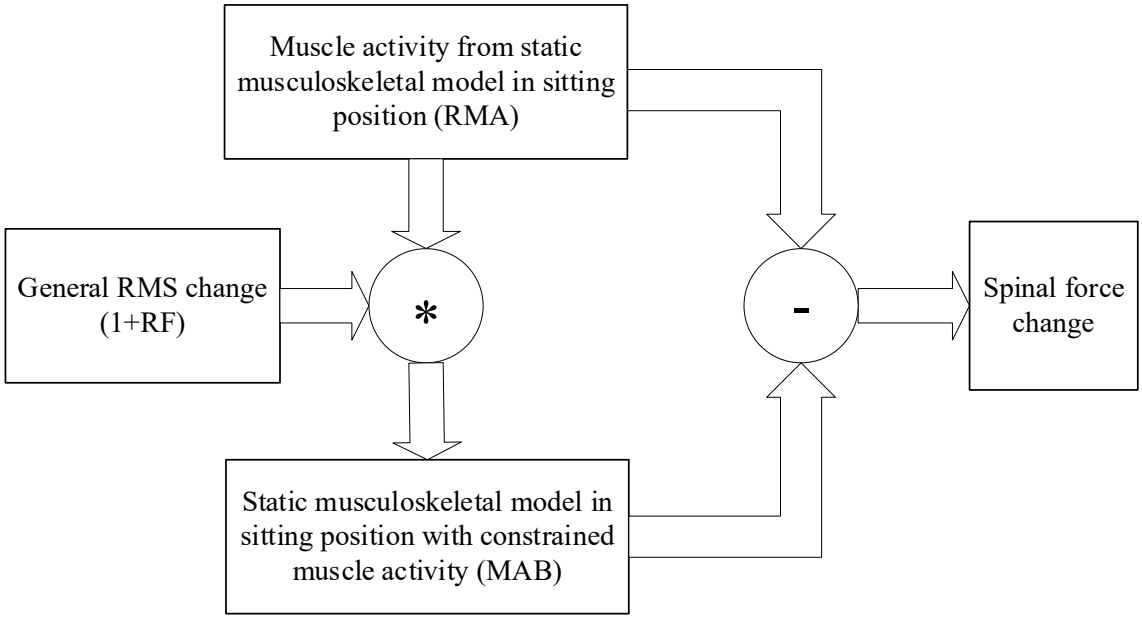


**Figure 2.5:** Workflow of EMG data applied to inverse kinematic simulation model. A baseline computation (RMA) provides the factor multiplied with the measured muscle activity resulting in muscle boundaries (MAB).

$$\mathrm{MAB_j} = \mathrm{RMA_j} * (1 + \mathrm{RF_j}) \tag{2.11}$$

with:

$\mathrm{MAB_j}$: Stress model muscle activation
$\mathrm{RMA_j}$: Relax model muscle activation
$\mathrm{RF_j}$ : Stress trial response factor

$$MA_i^{(M)} \geq 0, i \in [1 \dots m^{(M)}] \tag{2.12}$$

$$MA_j^{(M)} = MAB_j, \qquad j \in [(m+1)^{(M)} \dots n^{(M)}] \tag{2.13}$$

with:

$MA_i^{(M)}$ : Muscle activity boundary of muscles **not** measured during the experiment
$MA_j^{(M)}$ : Muscle activity boundary of muscle measured during experiment
$\mathrm{MAB_j}$ : Stress model muscle activation

This setting represents the mean condition during the respective stress trial. Rerunning the model with the new conditions outputs the joint reaction forces caused by the respective stressor. The modeling system optimizer readjusts the unstressed muscles to maintain equilibrium in the modeled static seated position.

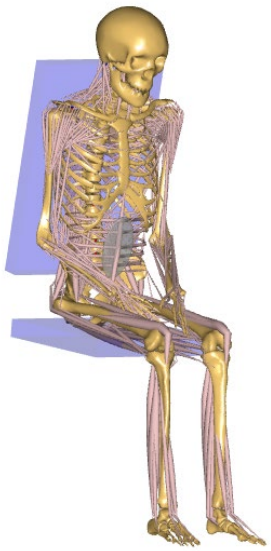

**Figure 2.6:** Illustration of the full body sitting musculoskeletal model used to simulate the spinal disc loads.

Since upper body motion can result in higher core muscle activity, a separate simulation model is developed to determine if the changes in motion due to mental loading are significant. The resulting spinal loads will be used as a characteristic value. It is expected that COS will produce significantly higher muscle activity that is the result of either the movement or the underlying CNS response. To clarify if this is the case, a reduced musculoskeletal model was created and used. Results from motion during baseline, COS, and stress-induced muscle recruitment will be compared. The changes in recruitment are applied as above. This approach provides a numerically stable simulation model with high time resolution.

The model itself is stationary according to the marker placement on the seat pan in the pelvic region. A marker at vertebra C7 initiates the thoracic movement (Figure 2.7). Since the change in thoracic motion only affects the lumbar muscles, both the arms and legs are turned off. All missing limb weights are replaced at the correct thoracic positions. This resulted in a high-resolution calculation at 200 Hz to account for even small changes in motion and load.

**Figure 2.7:** Illustration of the reduced motion capture model to simulate high-resolution motion data.

In addition to using descriptive statistics, the results are analyzed using a paired Student's t-test and a significance level of 0.05. Furthermore, the stressors in chapter two and their effects were tested using an analysis of variance (ANOVA) with a significance level of 0.05. Differences between group means were determined using Tukey multiple comparisons.

## 2.3. Results

Before stress induction, subjects showed positive mood and low arousal level. All stressors increased the participants' subjective stress level (Table 2.3). After affect induction (EMS) both dimensions of the affect grid changed significantly ($p < 0.001$) compared to baseline. The emotional stressors decreased the valence dimension and increased the arousal dimension. The NASA-TLX evaluation revealed a workload of 61 ± 12 for COS, indicating a high level of mental arousal. Scores above 46.0 can be interpreted as an above average workload (SAGE, 2015).

| Stressor | Mean (SD) valence | Mean (SD) arousal |
|---|---|---|
| EMS(movie) | 3.62 (1.63) *** | -2.18 (2.15) *** |
| EMS(recall) | 2.65 (1.69) *** | -2.47 (2.03 *** |

**Table 2.3:** Affect grid values of both emotional stressor for valence as well as for arousal ( $P < 0.05$*, $P < 0.01$**, $P < 0.001$***)

Table 2.4 shows the results of the range of motion (ROM) analysis for each stressor and the baseline trial. Significant changes ($P < 0.05$) are observed in the anterior-posterior direction during the COS. The CC 95$^{th}$ percentile values show that subjects remain nearly constant with a similar standard deviation during EMS. While during the COS, both the range and the deviation increase. Cranial-Caudal motion shows the greatest change between baseline and stressors. Here, motion is nearly constant with a mean of 2.5 mm during EMS (imagine) and a maximum during COS of 5.73 mm. In CC direction, COS causes less subject sway in contrast to ML. For EMS, the result is not clear because larger and smaller fluctuations occur. In the direction of AP, a reduction in size can generally be seen.

| C7 ROM | Baseline Mean (SD) | EMS(movie) Mean (SD) | EMS(imagine) Mean (SD) | COS Mean (SD) |
|---|---|---|---|---|
| ML ROM [mm] 95$^{th}$ percentile | 10.53(9.49) | 10.42(8.32) | 10.51(7.95) | 15.99(17.49) |
| ML ROM [mm] | 19.33(19.44) | 20.68(15.97) | 16.96(10.07) | 28.39(30.21) |
| AP ROM [mm] 95$^{th}$ percentile | 25.96(57.58) | 16.97(34.66) | 10.8(14.19) | 23.7(37.21)* |
| AP ROM [mm] | 36.17(65.5) | 29.05(43.57) | 22.09(23.02) | 33.76(49.95) |
| CC ROM [mm] 95$^{th}$ percentile | 29.77(138.87) | 4.55(6.27) | 2.5(1.83) | 5.73(7.29) |
| CC ROM [mm] | 50.66(205.88) | 8.47(12.46) | 4.43(3.69)* | 8.89(10.46) |

**Table 2.4:** Thorax ROM measured with marker C7. ( $P < 0.05$*, $P < 0.01$**, $P < 0.001$***)

The kinetic analysis (Table 2.5) shows a significant change ($P < 0.01$) in the motion parameters during COS. In the case of EMS all values drop with the greatest magnitude at the jerk root mean square from 27.12 $m/s^{-3}$ down to 1,86 $m/s^{-3}$. During COS, the mean acceleration on one side decreases while the RMS increases. The jerk halves for the average of the RMS value and decreases by more than 23 $m/s^3$.

| Value | Baseline Mean (SD) | EMS(movie) Mean (SD) | EMS(imagine) Mean (SD) | COS Mean (SD) |
|---|---|---|---|---|
| ACC mean [$m/s^2$] | 0.12(0.41) | 0.04(0.02) | 0.04(0.02) | 0.07(0.03) *** |
| ACC RMS [$m/s^2$] | 0.8(3.61) | 0.07(0.05) | 0.06(0.03) | 0.11(0.08)** |
| Jerk mean [$m/s^3$] | 4.09(14.46) | 1.3(0.76) | 1.26(0.64) | 2.05(1.14)** |
| Jerk RMS [$m/s^3$] | 27.12(122.56) | 2.11(1.73) | 1.86(1.13) | 3.21(2.4)** |

**Table 2.5:** Thorax acceleration and jerk measured with motion capture. Significate changes are found during COS. EMS shows no significant difference compared with the baseline ( $P < 0.05$*, $P < 0.01$**, $P < 0.001$***)

Table 2.6 shows parameters of motion smoothness that are commonly used in neuro-rehabilitation to evaluate the recovery process after a condition such as stroke. In general, these parameters assess the motion smoothness and thus the postural control of the subject. For both parameters, statistics indicate a significant change during COS. EMS (imagine) show a mixed picture as the LDLJ significantly ($P < 0.01$) increases from -27.34 to -26.27 (Figure 2.8) and the MSJ value does not significantly decrease. The EMS (movie) trial shows no significance despite the drop in value in both cases.

| Value | Baseline Mean (SD) | EMS(movie) Mean (SD) | EMS(imagine) Mean (SD) | COS Mean (SD) |
|---|---|---|---|---|
| MSJ | $1.6e^6(8.1e^6)$ | 744,15(1410,69) | 474,73(516,23) | 1606,79(2730,08)** |
| LDLJ | -27,34(1,81) | -26,73(3,86) | -26,27(1,31)** | -28,34(3,03)** |

**Table 2.6:** Smoothness parameter mean Squared Jerk (MSJ) and log dimensional jerk (LDLJ) show both a significant difference for COS. EMS does not cause a distinct effect. Only LDLJ is different for the imagine task. ( $P < 0.05$*, $P < 0.01$**, $P < 0.001$***)

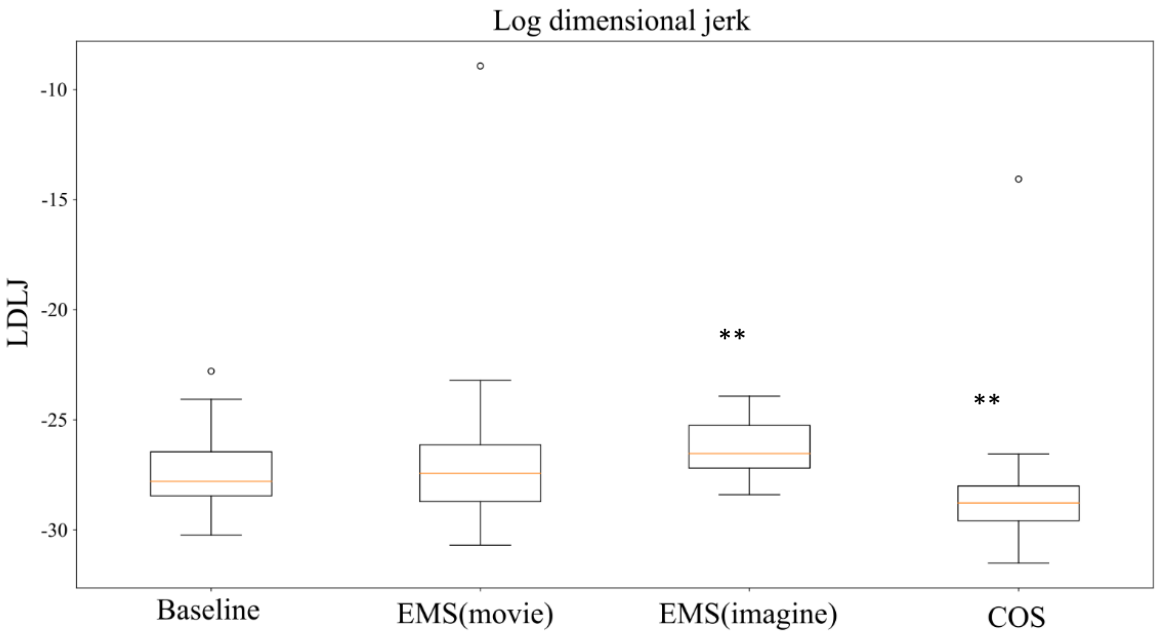


**Figure 2.8:** Box plot depicts the LDLJ parameter. Significant differences for COS and EMS (imagine) are found when compared to the baseline data. ( $P < 0.05$*, $P < 0.01$**, $P < 0.001$***)

All stressors resulted in a more pronounced activation level in the trapezius region. Cognitive stress resulted in higher muscle activation compared to emotional stressors with a mean increase of 137% ($p < 0.05$) and a peak increase of 596% ($95^{th}$ percentile) for the trapezius region. A significant difference ($P < 0.01$) between COS and EMS (movie) is found in the right trapezius ascending ($p < 0.01$). In addition, a significantly different pattern for emotional and cognitive stressors was found in the lumbar region with higher activation for COS. The right erector spinae longissimus was more activated compared to the left side ($p < 0.01$). Furthermore, the left ($p < 0.001$) and right erector spinae iliocostalis ($p < 0.001$) showed a significant difference to both EMS.

| EMG ID | COS Mean (SD) | EMS(movie) Mean (SD) | EMS(imagine) Mean (SD) | EMS 95th percentile | COS 95th percentile |
|---|---|---|---|---|---|
| 1 | 137.37(246.81) | 33.44(138.35)** | 43.89(137.04)* | 310.40 | 595.59 |
| 2 | 43.32(83.82) | 25.22(72) | 43.44(118.72) | 300.15 | 216.98 |
| 3 | 16.2(29.34) | 9.36(56.16) | 8.13(23.84) | 39.52 | 72.72 |
| 4 | 13.07(29.86) | 4.32(14.35) | 5.73(13.3) | 34.74 | 49.5 |
| 5 | 32.91(56.92) | 6.91(30.31)* | 25.52(95.89) | 100.32 | 108.14 |
| 6 | 43.59(74.65) | 4.77(17.38)** | 18.94(46.47)* | 117.14 | 192.35 |
| 7 | 17.75(38.75) | 0.81(19.46)** | -3.29(17.85)*** | 24.96 | 67.47 |
| 8 | 26.93(40.36) | 6.6(32.49)** | 7.99(41.64)* | 56.29 | 100.14 |
| 9 | 24.35(39.1) | 3.7(9.85)** | 3.02(8.31)** | 18.81 | 100.98 |
| 10 | 21.97(29.89) | 2.56(7.3)*** | 4.2(12.74)*** | 33.47 | 76.6 |
| 11 | 9.7(22.13) | 6.51(23.22) | 0.66(12.7) | 56.88 | 43.93 |
| 12 | 6.96(31.68) | 7.13(26.71) | 2.37(21.8) | 48.28 | 70.51 |

**Table 2.7:** Relative mean changes and standard deviation in comparison to baseline for EMG muscle activation for all sensor locations. Stars represent Tukey comparison significance between EMS Movie-COS and EMS Recall-COS ( $P < 0.05$*, $P < 0.01$**, $P < 0.001$***)

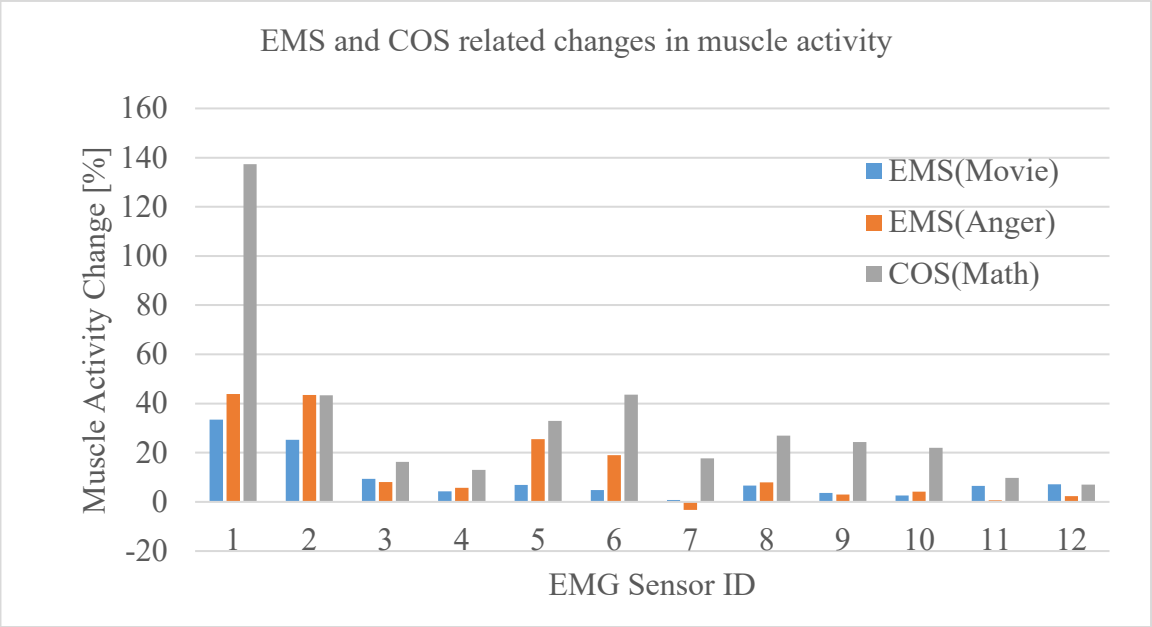


**Figure 2.9:** Change in muscle activity in the shoulder region is highest for COS in the right m. trapezius pars descendens. In general, EMS is affecting the upper back, whereas the lower back is effect by COS as well.

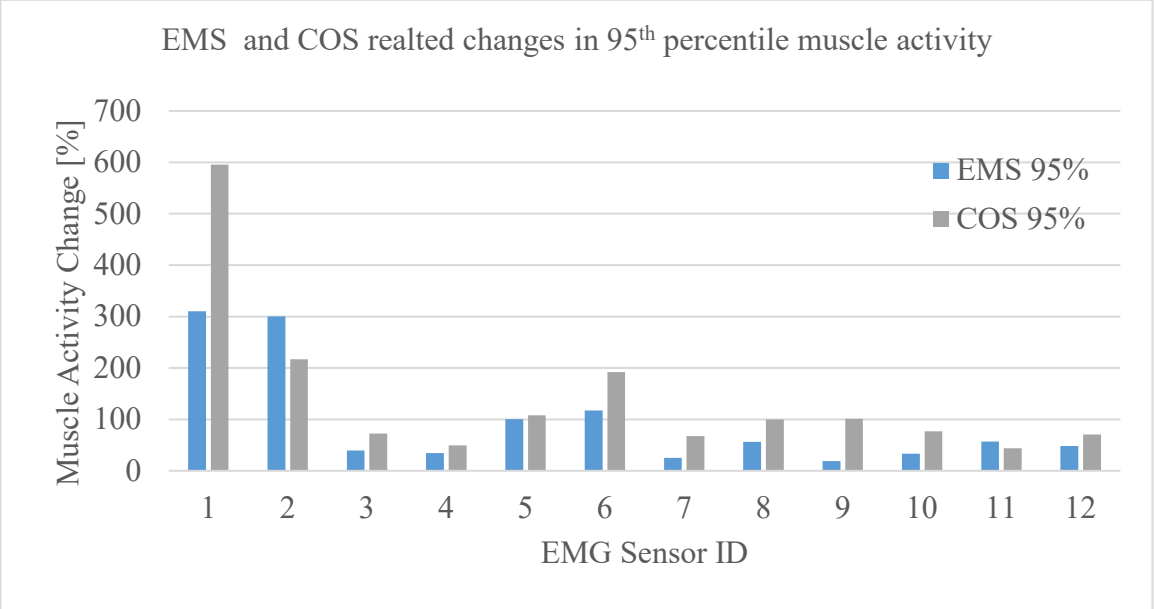


**Figure 2.10:** Peak increases are displayed using the 95th percentile. Muscle m. trapezius pars descendens is responding with more than 300% in the upper back. In the lower back m. erector spinae pars longissimus and m. erector spinae pars iliocostalis react the most but asymmetrical.

The standard sitting position without load results in a compression force in the cranial-caudal direction (CC) with a value of 143 N (disc level C7T1) at the cervical and 618 N (disk level L4L5) at the lumbar spine.

COS mean force increases in the lower cervical spine level by up to 189 N. Emotional stressors led to lower mean values of 31 N maximum. Detailed information on the force changes is presented in Table 2.8. Analysis of changes in peak (95th percentile) muscle activity revealed more dramatic force changes with an increase of up to 907 N at the C7T1 level. While only small changes were found in the medial-lateral (ML) direction, moderate force changes in anterior-posterior shear (AP) were observed from the standard sitting load (C7T1 10N; L4L5 68N). Mean force increases of up to 29 N in the lower lumbar levels under COS and peak muscle activation cause a force increase by around 100 N at the lower cervical and lower lumbar spine levels for anterior-posterior shear.

| Disc level | EMS(movie) [N] | | EMS(imagine) [N] | | COS [N] | | EMS 95th percentile [N] | | COS 95th percentile [N] | |
|---|---|---|---|---|---|---|---|---|---|---|
| | AP | CC | AP | CC | AP | CC | AP | CC | AP | CC |
| Cervical spine | | | | | | | | | | |
| C1C0 | -3 | 10 | -4 | 12 | -18 | 95 | -28 | 101 | -82 | 455 |
| C2C1 | -3 | 12 | -4 | 15 | -19 | 101 | -31 | 117 | -86 | 483 |
| C3C2 | -4 | 14 | -5 | 17 | -18 | 115 | -35 | 133 | -82 | 542 |
| C4C3 | -4 | 17 | -6 | 19 | -16 | 139 | -40 | 154 | -75 | 644 |
| C5C4 | -3 | 15 | -4 | 18 | -8 | 137 | -30 | 157 | -41 | 657 |
| C6C5 | -3 | 17 | -5 | 20 | -2 | 145 | -27 | 170 | -21 | 702 |
| C7C6 | -2 | 20 | -4 | 25 | 3 | 162 | -20 | 203 | 13 | 786 |
| C7T1 | -1 | 25 | -2 | 31 | 7 | 189 | -13 | 249 | -103 | 907 |
| Lumbar spine | | | | | | | | | | |
| T12L1 | -4 | 22 | -4 | 20 | -26 | 109 | -62 | 218 | 38 | 483 |
| L1L2 | -2 | 19 | -4 | 22 | -18 | 103 | -51 | 238 | -49 | 487 |
| L2L3 | -1 | 22 | -2 | 24 | -9 | 112 | -26 | 243 | -7 | 484 |
| L3L4 | 0 | 26 | -1 | 20 | -3 | 128 | 1 | 247 | 64 | 473 |
| L4L5 | 2 | 25 | 3 | 20 | 21 | 136 | 26 | 249 | 93 | 485 |
| L5Sacrum | 3 | 28 | 4 | 21 | 29 | 139 | 35 | 269 | 97 | 508 |

**Table 2.8:** Force changes in anterior-posterior (AP) and cranial-caudal (CC) direction for mean and 95th percentile muscle activation.

Figure **2.11** visualizes the trends for the spinal disc forces.

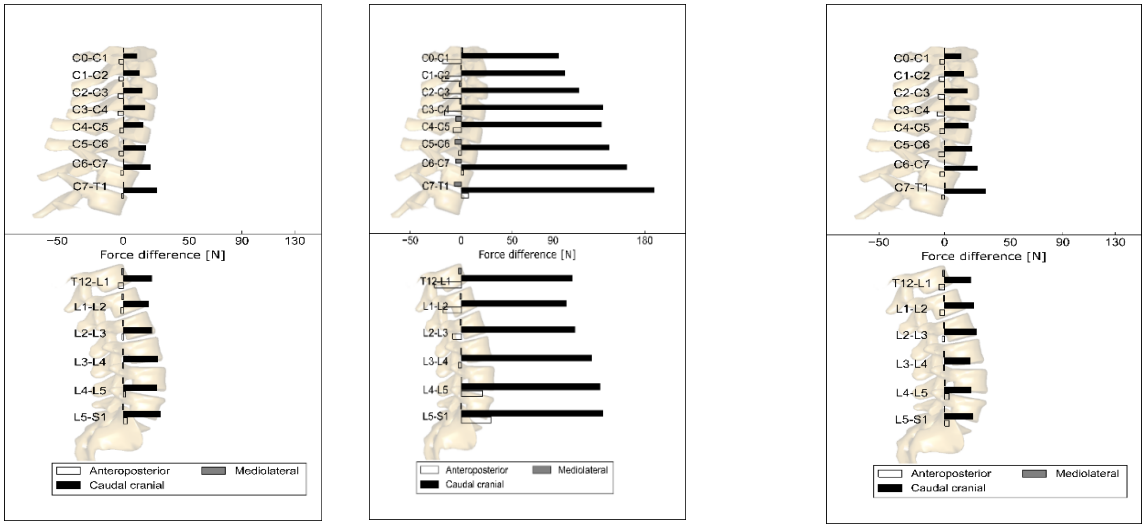


a) EMS(Movie) b) COS c) EMS(Recall)

**Figure 2.11:** Changes in spinal disc forces due to different stressors. a) EMS (movie), b) COS, c) EMS (recall). COS has the greatest influence with 189 at the cervical spine and 139 N at the lumbar spine in cranial-caudal direction.

Figure 2.12 depicts the simulation results of the L4L5 compression load. There is no significant difference between the models when only thoracic motion is considered. However, when the results of the kinematic model are compared with the models that include stress muscle activation, the loads are significantly different ($P < 0.01$). This pattern is seen across almost all disc loads for CC and AP except L4L5 downwards (Table 2.9).

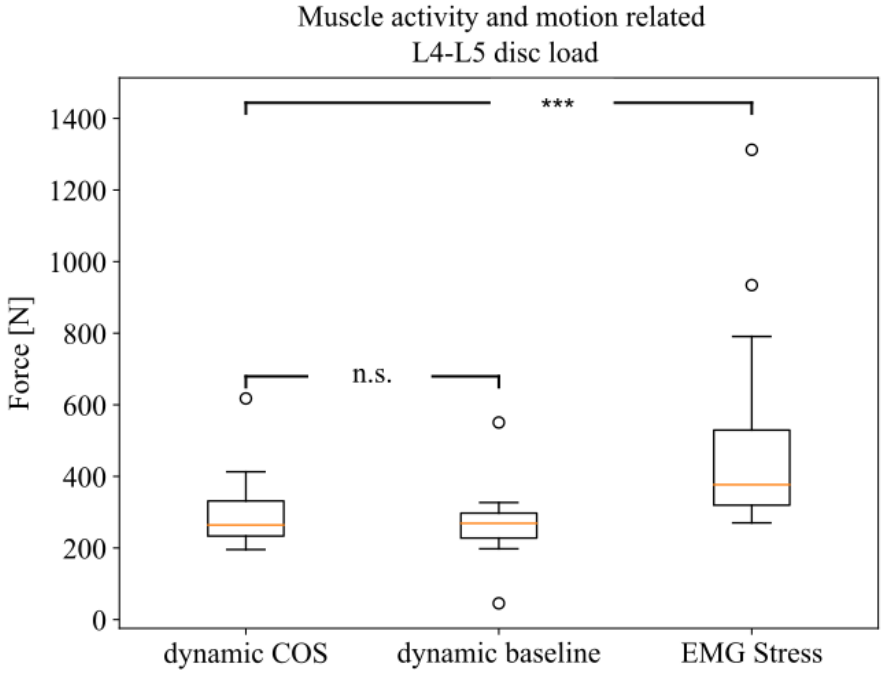


**Figure 2.12:** EMG stress data is significantly increasing the L4L5 CC disc load in comparison with the load resulting from motion. There is no significant influence caused by motion when compared to the baseline motion data. ( $P < 0.05$*, $P < 0.01$**, $P < 0.001$***)

| Disc Level | | EMG COS Mean (SD) [N] | Dynamic baseline Mean (SD) [N] | Dynamic COS Mean (SD) [N] |
|---|---|---|---|---|
| T12L1 | CC | 368.61(114.19)*** | 269.02(81.24) | 251.16(74.69) |
| | AP | -107.04(45.86)*** | -59.65(16.91) | -55.65(16.35) |
| | ML | 2.3(5.3) | 0.42(1.13) | 0.22(1.26) |
| L1L2 | CC | 377.02(121.01)*** | 273.59(86.37) | 254.93(78.12) |
| | AP | -89.03(42.52)*** | -48.4(14.31) | -44.91(13.23) |
| | ML | 3(5.16)** | 0.36(0.75) | 0.2(0.87) |
| L2L3 | CC | 367.79(132.5)** | 268.41(83) | 249.77(74.8) |
| | AP | -54.74(36.79)*** | -24.33(9.76) | -21.74(8.14) |
| | ML | 3.51(6.46)** | 0.21(0.44) | 0.09(0.5) |
| L3L4 | CC | 382.7(150.06)** | 273.06(86.89) | 253.99(77.34) |
| | AP | -28.86(23.35)*** | -9.27(6.16) | -8.41(6.13) |
| | ML | 0.08(3.98) | -0.16(0.42) | -0.15(0.35) |
| L4L5 | CC | 457.57(226.88)*** | 288.15(85.63) | 268.17(77.43) |
| | AP | 15.68(13.5) | 21.29(11.81) | 19.64(10.03) |
| | ML | 0.69(2.33) | -0.01(0.16) | 0.03(0.12) |
| L5Sacrum | CC | 571.58(334.08)*** | 318.49(82.8) | 297.68(78.52) |
| | AP | 37.69(12.56) | 32.7(10.64) | 30.28(9.38) |
| | ML | -0.13(0.98) | -0.13(0.44) | -0.03(0.44) |

**Table 2.9:** Overview of directional loads in disc levels caused by motion during COS and Baseline. EMG COS shows disc forces caused by changes in muscle recruitment. ( $P < 0.05$*, $P < 0.01$**, $P < 0.001$***)

## 2.4. Discussion

This study focused on examining hypothesis one, how emotional and cognitive stressors cause changes in back muscle recruitment. Furthermore, the resulting spinal loading for both cases was determined using musculoskeletal simulation. To investigate the effects on the subjects' movement, kinematics-related parameters were evaluated to answer hypothesis two.

Kinematic analysis of the thorax range of motion, show almost no significant differences between stress and baseline. These results are in agreement with other studies that also found no significant difference in postural sway during short-term memory tasks (Andersson et al., 2002; Riley et al., 2003). This seems to support their findings, in an increased resource level

during a dual-task situation and the accompanying arousal. Nevertheless, postural control may vary not only the range of motion or postural sway, but also other kinematic properties. Therefore, acceleration and jerk of the upper body were analyzed. Both emotional stressors did not significantly alter these properties, in contrast to COS. While the mean acceleration with its smaller value indicates smoother kinematics. Their RMS value increases and favors a significantly rougher trajectory. Despite the contradiction, when jerk is considered as a measure, both the mean and RMS values decrease, leading to smoother kinematics. Whether this is the result of limitations in the cognitive control, as suggested by resource theories (Wickens, 1991) or due to the rather young participants in this study, as suggested by the literature review by Ruffieux et.al. (Ruffieux et al., 2015) should be the subject of a separate study.

Not only dual-task research is devoted to motion smoothness, but also neuro-rehabilitation is devoted to these properties as a measure of various diseases such as Parkinson's disease or stroke recovery (Balasubramanian et al., 2015). In particular, the dimensionless and mean square jerk provides information about the patient's motion smoothness and condition. In this study, this parameter is used to determine which stressor may be contributing to changes in kinematics, leading to kinetic changes that affect muscle recruitment. Like the other parameters, mean squared jerk and LDLJ indicate a potential difference during cognitive stress. Based on the results of Balasubramanian et.al (Balasubramanian et al., 2012), the LDLJ may not be as stable as the mean squared jerk, so only COS will be analyzed if movement changes can significantly contribute, since in this case both properties show a difference.

With the help of inverse kinematic analysis, the responsibility of motion for a higher muscle activity could be declined. Even though the consideration of postural sway can only result from providing the computational result by speech (Dault et al., 2003; Taylor et al., 2015) or when the subject moves only above the lumbar spine, the results show no significant contribution. The conclusion can be drawn as both cases are modeled to increase lumbar spine muscle activity and contribute more load as a worst case scenario. On the other hand, stress-induced recruitment changes lead to significantly higher load on the intervertebral discs.

Emotional stressors appear to primarily increase the muscle activation in the cervical spine/ trapezius region, while cognitive stress also alters the biomechanical situation in the lumbar

region. Studies in literature did use a different setup by including work task-related kinematic changes but the data can be used to classify the results. Davis et al. (Davis et al., 2002b) analyzed lumbar spine compression load as influenced by serial mental processing and a physical loading with a defined lifting task. Their study resulted in a peak force increase between 70 N and 410 N. The results show similar results with a mean load of 139 N and a peak load increase of 508 N. In the current study, influences of the subjects' altered kinematics, training status, and coordinative abilities were minimized by a static sitting position setup. For trapezius descendants, the results regarding muscle activity differ from previous studies. We found an asymmetric activity increase with a dominant right-handed side for COS whereas Lundberg et al. (Lundberg et al., 2002) found an average increase between 9.4% and 51.6% during mental arithmetic. Regarding the left side, we are in a similar range to these findings (43%) while the right side is more affected in the study. This result may be due to a large number of right-handed subjects in the group with only three left-handed participants. Nevertheless, subject-specific muscle activation patterns should be the focus of further studies. Asymmetric load changes may have a significant impact on the musculoskeletal system with respect to force distribution in the thorax.

Emotional stressors resulted in a more symmetrical muscular response with a comparable magnitude (33 % EMS (movie); 43 % EMS (recall)) in the trapezius with respect to the findings of Lundberg et al. The cervical compression load increase is moderate at approximately 30 N during EMS. The mean compression load during COS is six times higher with up to 189 N. Peak loads are 249 N during EMS and 907 N during the application of COS. Peak anterior-posterior forces increase up to 103 N when participants were exposed to COS. Literature suggests compression loads of approximately 1200 N during daily activities in the cervical spine and shear loads of one-tenth of this value (Moroney et al., 1988). These loads are brief peak values occurring during head motion, while the increase in force caused by stress persists throughout the duration of the stressful situation. Therefore, the determined increase in force represents a relevant stress-induced load contribution to the spine. Prolonged sitting is a dominant human working position (Putzer) position associated with static loads that lead to loss of disc height, disc degeneration, spinal stiffness, and low back pain (Pape et al., 2018). An increase in static load due to psychological stress could accelerate and amplify these outcomes.

These results suggest that EMS affects only the cervical spine, but COS affects the entire back. To examine different reaction patterns on a subject level it is necessary to enlarge the number of participants and group the participants according to their reaction patterns. To evaluate the isolated effect of mental stressors on musculoskeletal loading, we used a combination of experimental and state-of-the-art numerical methods. Stressors were selected to target emotional and cognitive components representing a broad spectrum of mental stress. The experimental conditions were designed for optimal control with a minimized influence of altered loading due to trunk motion. Nevertheless, some subjects might have experienced a small amount of trunk movement in response to the stressor (Woollacott and Shumway-Cook, 2002). As a result, trunk movement could directly lead to an increase in muscle activation and spinal forces in an individual but was excluded for the study group in total. There are other limitations in this study that could potentially affect the results. Much emphasis was placed on proper EMG sensor placement and appropriate skin preparation. The surface EMG signal during static sitting is rather low during both baseline measurement and stressor. Therefore, small changes in the baseline measurement could have affected the result. For this reason, we chose a conservative approach by only looking at mean values and not excluding subjects with no significant difference between the baseline and a given stressor. This approach was intended to reduce the influence of outliers.

We chose a linear transfer function to correlate the simulated muscle activity and EMG measurement. This approach has been evaluated and used in other studies (Dubowsky et al., 2008; Zee et al., 2007). However, the appropriate transfer function depends on muscle size, motor recruitment, and muscle fiber composition (Kuriki et al., 2012). Furthermore, differences between genders have been neglected, as effects by stress seem to be rather equal (Swedish Council on Health Technology Assessment (SBU), 2014 Oct).

## 2.5. Conclusion

In summary, the results presented in this study provide insight into the biomechanical response in the back while sitting under different stressors. Cognitive and emotional stress affect muscle tone differently, supporting hypothesis one. The corresponding increased biomechanical load provides the information to confirm hypothesis two. The workflow presented in this study can be used to investigate the biomechanical influence of stressors under workplace conditions. In particular, cognitive stress contributes to high loading in both the cervical and lumbar spine with up to 189N on average and even higher peak values (907 N). Further studies should be conducted to examine the occurrence of the different stressor types and levels in daily life. This additional insight into the duration of stress exposure and the number of load peaks can help provide further information about how much additional exposure a person is exposed to and its effects.

# 3. Experimental study dynamic to investigate trunk extension flexion

## 3.1. Introduction

The first part of this work aimed to gather basic knowledge about the effect of emotional and cognitive stressors. The absence of motion and external loading demonstrates the isolated effects of these stressors on the cervical and lumbar spine.

Several studies examined how psychological stress alters muscle tension (Chapter 1). However, the recruitment of back muscles involving the upper and lower parts has not been studied in detail. . In addition, the advantages offered by musculoskeletal models have not been used to determine spinal disc loads.. To the author's knowledge, only Davis et al. (Davis et al., 2002a) have used forward dynamic simulation to determine the additional loading on the lumbar spine, but have not included the upper back. The use of this type of model limits the results to an overall conclusion, but does not allow categorization of the findings based on muscle tension or kinetic changes.

In this part, the influence of cognitive stress on changes in muscle recruitment during exercise with an additional moderate load is examined in the context of hypotheses two and three. Thus, the development of an experimental and numerical method provides the necessary tools to study muscle recruitment and load changes during trunk extension and flexion. The use of inverse kinematic simulation helps to distinguish between kinetic and muscle tension effects.

## 3.2. Methods

The present study investigates the stress-induced recruitment of the back muscles using a controlled experimental setup. It controls and measures movement and torque using a dynamometer (CON-TREX® WS; PHYSIOMED AG). The placement and fixation of the subjects was done according to the device specifications. In addition, the thoracic motion of

the subject is limited with a TP 500 adapter (**Fehler! Verweisquelle konnte nicht gefunden werden.**). This device setup has four connection points between the human and the device. Fixation of the subject at the pelvis and below and above the knee provides a stable standing position for the participant. A clamp attached to the shoulder limits trunk movement with a padded strap. The device settings align the center of rotation at the L4L5 vertebral disc level. Padding on all contact points ensures pain-free force transmission. The custom padded shoulder support replaces the original pad. This was necessary to allow access to the m. trapezius transversa.

The anthropometric data were collected after the subjects were informed about the further procedure and the experiment in general. These data included general subject-specific information such as age; weight; height; thoracic length (C7 - sacrum); femoral length (greater trochanter - knee condyles); shaft length (knee condyles - ankle); and device measurements: shoulder pad position; knee pad position; pelvic pad position. The numerical part of this work uses these data for subject-specific modeling.

Forty-one healthy subjects with no history of back pain or mental illness were enrolled in this study. The group included 13 females and 28 male participants. Their mean age was 22.8±2.4 (SD) with a weight of 75±13 kg and a mean height of 178±8 cm. To exclude individuals with an acute mental situation, all subjects were examined by a psychologist. Before the experiment, each participant had to give informed consent regarding possible risks and blinded data processing. The local ethics committee granted ethical approval for this study.

The muscle activities of:

- m. multifidi,
- erector spinae pars longissimus,
- m. erector spinae pars iliocostalis,
- m. tra.pezius ascendens,
- m. trapezius pars transversa
- m. trapezius pars descendens

were measured using TRIGNO IMU EMG sensors. The placement followed the recommendations of Criswell et al. and corresponds to chapter 2.2. A Qantum X 840 amplifier (Hottinger Baldwin Messtechnik GmbH) provided the synchronization between the EMG system and the sampling of the analog outputs of the CON-TREX WS. The data stream provided the current torso angle as well as the torque applied to the device by the subject. The sampling rate of the measurement was 300 Hz.

Normalization of muscle activities measured by EMG is necessary to compare them between subjects and is achieved by MVC measurements. Konrad et. al. (Konrad, 2005) give procedures for limb and trunk position and force directions (Chapter 1.5.3). The supervisor asked each subject to increase the force to the maximum within three seconds and maintain it for five seconds. After a recovery period of 60 seconds, the procedure was repeated. MVC for m. erector spinae pars longissimus, m. erector spinae pars iliocostalis, m. multifidi require the trunk to be pushed backward in the TP500 adapter. The subject in a 12.5-degree flexion position applied maximum torque. All tests involving the trapezius were performed in a seated position with a trunk and knee flexion angle of 90 degrees. The main trapezius pars descendens motion direction elevates the humerus joint. As the subject pushed upward, a pressure plate adjusted at the clavicular prevented any motion. The subject's arm position,

with humeral abduction and elbow flexion of 90 degrees, provides a stable platform for measuring the maximum value for the m. trapezius pars transversa. A static grip at the hand position allows the subject to grasp and pull with maximum muscle force. The m. trapezius pars ascendens was measured in almost the same way as the M. trapezius pars descendens but with a 90 degrees humerus pronation and a downwards pull.

Since the position and controlled trunk extension/flexion movement in a device like the TP500 is unfamiliar, uncontrolled trunk movement may occur during the first use, especially in the movement reversal points. Therefore, all subjects were asked to practice the movement and find a comfortable pace on the device before the experiment began. There was no time limit on the training phase to ensure smooth operation during the baseline and stress trial.

To determine the COS response, a two-phase protocol was developed that included a trunk movement with a top dead center at 5 degrees and a bottom dead center at 30 degrees. All subjects were required to apply 1Nm of torque during flexion and five percent of the MVC value throughout extension. The CON-TREX WS was set to isokinetic mode with the ballistic option enabled to account for device weight. With these device settings, a baseline measurement was first performed, which lasted 120 seconds. The subject was then released from the device to relax for at least five minutes. This procedure was intended to reduce the influence of muscle fatigue and discomfort on the participant's stress response. In the following stress trial, the subject was exposed to the COS for 120 seconds (Figure 3.1). After each trial, the subject had to answer the NASA-TLX stress assessment questionnaire.


**Figure 3.1:** General study workflow. A recovery follows training phase. Afterwards the baseline and COS stressor measurements take place.

To calculate the reference muscle activity, the MVC signal is smoothed by an overlapping 0.5-second sliding window and then the maximum value is determined. This procedure is consistent with the recommendations of Konrad et al. (Konrad, 2005) for static or slow movements. The trial muscle activity is determined with the RMS algorithm (3.1 chapter 1.5.2) using a 50 ms sliding window. Then the reference value is used to normalize each EMG channel accordingly.

Kinetic properties help to detect motion changes due to loss of postural control. Considered are:

| | |
|---|---|
| Angular velocity : | $\omega(t)$ |
| Angular acceleration : | $\frac{d\,\omega(t)}{dt}$ |
| Angular jerk : | $\frac{d^2\,\omega(t)}{dt^2}$ |

as these properties influence the muscle recruitment directly.

To investigate the contribution of mental stress to the disc force, a mean trajectory is calculated. This is achieved by dividing each trial into cycles. A complete cycle is defined by the last zero velocity point in the upper position. This definition is necessary as a turning in the upper position is not instantaneous, but a stop and start process where the trunk motion is generating a tremor due to postural control. This series of upper positions describes cycle times that divide the torque and EMG channels into intervals that represent each cycle. To gain a broader knowledge of how COS affects back muscle recruitment, the movement is divided into four sections. Two sections contain the reversal points and one contains the forward movement and the backward movement. A two-degree offset from the dead centers define the upper and lower sections, while the remaining trajectory describes the forward and backward motion (Figure 3.2). Descriptive statistics calculate various muscular and kinetic properties for each section. Mean muscle activity (MMA) defines changes in muscle recruitment (3.1):

$$MMA_{EMG\ ID} = \frac{\sum_{i=1}^{N} MA_i^{EMG_{ID}}}{N} \tag{3.1}$$

*with:*

*MMA: Mean Muscle Activity*

*MA: Muscle activity*

*N: Number of samples*

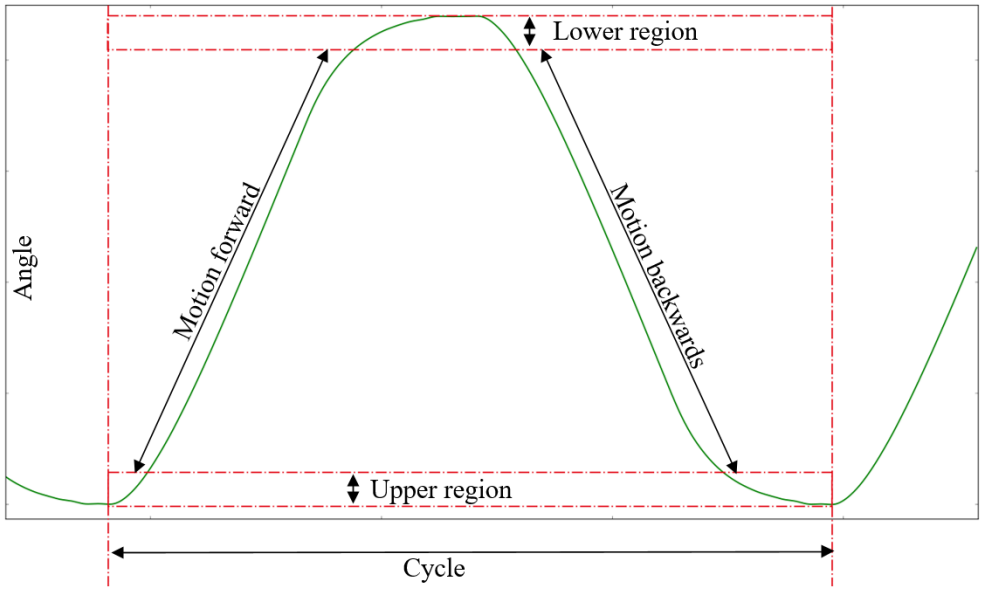


**Figure 3.2:** Green line represents the angle of thorax motion. The motion is split into four parts. The lower and upper region contain the turning points. The backward motion follows the lower region and the forward motion the upper one.

The average duration for completion is calculated from all cycles and mapped linearly to a scale from zero to average duration. This procedure allows the analog signal to be sampled at a rate of 300 Hz, which corresponds to CON-TREX WS recording. After all cycles have been processed in this way, the calculation of one cycle creates an average value at a specific point in time.

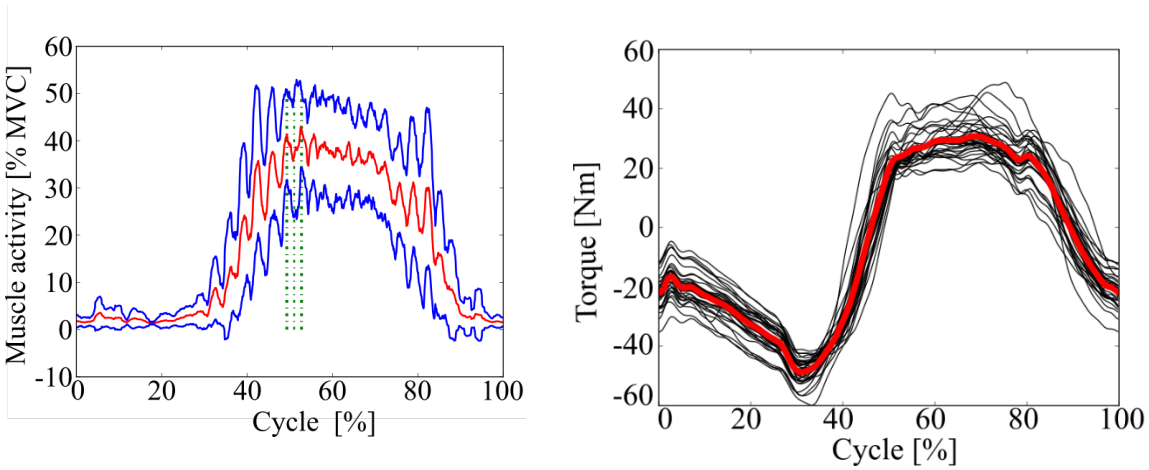


This provides in total one trajectory for motion, torque (**Fehler! Verweisquelle konnte nicht gefunden werden.**), and for each muscle group for both stressed and unstressed

activation (**Fehler! Verweisquelle konnte nicht gefunden werden.**). By normalizing the EMG stress signal with the baseline data for each time step, the resulting response curve can be used in the simulation.

The inverse kinematics software AnyBody Modeling SystemTM (version 7.1 Anybody Technology A/S) is used to determine the biomechanical loads imposed by the COS by simulating muscle recruitment in combination with the movement patterns. The standing model from the AnyBody Managed Model Repository (AMMR) version 2.1.1 was adapted to model the experimental conditions. To simulate the participant in the TP500 adapter, a simulation model is developed that includes connection nodes at the same locations where the adapter is attached to the human body. These include both feet, below and above the knees, and at the pelvis. These contact nodes connect to the global coordinate system with reaction forces and form support and fixation points (Figure 3.3).

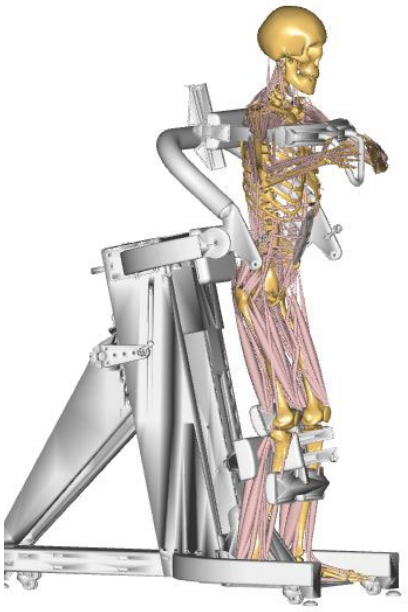

**Figure 3.3:** Simulation model of the experiment. The manikin is placed in a TP500 adapter. The correct power transmission is ensured with reaction forces in the foot, knees, hip and sternum. The measured force is applied at the sternum.

The force measured during the experiment is applied to the sternum. Therefore, a node was created in the model at the same position. At this node, an AnyForce3D element generates the force applied by the machine. Since the trajectory may not be at the same sampling rate as the simulation, the input data is filtered using a B-spline interpolation function.

The predefined AnyKinEqInterPolDriver replaced the standard thorax motion driver to apply the average motion curve for each time step. Again, a B-spline function was used for this interpolation. The generic model was length-mass-fat scaled for the simulation to fit the subject-specific anthropometry. To account for the different fitness levels of the participants, the model was also force-scaled. . To obtain this scaling factor, the thoracic MVC test was simulated. This was done by applying a thoracic flexion of 12.5 degrees and the measured force to the model. Since this test introduces maximum muscle activity into the human body, the thoracic force parameter of the model was set to correspond to 100% muscle activity.

In a multi-stage process, the subject-specific model simulates the mean motion and torque trajectories. In the first run, the baseline data form the basis for calculating the simulated muscle activity without the influence of mental stress . In a second run, this muscle activity is used to generate the muscle activity boundary for each measured muscle group. This is done by deriving a scaling factor from the experimental EMG data for each position in the movement trajectory. As described in chapter 2.2 these constraints are applied to each individual muscle with muscle boundaries. Unlike the static model where there is only one scalar value, the underlying motion requires a function over time to force a specific muscle activity and forms a muscle recruitment model (MRM). The baseline kinetic data provides the additional model input. The third simulation uses the stress-related kinetic trajectories (Figure 3.4). This approach results in a kinetic musculoskeletal model (KMM).

As the experimental muscle activity and kinetic data were not normally distributed, they were examined with a non-parametric Wilcoxon signed-rank test. For the simulated disc loading, Bonferroni-Holm multi comparison was performed. In addition, descriptive statistics is used to describe all variables and presented with mean values as well as standard deviations. The Python 2.7 library scipy formed the basis of all analyses.

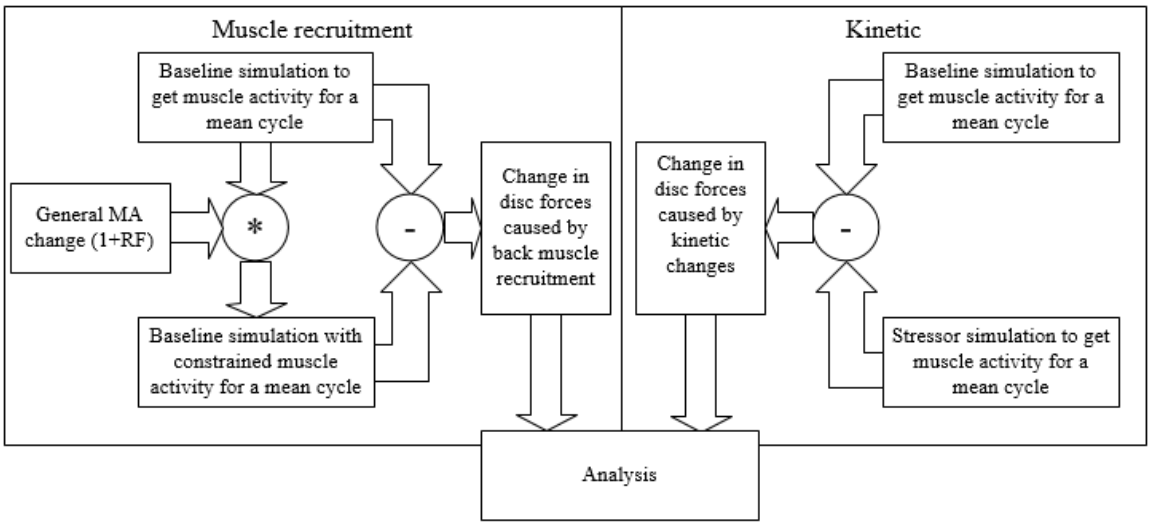


**Figure 3.4:** Workflow of force analysis. On the left side in the muscle recruitment model (MRM), changes in muscle activity in combination with the baseline simulation data are applied as boundary conditions. In the kinetic model (KMM) the baseline and COS data is used for simulation. The analysis compares the force changes of the muscle recruitment and kinetic model.

## 3.3. Results

Table 3.1 shows the result of the stress assessment. The stressor showed a significant ($P < 0.001$) influence on both physical and mental workload. This resulted in an overall increase in the NASA -TLX score from 36.58 to 57.61. Scores above 46.0 can be interpreted as above average stressful workload (SAGE, 2015).

| Value | Baseline<br>Mean (SD) | COS<br>Mean (SD) |
|---|---|---|
| Mental Demand | 24.36 (17.96) | 71.54 (20.65)*** |
| Physical Demand | 60.26 (20.80) | 55.26 (25.31)*** |
| Frustration | 14.87 (10.23) | 43.08 (26.15)*** |
| NASA-RTLX | 36.58 (10.27) | 57.61 (13.61)*** |

**Table 3.1:** Overview of personal stress assessment. COS shows a significant increase in all categories. This indicates a positive stress response and a successful stress introduction. ($P < 0.05$*, $P < 0.01$**, $P < 0.001$***)

The data was divided into four segments to analyze the data during the thorax extension flexion movement (Figure 3.2). Table 3.2 shows the mean muscle activities during each section for the measured muscle groups. All individual activities are normalized with the corresponding maximum values recorded during the MVC test.The right m. trapezius pars transversa, m. trapezius ascendens and m. trapezius pars descendens and are different in the lower region and during the backward motion. However, the latter increases with 8%. The others are below 3%. Higher changes are observed in the forward thoracic position and during the backward movement where the external load was applied. In the forward-leaning position, the largest increase in the lower region is observed in the right m.multifidi with 9% from 25% to 34%. In general, the muscle activity in the lower back increased from a range of 15% - 25% up to 19% - 34%. During backward movement, the overall muscle activity is overall greater, increasing from a minimal value of 25% up to a maximum of 48%. In detail with a growth of 9% at the m. multifidi from 39% to 48% and m. erector spinae pars iliocostalis from 26% to 34% reacts the most ($P < 0.001$) (Table 3.2).

| | Upper region Mean (SD) [%MVC] | | Motion forward Mean (SD) [%MVC] | | Lower region Mean (SD) [%MVC] | | Motion backward Mean (SD) [%MVC] | |
|---|---|---|---|---|---|---|---|---|
| EMG ID | Baseline | COS | Baseline | COS | Baseline | COS | Baseline | COS |
| 1 | 8(22) | 14(55) | 7(17) | 11(42) | 6(17) | 13(58) | 9(27) | 17(75)* |
| 2 | 4(3) | 4(3) | 4(4) | 4(3) | 3(3) | 3(3) | 3(3) | 4(3) |
| 3 | 4(5) | 4(5) | 3(3) | 4(4) | 6(9) | 6(5)** | 8(13) | 9(10)** |
| 4 | 4(3) | 4(3) | 3(2) | 3(3) | 5(3) | 6(6) | 6(5) | 8(11) |
| 5 | 7(6) | 8(9) | 6(6) | 7(8)* | 10(8) | 13(10)** | 13(11) | 18(15)* |
| 6 | 10(15) | 10(17) | 8(13) | 7(8) | 11(10) | 13(12)* | 16(17) | 19(19) |
| 7 | 14(12) | 14(13) | 9(8) | 9(9) | 20(12) | 24(13)*** | 33(24) | 40(26)*** |
| 8 | 15(12) | 15(13) | 10(8) | 10(9) | 21(12) | 26(14)*** | 36(25) | 44(26)*** |
| 9 | 12(9) | 13(11) | 8(7) | 9(9) | 15(8) | 19(10)*** | 25(17) | 32(20)** |
| 10 | 13(10) | 16(20) | 9(9) | 11(21) | 15(9) | 21(12)*** | 26(18) | 34(19)*** |
| 11 | 23(23) | 24(26) | 21(30) | 22(34) | 25(20) | 34(26)*** | 39(31) | 48(33)*** |
| 12 | 20(15) | 21(17) | 20(39) | 14(13) | 24(12) | 29(12)*** | 39(16) | 45(19)** |

**Table 3.2:** Muscle recruitment changes split into upper and lower region and the forward and backward motion. The lumbar spine is significantly reacting in the lower region and backward motion. ( $P < 0.05$*, $P < 0.01$**, $P < 0.001$***)

Figure 3.5 to Figure 3.8illustrate the muscle activity of all measured muscles for baseline, COS in the individual sections.

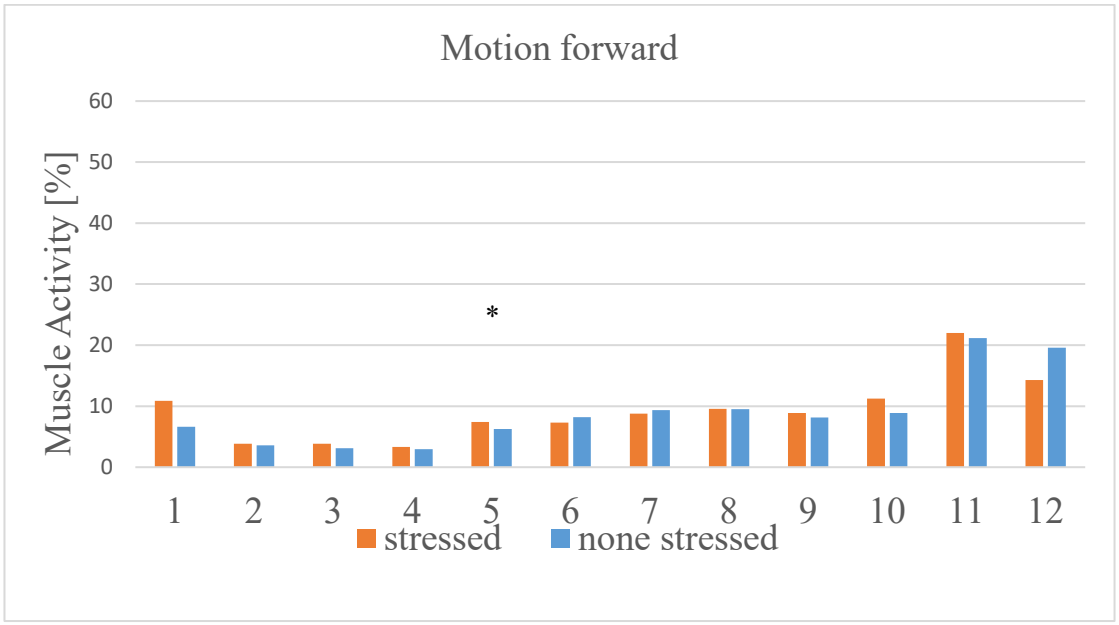


**Figure 3.5:** Normalized mean muscle activities during forward motion. The greatest activity is in the m. multifidi region with above 20% MVC. ( P < 0.05*, P < 0.01**, P < 0.001***)

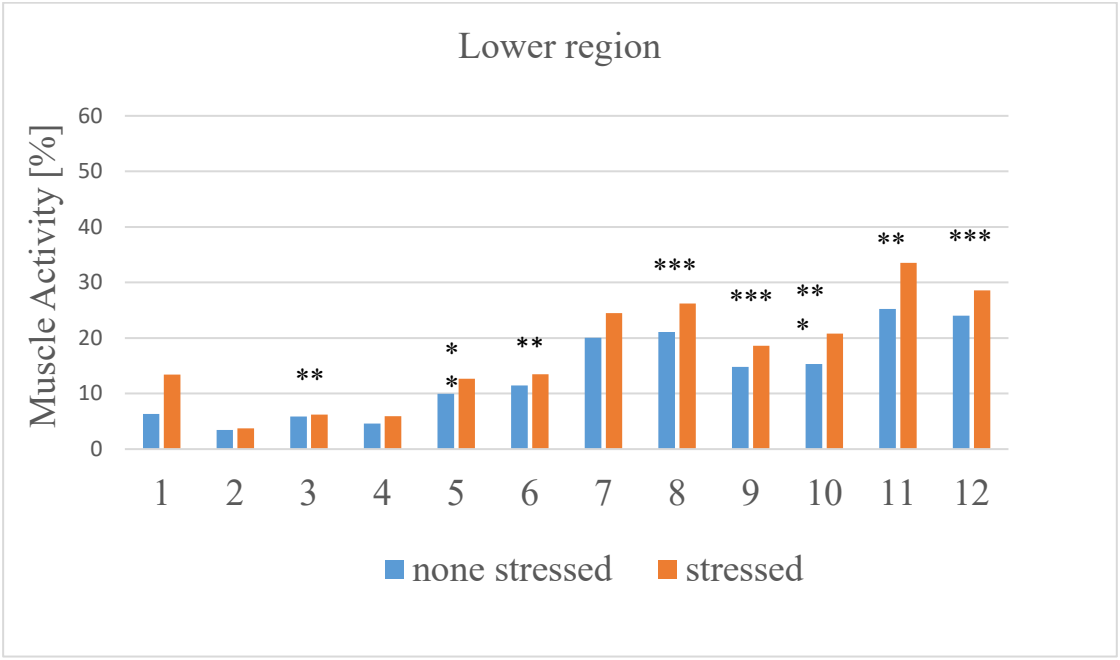


**Figure 3.6:** Normalized mean muscle in the lower region. The greatest activity is in the m. multifidi region and m. erector spinae pars longissimus with above 20% MVC. ( P < 0.05*, P < 0.01**, P < 0.001***)

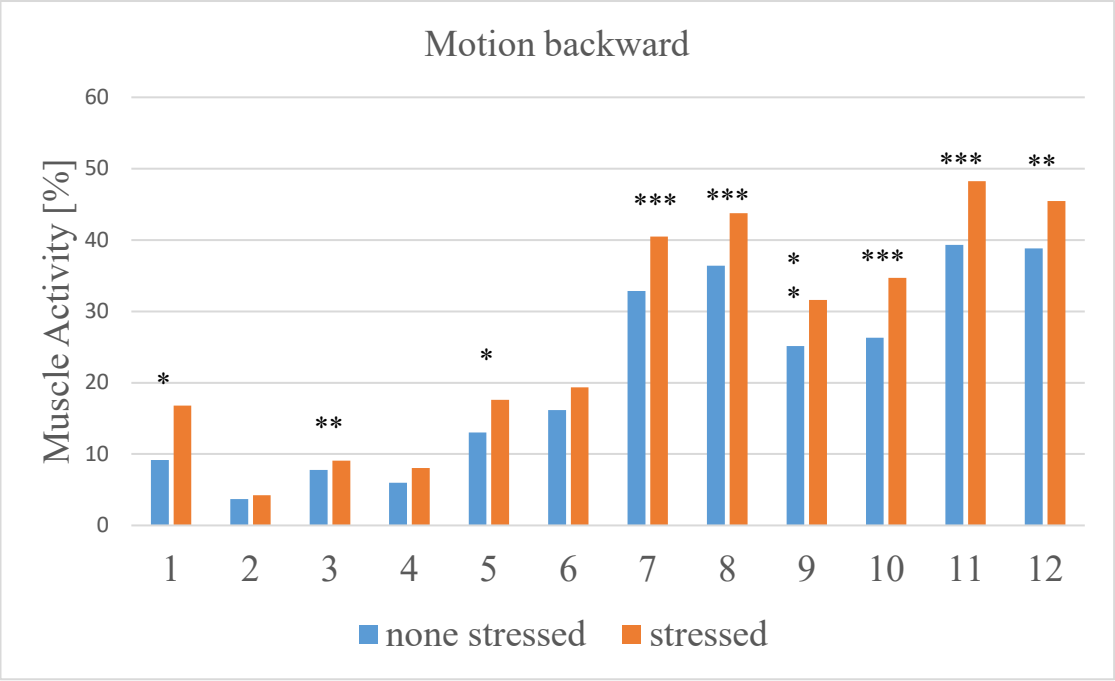


**Figure 3.7:** Normalized mean muscle activities during backward motion. The highest reaction is in the lower back with activities greater than 25%. ( P < 0.05*, P < 0.01**, P < 0.001***)

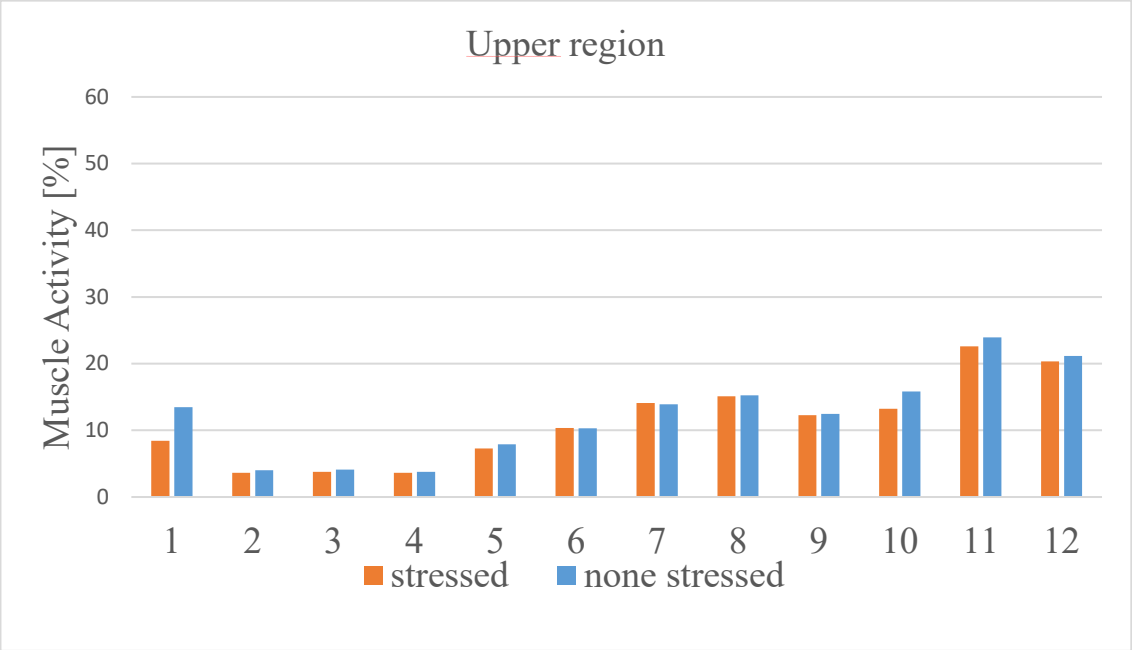


**Figure 3.8:** Normalized mean muscle in the upper region. The greatest activity is in the m. multifidi region with above 20% MVC. ( P < 0.05*, P < 0.01**, P < 0.001***)

**Table 3.3** and **Table 3.4** describe the results of the basic kinetic parameters. In contrast to the muscle activity, where the backward movement and the lower range showed differences, here the upper and lower range are of interest. The LDLJ and acceleration RMS increase at these upper and lower dead center. LDLJ increase at 0.63 and 0.44 while the acceleration increases at $0.066e^{-3}°/s^2$ and $0.106e^{-3}$ $°/s^2$.

| Parameter | LDLJ Mean (SD) | | ACC RMS Mean (SD) [°/s²] | | Jerk RMS Mean (SD) [°/s³] | |
|---|---|---|---|---|---|---|
| Trial | Baseline | Stress | Baseline | Stress | Baseline | Stress |
| Upper region | -9.03 (1.17) | -8.4 (0.87)*** | 0.964e-3 (0.143e-3) | 1.03e-3 (0.11e-3)*** | 0.032 (0.005) | 0.032 (0.004) |
| Motion forward | -7.5 (1.14) | -7.26 (0.66) | 0.861e-3 (0.029e-3) | 0.866e-3 (0.023e-3) | 0.02 (0.002) | 0.019 (0.001) |
| Lower region | -8.97 (1.17) | -8.53 (0.9)** | 0.889e-3 (0.162e-3) | 0.955e-3 (0.158e-3)** | 0.028 (0.006) | 0.029 (0.006)* |
| Motion backward | -7.4 (1.07) | -7.15 (0.49) | 0.77e-3 (0.151e-3) | 0.805e-3 (0.111e-3) | 0.017 (0.003) | 0.018 (0.002) |

**Table 3.3:** Parameter LDLJ show significant differences in the upper and lower region. RMS acceleration shows the same reaction. ( P < 0.05*, P < 0.01**, P < 0.001***)

| Parameter | MSJ Mean (SD) | | ACC Mean (SD) [°/s²] | | Jerk Mean (SD) [°/s³] | |
|---|---|---|---|---|---|---|
| Trial | Baseline | Stress | Baseline | Stress | Baseline | Stress |
| Upper region | 0.16 (0.05) | 0.16 (0.03) | 5e-4 (1.5e-4) | 5e-4 (1.2e-4)*** | 4.6e-4 (4.8e-4) | 5.5e-4 (4.2e-4) |
| Motion forward | 0.06 (0.01) | 0.06 (0.01) | -9.4e-5 (3.7e-5) | -9.8e-5 (2.7e-5) | -1.9e-3 (4.9e-4) | -2e-3 (4.1e-4) |
| Lower region | 0.12 (0.05) | 0.13 (0.06)* | -4.5e-4 (2e-4) | -5.4 (1.3e-4)** | -5.8e-4 (3.9e-4) | -6.8e-4 (3.1e-4) |
| Motion backward | 0.04 (0.01) | 0.05 (0.01) | 9.5e-5 (4.7e-5) | 1.1e-4 (2e-5)* | 2e-3 (5.5e-4) | 2.1e-3 (3.4e-4) |

**Table 3.4:** The lower region is the only section where MSJ shows a significant difference. Mean jerk shows no difference at all in contrary to the ACC, which is only not different during the forward motion. ( P < 0.05*, P < 0.01**, P < 0.001***)

A similar result is reflected in the dwell times of the sections (Table 3.5). In the upper (P < 0.01) and lower region (P < 0.05), COS causes motion to be 140 ms faster on average (P < 0.05). The shorter times are consistent with the accelerations, as the amounts are lower in the upper region where the acceleration is greater.

| Trail | Baseline<br>Mean (SD) [s] | COS<br>Mean (SD) [s] |
|---|---|---|
| Upper region | 0,91(0,27) | 0,77(0,2)** |
| Motion forward | 1,11(0,58) | 1,01(0,13) |
| Lower region | 1(0,44) | 0,86(0,28)** |
| Motion backward | 1,13(0,51) | 1,02(0,18) |
| Total | 4,1 | 3,6 |

**Table 3.5:** Average length of time spent in each section. In the upper and lower region, the length of stay decreased significantly. Overall the subjects moved faster during the COS trial ( $P < 0.05$*, $P < 0.01$**, $P < 0.001$***)

Despite the predefined and controlled torque by the dynamometer, the subject can produce a slightly deviating value in combination with the device. This is possible because the control algorithm reacts to the subjects movement and kinetics. The sign of the values reflects its direction. Statistical analysis shows a difference ($P < 0.05$) in all sections . The largest differences are found in the forward and backward motion with an increase of 20 and 16 Nm ($P < 0.01$) due to COS.

| Trial | Baseline<br>Mean (SD) [Nm] | Stress<br>Mean (SD) [Nm] |
|---|---|---|
| Upper region | 17(18,8) | 9,48(20,28)** |
| Motion forward | -35,62(27,98) | -55,84(45,64)** |
| Lower region | -17,29(18,92) | -12,29(22,49)* |
| Motion backward | 49,04(35,25) | 65,43(46,98)* |

**Table 3.6:** Torque applied in each section. Significant differences are found in all but one. ( $P < 0.05$*, $P < 0.01$**, $P < 0.001$***)

The analysis of the kinematic changes due to stress shows most differences in the upper and lower regions, which are the turning points in the trajectories. Significant changes in muscle activity occur in the lower region as well as during the backward movement, which is the part where the extra load is applied. Both results increase the load on the internal structures.

Intervertebral disc loads represent a general measure, since that is also, where the most vulnerable tissue is located. To account for the varying physiology of the subjects, the spinal loads are normalized by the mass of the individual and represent the change as a percentage of body weight. As described in method section 3.2 the musculoskeletal model is symmetrical in the medio-lateral direction. This results in zero disc loading in this direction throughout the simulation. Figure 3.9 visualizes the average load difference due to kinematic changes of the spine during backward motion. The highest increase is found in disc L4L5 and L5Sacrum compression with 20% BW. The anterior-posterior direction experiences almost half the load increase with 8% BW in disc T12L1. The results in detail are shown in Table 3.7. In the upper region, the load change is similar to the backward movement. The load increases up to 24% BW in the disc L1L2 for compression and 8% in T12L1 in anterior-posterior direction. In the lower region, the maximum load increase of 14% BW happens in L3L4 and L4L5 from 139% BW to 153% BW. Anterior-posterior load increases are below 5% BW. The smallest load increase occurs during the trunk forward motion. The increases in value do not exceed 11% BW for compression in T12 L1 and 2% BW in the anterior-posterior direction.

| | | Motion forward Mean (SD) [%BW] | | Lower region Mean (SD) [%BW] | | Motion backward Mean (SD) [%BW] | | Upper region Mean (SD) [%BW] | |
|---|---|---|---|---|---|---|---|---|---|
| Disc level | dir | Baseline | COS | Baseline | COS | Baseline | COS | Baseline | COS |
| T12L1 | AP | -35 (8) | -37 (13) | -51 (10) | -56 (12)** | -80 (26) | -88 (27)* | -46 (13) | -54 (9)*** |
| | CC | 110 (31) | 121 (47) | 139 (25) | 151 (30)** | 196 (54) | 211 (55)* | 123 (26) | 144 (22)*** |
| L1L2 | AP | -23 (6) | -22 (7) | -39 (9) | -43 (12)** | -68 (24) | -75 (25)* | -36 (12) | -42 (8)* |
| | CC | 109 (31) | 119 (46) | 143 (26) | 156 (31)** | 206 (60) | 222 (61)* | 125 (29) | 149 (23)*** |
| L2L3 | AP | -9 (5) | -7 (4)** | -22 (7) | -25 (9)* | -44 (18) | -50 (18) | -21 (9) | -24 (6)* |
| | CC | 104 (29) | 113 (43) | 139 (26) | 151 (31)** | 203 (63) | 221 (64)* | 122 (30) | 145 (24)*** |
| L3L4 | AP | 5 (4) | 7 (5)* | 1 (2) | 1 (3) | -7 (5) | -9 (6) | -2 (3) | 0 (2)** |
| | CC | 101 (29) | 109 (41) | 139 (28) | 153 (34)** | 211 (68) | 230 (70)* | 123 (33) | 146 (26)*** |
| L4L5 | AP | 17 (4) | 18 (6) | 26 (5) | 28 (6)** | 39 (12) | 43 (13)* | 22 (6) | 27 (5)*** |
| | CC | 98 (28) | 105 (38) | 139 (29) | 153 (35)** | 216 (72) | 236 (73)* | 125 (35) | 147 (26)*** |
| L5 Sacrum | AP | 24 (5) | 24 (7) | 37 (7) | 41 (9)** | 58 (18) | 63 (19)* | 32 (9) | 39 (6)*** |
| | CC | 102 (28) | 109 (39) | 142 (29) | 155 (35)** | 220 (72) | 240 (74)* | 129 (35) | 150 (27)*** |

**Table 3.7:** Mental stress not just changes the muscle recruitment but also the thorax kinetic. This table present disc loads in each individual disc level in body weight percent caused by different kinetic. ( $P < 0.05$*, $P < 0.01$**, $P < 0.001$***)

Not only kinetic changes influence the spinal disc loads, but also the increase in muscle tone. To evaluate these changes the loads presented in this chapter are calculated as described in chapter 3.2 with the help of musculoskeletal models. Again, significant ($P < 0.01$) differences are found in all sections. In general, (Figure 3.10) the altered muscle tonus leads to higher disc loads during motion. During backward motion, CC increases to a maximum of 72% BW in T12L1. In almost all levels, an increase of at least 67% BW occurs. In the upper region, the magnitude is not as great with a maximum of 48% BW. Figure 3.10 shows an overview of the mean load changes during backward motion.

Maximum anterior-posterior changes occur in the upper region and during the backward motion with up to 24% BW from -80% BW to -104% BW in disc T12L1. In the lower region and during forward motion, no disc level exceeds 10% BW found in disc T12L1. Table 3.8 shows a summary of all values.

| | | Motion forward Mean (SD) [%BW] | | Lower region Mean (SD) [%BW] | | Motion backward Mean (SD) [%BW] | | Upper region Mean (SD) [%BW] | |
|---|---|---|---|---|---|---|---|---|---|
| Disc Level | | Baseline | COS | Baseline | COS | Baseline | COS | Baseline | COS |
| T12L1 | AP | -35 (8) | -40 (15)* | -51 (10) | -61 (18)*** | -80 (26) | -104 (47)** | -46 (13) | -62 (16)*** |
| | CC | 110 (31) | 123 (45) | 139 (25) | 167 (47)*** | 196 (54) | 268 (126)** | 123 (26) | 170 (46)*** |
| L1L2 | AP | -23 (6) | -26 (11)* | -39 (9) | -45 (14) | -68 (24) | -84 (37) | -36 (12) | -48 (12)*** |
| | CC | 109 (31) | 122 (45) | 143 (26) | 171 (48)*** | 206 (60) | 275 (125)** | 125 (29) | 173 (45)*** |
| L2L3 | AP | -9 (5) | -11 (8)* | -22 (7) | -26 (9)*** | -44 (18) | -53 (22)** | -21 (9) | -28 (7)** |
| | CC | 104 (29) | 117 (44) | 139 (26) | 167 (47)*** | 203 (63) | 273 (124)** | 122 (30) | 170 (46)*** |
| L3L4 | AP | 5 (4) | 5 (4) | 1 (2) | 1 (3) | -7 (5) | -6 (7) | -2 (3) | 0 (2)* |
| | CC | 101 (29) | 114 (44) | 139 (28) | 168 (48)*** | 211 (68) | 278 (123)** | 123 (33) | 171 (46)*** |
| L4L5 | AP | 17 (4) | 19 (8) | 26 (5) | 31 (10)** | 39 (12) | 52 (27)** | 22 (6) | 31 (9)*** |
| | CC | 98 (28) | 112 (42) | 139 (29) | 167 (48)*** | 216 (72) | 283 (123)** | 125 (35) | 172 (45)*** |
| L5 Sacrum | AP | 24 (5) | 27 (9) | 37 (7) | 43 (12)** | 58 (18) | 73 (31)** | 32 (9) | 44 (10)*** |
| | CC | 102 (28) | 115 (43) | 142 (29) | 171 (48)*** | 220 (72) | 288 (124)** | 129 (35) | 176 (46)*** |

**Table 3.8:** Overview of disc loads in body weight percentage caused by COS and baseline kinetic data. Only during the forward motion no significant changes occur. ( $P < 0.05$*, $P < 0.01$**, $P < 0.001$***)

When directly comparing the resulting disc forces caused by kinetics and muscle recruitment, the most significant differences ($P < 0.001$) occur during the backward motion and in the upper region. Differences up to 57% BW are found during backward motion for T12 L1 compression. Anterior- posterior forces increase up to 16% BW at the same disc level. In the upper region, the highest value of 26% BW is also found in T12 L1 for compression. For forward motion, no value exceeds 10% BW, while in the lower region, forces are around 15% BW in the cranial-caudal direction. Anterior-posterior load differences are below 5% BW at all levels. Table 3.9 summarizes all section values.

| | | Motion forward Mean (SD) [%BW] | | Lower region Mean (SD) [%BW] | | Motion backward Mean (SD) [%BW] | | Upper region Mean (SD) [%BW] | |
|---|---|---|---|---|---|---|---|---|---|
| Disc Level | Dir. | Kinetic | Muscle | Kinetic | Muscle | Kinetic | Muscle | Kinetic | Muscle |
| T12L1 | AP | -37 (13) | -40 (15) | -56 (12) | -61 (18)* | -88 (27) | -104 (47)** | -54 (9) | -62 (16)*** |
| | CC | 121 (47) | 123 (45) | 151 (30) | 167 (47) | 211 (55) | 268 (126)*** | 144 (22) | 170 (46)*** |
| L1L2 | AP | -22 (7) | -26 (11) | -43 (12) | -45 (14) | -75 (25) | -84 (37)** | -42 (8) | -48 (12)*** |
| | CC | 119 (46) | 122 (45) | 156 (31) | 171 (48)* | 222 (61) | 275 (125)** | 149 (23) | 173 (45)*** |
| L2L3 | AP | -7 (4) | -11 (8)** | -25 (9) | -26 (9) | -50 (18) | -53 (22) | -24 (6) | -28 (7)** |
| | CC | 113 (43) | 117 (44) | 151 (31) | 167 (47)** | 221 (64) | 273 (124)*** | 145 (24) | 170 (46)*** |
| L3L4 | AP | 7 (5) | 5 (4) | 1 (3) | 1 (3) | -9 (6) | -6 (7) | 0 (2) | 0 (2) |
| | CC | 109 (41) | 114 (44) | 153 (34) | 168 (48)* | 230 (70) | 278 (123)*** | 146 (26) | 171 (46)*** |
| L4L5 | AP | 18 (6) | 19 (8) | 28 (6) | 31 (10)* | 43 (13) | 52 (27)** | 27 (5) | 31 (9)*** |
| | CC | 105 (38) | 112 (42) | 153 (35) | 167 (48)* | 236 (73) | 283 (123)*** | 147 (26) | 172 (45)*** |
| L5 Sacrum | AP | 24 (7) | 27 (9) | 41 (9) | 43 (12) | 63 (19) | 73 (31)** | 39 (6) | 44 (10)** |
| | CC | 109 (39) | 115 (43) | 155 (35) | 171 (48)* | 240 (74) | 288 (124)*** | 150 (27) | 176 (46)*** |

**Table 3.9:** Summary compares stress related spinal load changes caused by kinetic and muscle recruitment differences. Especially during the backward motion and in the upper region the muscle recruitment is generating higher loads.

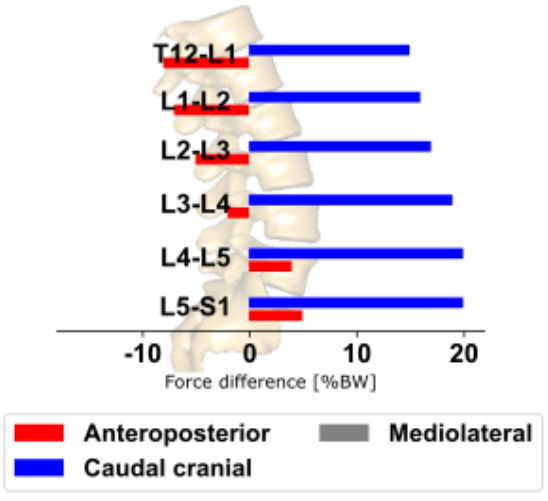


**Figure 3.9:** Force differences in each individual disc level between baseline and COS trial caused by changes in kinetic during the backward motion. The force increases up to 20% BW in disc L5-S1.

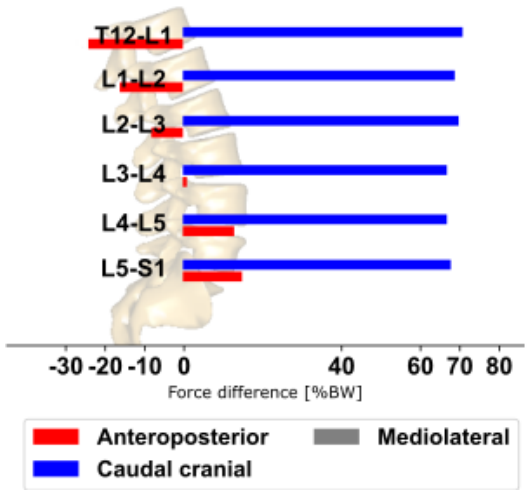


**Figure 3.10:** Force differences in each individual disc level between baseline and COS trial caused by changes in muscle recruitment during the backward motion. The force increases up to 70% BW in disc L2-L3.

## 3.4. Discussion

Using inverse kinematic simulation models and adapting them to include the psychological muscle response, hypothesis three was investigated. The novel approach in splitting the evaluation into the kinetic and psychological response allows for the determination of pure stress-induced biomechanical loading. By looking at the upper and lower muscles simultaneously, a recruitment pattern is found that helps to understand how movement, stress and loading contribute to lower back pain and muscle tension.

Despite the dual-task character, the subjects are faster in the turning points and no significant difference is found during the movement. This leads to an overall faster motion during the dual-task trial. The faster movement can be associated with higher accelerations in the turning regions for both the mean and RMS values. The much higher RMS values suggest higher peak values during COS. Similar studies with dual tasks and movements use gait analyses to examine competition between shared resources (Wrightson et al., 2016). In his systematic review, Al-Yahya et.al. (Al-Yahya et al., 2011) showed in his systematic review that gait speed is usually slower under dual-task conditions in subjects with and without disorders. Specifically, this results in reduced stride length but increased stride time in concert with higher cadence. In contrast, this study yields reduced variability for times and accelerations. Since gait is a rather complex and high-dimensional movement, the restricted movement might have influenced the behavior of the subjects. Nevertheless, to allow a detailed comparison, the gait cycle should be divided into its phases. Hamacher et.al. (Hamacher et al., 2017) showed in their study a phase-dependent variability especially in the swing phase, which is comparable to the forward and backwards movement and result in a contradicting observation.

Both kinetic and stress-induced muscle tension contribute to changes in the lumbar spine during backward motion turning point but only minor in the trapezius. During the backward movement there is an increase of 8% in the right m. trapezius pars descendens. Since this occurs only during the application of the force, the question arises whether the increase is the result of an increased right-sided push or a stress-induced tonus increase. However, the increase is smaller compared to other studies. Larsson et.al. (Larsson et al., 1995) found a 20% increased during static load. Relatively low physical load during typewriting resulted in an asymmetric increase of 67% on the left and almost 8% on the right side (Leyman et al., 2001; Leyman et al., 2004). Shahidi et. al. (Shahidi et al., 2013) indicate the independent response of the trapezius from

concentration and posture. Similar results were reported by Rissen et.al. (Rissén et al., 2002) who studied female cashiers before and after work. While most of the studies do not involve motion with additional loading, in this work the subjects were strained during a basic upper body motion. The result suggests a small response of the trapezius during motion, but does not exclude the stress response that could occur after exercise/work.

The picture is different in the lumbar spine with a significant increase in muscle activity averaging 8% - 9% in the m. multifidi and m. erector spinae pars iliocostalis. A similar experiment was performed by (Davis et al., 2002a) using a complex material handling task with 90° clockwise and counterclockwise rotation. They found an increase in muscle activity in the range of 2% - 7%. In addition, they used a forward dynamic musculoskeletal simulation to calculate changes in peak mean spinal loads that increased by 160 N (23% BW) in lateral shear, 80 N (12% BW) of anterio-posterior shear and 700 N (101% BW) of compression. As discussed in chapter 1.7 forward dynamic simulation incooperates EMG data into the muscle recruitment. In this work, an extended inverse kinematic approach is adopted to calculate the resulting lumbar loads for a different kinematic and recruitment pattern. Overall, kinetic changes in AP direction increase loads by 8% BW, while CC loads increase by 24% BW. This load increase is reasonable and reflects the higher mean torque as well as the faster motion during the COS. To incorporate the muscle activity changes the measured recruitment pattern is applied which results in a higher spinal load of 24% BW and 72% BW.

In the following, the loads at disc level L4L5 are used as an indicator whether a possible additional muscle tension due to COS contributes to the load increase or whether it is only due to kinetic changes. Looking at the compression force, the load increases significantly from 216% BW during baseline motion to 236% BW (Table 3.7). This is due to the shorter section time of 1.02 sec and the corresponding higher torque of 65 Nm, an increase of 16 Nm compared to the baseline.

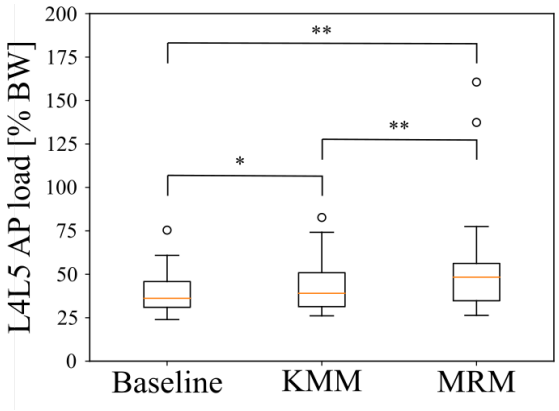


**Figure 3.11:** Mean anterior-posterior disc load in L4 L5 during the backward motion. There is a significant difference between the baseline, muscle recruitment (MRM), and kinetic musculoskeletal model. The significance between the MRM and KMM model indicates stress-related muscle tension. . ( $P < 0.05$*, $P < 0.01$**, $P < 0.001$***)

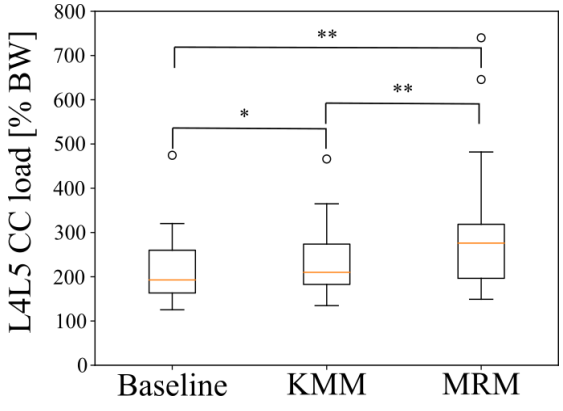


**Figure 3.12:** Mean cranial-caudal disc load in L4 L5 during the backward motion. There is a significant difference between the baseline, muscle recruitment (MRM), and kinetic musculoskeletal model. The significance between the MRM and KMM model indicates stress-related muscle tension. ( $P < 0.05$*, $P < 0.01$**, $P < 0.001$***)

To test whether the measured changes in recruitment are simply a consequence of the difference in kinetics, the EMG changes in recruitment are applied as boundary conditions during a separate simulation of the baseline trajectory. Table 3.9 shows a significant difference due to the change in muscle recruitment. In the case of CC force, the higher muscle activity contributes 47% BW in this direction. The results in AP are similar, although the magnitude is smaller at 9% BW, but may have more influence on the disc tissue as it acts in the shear direction. A similar result is found in the upper region the force differs 25% BW in CC direction and 4% AP. In the lower region the difference, gets smaller with 14% BW. As in this section the mean, RMS acceleration and dwell time indicates a lack of postural control due to shared similar during gait where higher stride times can be observed (Al-Yahya et al., 2011).

There are limitations to this study. Not randomizing the study prolonged the exercise training phase and contributed to better exercise control during COS. Another disadvantage arises from the use of the dynamometer. It only records torque and motion in one axis, which prevents modeling of lateral forces and imbalances. Despite the emphasis on the subject's training phase, motor control and the subject's ability to learn a new task could influence the outcome, and one cannot 100% rule out the contribution. This inability could influence the baseline measurement more than the loading study and reduce the response magnitude between both trials. A linear

approach was used to model the measured muscle activity in the musculoskeletal model. Although this approach has been evaluated (Dubowsky et al., 2008; Zee et al., 2007) the actual transfer function may differ because it depends on muscle composition and motor recruitment (Kuriki et al., 2012).

## 3.5. Conclusion

In summary, this study confirms hypothesis three. The results show that COS contributes to an increase in disc load by altering both thoracic kinetics and muscle recruitment. The use of simulation provides a novel method to incorporate changes in muscle activity into inverse kinematic musculoskeletal models. This approach allows the subject's mental stress response to be split into a kinetic and a muscular recruitment component. The resulting loads show a significant higher disc compression of 47% BW increasing from 236% BW to 283% BW, at disc level L4L5 (Figure 3.12). In addition, no significant difference in muscle activity was found at the cervical spine. This information can help to develop prevention schemas in ergonomics. For example to include or adapted thorax movements in workplaces with a high work demand in order to avoid muscle tension in the upper back.

# 4. Muscle activity prediction for usage in musculoskeletal modeling

## 4.1. Introduction

The relationship between mental stress and muscle activity has been the subject of numerous studies over the years (chapter 1.6). The usage of EMG measurements play an essential role in these studies and reflects muscle activity and tension. Significant differences in muscle recruitment in different muscle groups have been found. Numerous studies link both emotional and cognitive stress to higher short-term response of the trapezius. Despite the smaller number of studies linking lower back muscle activity to psychological stress, a correlation appears to be present especially when not only muscle activity but also the resulting spinal loads are considered. Typically, this type of study is conducted at specific workstations during or after a specific task in laboratory environments for very specific conditions. The inability to take measurements in a specific environment makes it very difficult to study biomechanical effects for these circumstances. This is the case, for example, when motion or pressure artifacts during EMG measurements provide false or inaccurate results. A similar situation is possible for motion measurements. In Chapter 3, experimental EMG data provides an additional dimension and extend inverse kinematic musculoskeletal simulation models. In addition, several studies demonstrated the usability of EMG data in combination with artificial neural networks to predict muscle activity, kinematics, and loads on musculoskeletal structures.

For gait analysis Heller et al. (Heller et al., 1993) used machine learning techniques to reconstructed muscle activity dependent on kinematic data like walking speed as well as joint kinematics. With moderate static loading, Nussbaum et al. (Nussbaum et al., 1995; Nussbaum et al., 1997) used experimental data to train and predict lumbar muscle recruitment. Input data of thoracic angle and external load predicted measured activity of erector spinae, rectus abdominus, oblique externus, and latissimus dorsi. Luh Chang et al. (Luh et al., 1999) and Wang et al. (Wang and Buchanan, 2002) used arm muscle activity in combination with kinematics to train neural network to predict joint torque. Savelberg et al. (Savelberg and Herzog, 1997) and Liu et al. (Liu et al., 1999) used similar approaches to prove the feasibility of the methods for muscle and tendon forces during walking of cats. In addition to predicting internal load Oh Choi et al. (Oh et al., 2013) used gait dynamic parameters for training and predict ground reaction

forces for each step. The existing studies demonstrate the wide application of neural networks in biomechanics.

The combination of numerical models and experimental data offers a method to provide data for submaximal stress levels as well as to simulate arbitrary motions with and without stress. The method presented in this work is based on a combination of numerical baseline computation and the application of measured muscle activity. This approach assumes knowledge of how stress alters muscle recruitment and allows application of these data to musculoskeletal models as in Chapter 3. Thus, prediction of muscle activity is sufficient to generate information for musculoskeletal simulation. From a mathematical perspective, this problem is defined as a nonlinear regression model.

Due to the popularity of machine learning methods in recent years for prediction problems, neural networks and gradient amplification methods are investigated in this work to map kinetic trajectories and load-related muscle recruitment data.

This feasibility study investigates hypothesis 4 and the possibility of applying such procedures in principle.

## 4.2. Method

The numerical average trajectories from chapter 3 provides the training dataset for this part of the work. The records are divided into baseline and stress data and it is assumed that the subject was maximally stressed and minimally relaxed. Based on this assumption, the stress level feature is set to zero for the baseline data and one otherwise. Resampling and processing the experimental data at 300 Hz allows the generation of mean trajectories for each subject. A single training data set contains the kinematic variables: Position, Velocity, Acceleration, and Torque. The subject specific data weight, height are added to the time series data and provide a sample for training. This results in 28297 data points containing all 41 subjects.

- **Gradient Boosting**

The library XGBoost (2020d) is the basis for the implementation. This library supports several programming languages like Python, C++; R; Ruby etc. as well as GPU support. The wide

variety of implementations allows this approach to be applied to other platforms. In this work, the python version is used. First, the data is collected, then stored in a pandas DataFrame and written to disk as a Python pickle object. This approach allows the data to be loaded into memory during the computational steps and saves the time for device access and file parsing. The training includes the following parameters and their corresponding values, and only values without defaults are listed here. For all other values I refer to the official XGBoost documentation (2020d):

- eta: 0.1 Step size shrinkage used in update to prevents overfitting. After each boosting step, we can directly get the weights of new features, and eta shrinks the feature weights to make the boosting process more conservative.
- gamma:0 Minimum loss reduction required to make a further partition on a leaf node of the tree. The larger gamma is, the more conservative the algorithm will be.
- max_depth 9 Maximum depth of a tree. Increasing this value will make the model more complex and more likely to overfit. 0 is only accepted in lossguided growing policy when tree_method is set as hist and it indicates no limit on depth. Beware that XGBoost aggressively consumes memory when training a deep tree.
- min_child_weight: 6 Minimum sum of instance weight (hessian) needed in a child. If the tree partition step results in a leaf node with the sum of instance weight less than min_child_weight, then the building process will give up further partitioning. In linear regression task, this simply corresponds to minimum number of instances needed to be in each node. The larger min_child_weight is, the more conservative the algorithm will be.
- subsample 0.7: Subsample ratio of the training instances. Setting it to 0.5 means that XGBoost would randomly sample half of the training data prior to growing trees and this will prevent overfitting. Subsampling will occur once in every boosting iteration.

Using these hyperparameters, a machine learning model is trained for each mean EMG channel in the low back as an outcome variable and as a function of subject height, weight, stress level, thoracic flexion angle, thoracic velocity, thoracic acceleration, and applied torque. In the case of the stress level feature, baseline data are coded with a value of zero and one for the stress test. This approach assumes that the subject was in a 100% arousal state and allows prediction of submaximal muscle activity for a lower stress level.

- **Neural Network**

Similar to the gradient tree model, a third-party Python library is used for the NN implementation. TensorFlow (2020b) as an open source multi language library, supports various types of devices and was therefore selected for this implementation. The pre-collected data is used for grid search and Bayesian optimization to perform hyperparameter optimization. The following parameters are part of the optimization: Learning Rate; Epochs, Batch size; Number of neurons in layer 1 - 3. The following table (Table 4.1) shows the outer boundaries of the search space.

| Boundary | Learning rate | Epochs | Batch Size | Layer 1 | Layer 2 | Layer 3 |
|---|---|---|---|---|---|---|
| - | 0.01 | 10 | 50 | 14 | 14 | 14 |
| + | 0.001 | 50 | 500 | 28 | 28 | 28 |

**Table 4.1**: Parameter boundaries used for hyperparameter grid search. Bayesian optimization uses the optimal parameters as starting parameters.

The result of the grid search is used as the initial value for the Bayesian optimization package (2020a). The parameter space was further extended to include learning rate; neurons in input layer, number of hidden layers; number of neurons in hidden layer; activation function: batch size; epoch size. Tanh, Relu and linear function served as possible activation function for best data fit. Predefined parameters and ranges are adopted by Montavon et.al. (Montavon et al., 2012).

During the training process, Bayesian optimization results are used to generate the NN. First, all input variables are mapped to a range between zero and one. This is necessary to avoid any bias due to the different scales of variables. Then, the data is fed into the Tensorflow training routine with a validation sample size of five percent. The mean absolute error (MAE) (4.1) was chosen to quantify the model quality. The training process was stopped if this value did not change over 10 iterations.

$$MAE = \frac{1}{n}\sum_{i=1}^{n}|Y_i - X_i| \tag{4.1}$$

$$RMSE = \sqrt{\sum_{i=1}^{n}\frac{(Y_i - Y_t)^2}{n}} \tag{4.2}$$

with:

n: Number of prediction
$Y_i$: Prediction values
$X_i$: Observation values

The muscle activity models are evaluated with the training data of their specific trial using MAE, RMSE (4.2) and person correlation. To assess the submaximal stress response, the stress level characteristic was set to 0.5 and the baseline data for the remaining input data.

## 4.3. Results

Table 4.2 shows the result of the grid search. The EMG data of the right m. multifidi delivers the most variations. Both the number of neurons and the learning rate are different. A difference is found in the right m. erector spinae pars iliocostalis, where the batch size and neurons in layer 3 vary.

| EMG ID | Learning rate | Layer 1 | Layer 2 | Layer 3 | Batch size | Epochs |
|---|---|---|---|---|---|---|
| 7 | 0.01 | 28 | 28 | 28 | 50 | 50 |
| 8 | 0.01 | 28 | 28 | 28 | 50 | 50 |
| 9 | 0.01 | 28 | 28 | 28 | 50 | 50 |
| 10 | 0.01 | 28 | 28 | 14 | 500 | 50 |
| 11 | 0.01 | 28 | 28 | 28 | 50 | 10 |
| 12 | 0.001 | 28 | 14 | 14 | 50 | 50 |

**Table 4.2**: Result of hyperparameter grid search. Right m. multifidi delivers the most dissimilarities including a batch size of 500.

Table 4.3 show the results of the Bayesian hyperparameter optimization. The parameters are quite different for all muscle activity models. The learning rate varies from 0.001 to 0.005 with at least three hidden layers simultaneously. M. multifidi shows differences in the neuron configuration with more than 26 neurons in the input layer and fewer in the hidden layer. Erector spinae pars longissimus has the most number of layers with five. Moreover, no symmetry can be observed between the models for the right and left muscle groups.

| EMG ID | Learning rate | Number of hidden layers | Number of input layer neurons | Number of hidden layer neurons | Activation function | Batch size | Epochs |
|---|---|---|---|---|---|---|---|
| 7 | 0.004 | 5 | 32 | 33 | relu | 51 | 97 |
| 8 | 0.005 | 4 | 25 | 34 | relu | 191 | 100 |
| 9 | 0.001 | 3 | 24 | 35 | relu | 113 | 98 |
| 10 | 0.004 | 4 | 28 | 35 | relu | 213 | 76 |
| 11 | 0.003 | 4 | 26 | 33 | relu | 150 | 90 |
| 12 | 0.002 | 3 | 35 | 22 | relu | 225 | 88 |

**Table 4.3:** Results of the hyperparameter search for the TensorFlow models. Besides the same activation function, the results differ in the number of neurons per layer as well as hidden layers.

Table 4.4 shows the differences between prediction and training data. In general, XGBoost shows better results than the TensorFlow neural network (TNN). This is true for both baseline and stress data. The XGboost models are able to model the data with an MAE below 2.53% m. multifidi muscle activity. In contrast, the TNN error is much larger with up to 68.6% muscle activity in the m. erector spinae pars iliocostalis. The RMSE shows similar trend with the greatest error in the erector spinae pars longissimus to the m. multifidi.

The similarity analysis with the Pearson correlation coefficient r shows a strong correlation with over 0.78 for the TNN regression model. In this case, the correlation becomes smaller following the increase of MAE. The XGBoost model shows a strong correlation for all muscle activity models above 0.99.

In the case of the 50% stress level prediction, both models show different results. In general, the MAE for the XGBoost prediction is lower and closer to the baseline data. Whereas it has its maximum values with 39% and 48% muscle activity in the m. multifidi, the TNN model has its maximum in the m. erector spinae pars iliocostalis with 68% and 113% muscle activity to the baseline and maximum stress.

The Pearson correlation coefficient r is smaller for the TNN model with a range from 0.75 to 0.91 compared to the baseline data and 0.74 to 0.89 for the stress correlation. The XGBoost model varies from 0.85 to 0.95 and 0.77 to 0.92, respectively.

| EMG CH. | Baseline | | Stress | | 50% level to Baseline | | 50% level to Stress | |
|---|---|---|---|---|---|---|---|---|
| | TNN | XGboost | TNN | XGboost | TNN | XGboost | TNN | XGboost |
| | RMSE | | | | | | | |
| 7 | 2.27 (1.03) | 0.28 (0.12) | 2.70 (1.53) | 0.38 (0.22) | 7.58 (3.75) | 3.79 (2.68) | 8.69 (5.4) | 6.41 (5.89) |
| 8 | 3.22 (1.67) | 0.30 (0.13) | 4.09 (2.06) | 0.39 (0.19) | 5.97 (2.39) | 4.71 (2.78) | 8.61 (4.9) | 6.48 (4.48) |
| 9 | 2.49 (1.01) | 0.2 (0.08) | 3.01 (1.54) | 0.26 (0.12) | 6.42 (4.37) | 3.70 (2.87) | 8.97 (6.47) | 5.91 (6.10) |
| 10 | 18.81 (11.07) | 0.35 ( 0.31) | 25.37 (19.56) | 0.45 (0.56) | 18.81 (11.07) | 6.42 (10.56) | 25.37 (19.57) | 7.29 (8.12) |
| 11 | 9.10 (7.93) | 0.84 (0.69) | 12.77 (14.49) | 1.47 (3.23) | 14.28 (23.08) | 11.65 (21.57) | 15.37 (15.96) | 13.23 (18.53) |
| 12 | 9.06 (9.64) | 0.54 (0.74) | 8.74 (5.13) | 0.61 (0.97) | 13.68 (27.67) | 9.56 (28.05) | 14.07 (12.18) | 8.91 (8.36) |
| mean | 7.49 | 0.42 | 9,45 | 0.59 | 11.12 | 6.64 | 13.51 | 8.04 |
| | MAE | | | | | | | |
| 7 | 13.55 (4.28) | 1.01 (0.48) | 14.11 ( 5.99) | 1.08 (0.63) | 7.58 (3.75) | 17.72 (8.44) | 8.69 (5.4) | 26.85 (18.48) |
| 8 | 19.06 (10.2) | 1.12 (0.55) | 19.59 (10.47) | 1.33 (1.37) | 5.97 (2.39) | 21.32 (10.65) | 8.61 (4.9) | 28.22 (15.99) |
| 9 | 17.62 (7.7) | 1.00 (0.69) | 20.95 (14.62) | 0.99 (0.69) | 51.87 (39.58) | 21.25 (13.17) | 69.28 (75.20) | 32.78 (33.12) |
| 10 | 49.34 (82.34) | 2 (1.81) | 68.60 (176.99) | 1.70 (1.49) | 68.21 (96.73) | 29.59 (24.91) | 113.96 (241.56) | 35.06 (27.8) |
| 11 | 35 (16.35) | 2.21 (1.34) | 45.28 (30.28) | 2.53 (2.87) | 43.87 (31.65) | 39 (35.64) | 57.24 (46.31) | 48.08 (41.37) |
| 12 | 34.48 (12.85) | 2.11 (3.97) | 32.10 (14.42) | 1.7 (1.67) | 44.21 (37.57) | 30.42 (52.9) | 56.66 (43.41) | 31.4 (21.62) |
| mean | 28.17 | 1.58 | 33.44 | 1.56 | 36.95 | 26.55 | 52.41 | 33.73 |
| | Pearson r | | | | | | | |
| 7 | 0.97 (0.03) | 0.999 (0.0008) | 0.98 (0.02) | 0.99 (0.001) | 0.84 (0.16) | 0.95 (0.07) | 0.83 (0.16) | 0.92 (0.07) |
| 8 | 0.96 (0.04) | 0.999 (0.0003) | 0.97 (0.02) | 0.999 (0.0004) | 0.91 (0.07) | 0.94 (0.08) | 0.89 (0.08) | 0.92 (0.08) |
| 9 | 0.95 (0.04) | 0.999 (0.001) | 0.95 (0.04) | 0.999 (0.001) | 0.79 (0.27) | 0.93 (0.08) | 0.77 (0.25) | 0.88 (0.12) |
| 10 | 0.86 (0.28) | 0.999 (0.002) | 0.87 (0.27) | 0.999 (0.003) | 0.75 (0.27) | 0.93 (0.06) | 0.74 (0.27) | 0.89 (0.08) |
| 11 | 0.82 (0.19) | 0.996 (0.004) | 0.78 (0.35) | 0.99 (0.03) | 0.75 (0.29) | 0.85 (0.23) | 0.74 (0.31) | 0.77 (0.27) |
| 12 | 0.86 (0.11) | 0.999 (0.001) | 0.87 (0.14) | 0.999 (0.003) | 0.79 (0.22) | 0.902 (0.17) | 0.78 (0.25) | 0.85 (0.17) |
| mean | 0,90 | 0.999 | 0.90 | 0.996 | 0,81 | 0.92 | 0.79 | 0.87 |

**Table 4.4:** RMSE, MAE and person r values for the TNN and XGBoost training evaluation data. In general, the XGBoost models are able to predict the experimental data better than the Tensorflow models.

Figure 4.1 and Figure 4.2 depict the prediction of all values for a random subject in the erector spinae pars longissimus.

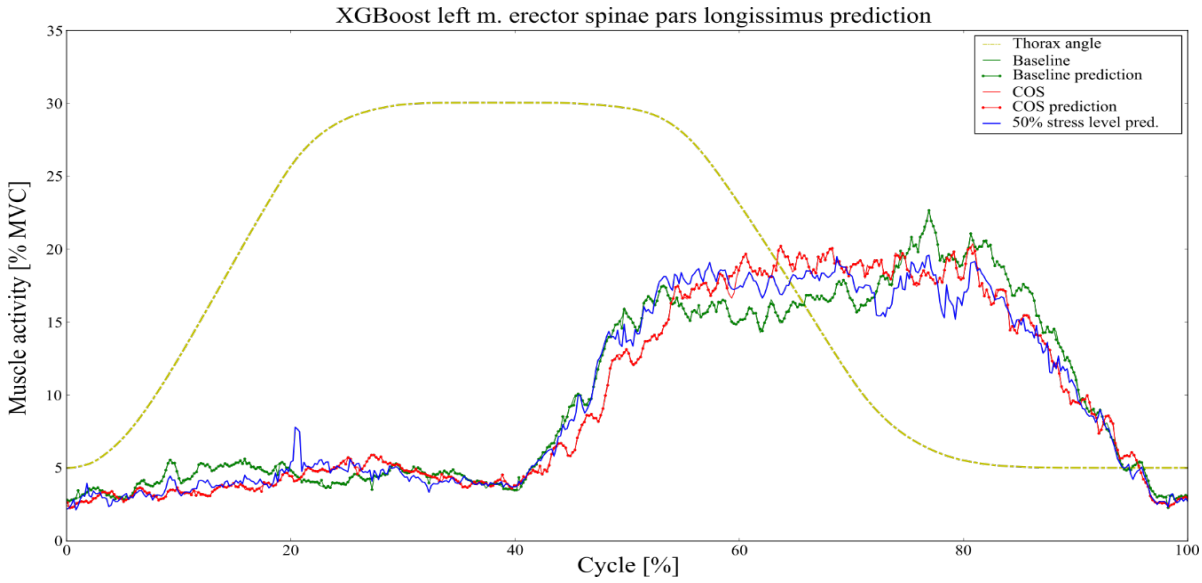


**Figure 4.1:** Result of XGBoost model prediction and target muscle activity of m. erector spinae pars longissimus. The yellow line indicates the thoracic angle. At the 40% position in the cycle, the prediction and target values increase as the subject moves backward. The curve for the 50 % stress level follows the baseline except in the middle of the backward movement where it moves closer to the stress data. Overall, the predictions are following the experimental data quite well.

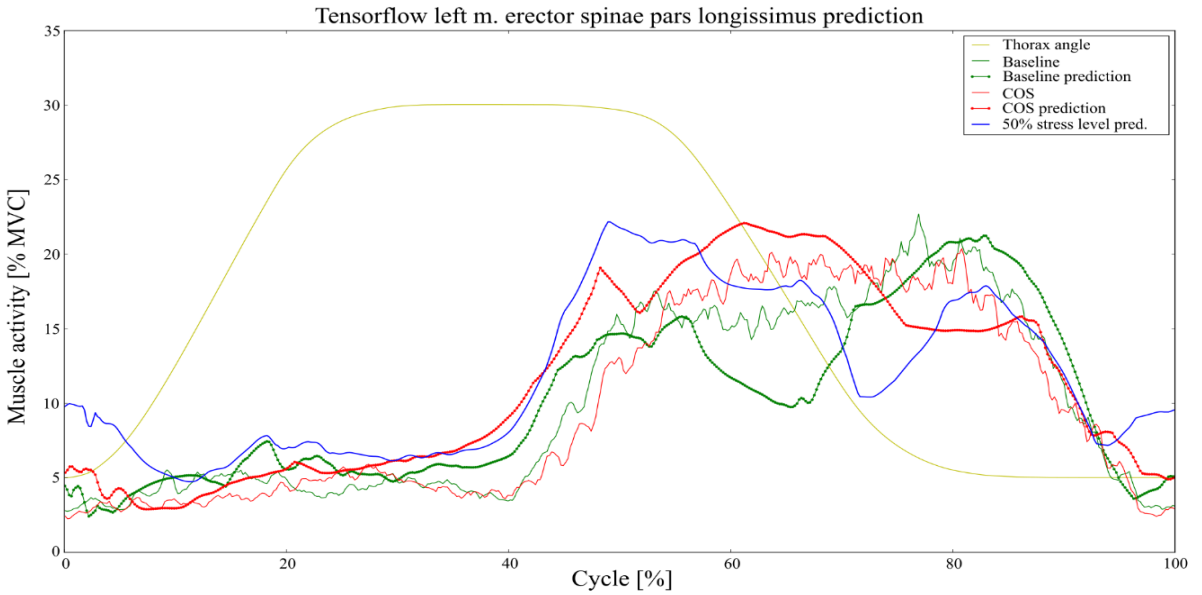


**Figure 4.2:** TensorFlow model prediction result and target muscle activity of the m. erector spinae pars longissimus. The yellow line indicates the thoracic angle. At a position of 40% in the cycle, the prediction and target values increase as the subject moves backward. The baseline and COS prediction do not follow the target values very closely. The prediction of the load level at 50% reflects this trend.

## 4.4. Discussion

Machine learning models of lumbar muscle recruitment were developed to predict muscle activity for thoracic movements in response to cognitive stress. The model represents the central nervous system and its kinetic and muscular response. Both the XGBoost and TNN models are able to predict the activation pattern as a function of thoracic flexion angle, velocity, torque, and stress level, but with different levels of precision.

In particular, the gradient boost approach shows greater accuracy for the relatively small amount of sample data. Compared to TNN, the MAE is below 2.53% as opposed to 68.6%. For the person correlation, this trend is repeated with a higher R-value for the gradient-boost method. Despite the limited number of other studies modeling EMG data, comparison of the results with other studies using neural networks to predict muscle activity reveals a similar result to this study. Nussbaum et al. (Nussbaum et al., 1995) used artificial neural networks to predict lumbar muscle activities. The average $r^2 = 0.83$ is below the value of $r^2 = 0.9$ in this study. In contrast, the gradient-boost model was able to increase the correlation $r^2 = 0.996$, which is higher and suggests an advantage for this type of model. With an MAE below 2.53 % and RMSE below 1.5 % in the case of the gradient-boost model, the prediction is quite accurate, especially considering that the RMSE value is dominated by the peaks. Despite a good correlation for the maximum and minimum stress data, this trend is not as accurate for the 50% stress level. In this case, one would expect an approximately equal RMSE value when comparing the prediction to the baseline and stress curves, but this is not the case. This situation may be caused by a nonlinear transformation from the baseline to the loading data or by missing features such as lateral torque in the model. In addition, the stress-related kinetic changes are influencing the muscle activity, which may be represented by a non-uniformly distributed RMSE value. The accessibility to such models allows numerical studies to identify kinetic parameters causing additional stress-related loads. The NN example in Figure 4.2 shows a general underestimation and overestimation of muscle activity during backward movement. This leads to a less accurate estimate of submaximals. This trend is smaller in the case of the gradient boost method, but is still present and likely results from the overall higher accuracy.

The relative small sample size and the unknown actual stress level of the subject directly affect the models and cause the lower accuracy of the TNN model. The use of the data for training and analysis is a direct result of the small sample size. Nevertheless, this approach was taken

to establish and identify a procedure if more data were available to train a general model. Prediction of the submaximal stress pattern using kinetic data from the baseline study may not reflect the correct trajectory of motion and may result in a less accurate prediction. In addition, to provide training data for submaximal loads, there is a limitation in accurately determining the stress level. Using an individual scaled value that is independent of personal assessment, submaximal measurements are possible. This option would provide the missing data point and allow for much more accurate training. Therefore, a study design that performs submaximal measurement is necessary to capture a range of stress responses.

## 4.5. Conclusion

In general, machine-learning algorithms, particularly gradient boost, appear to be a valid approach for estimating muscular stress response and confirms hypothesis four. The use of such models can help to study and understand the effects of psychological stress on musculoskeletal structures, such as disc loads and muscle recruitment.

After accurate prediction under a simplified setup, extending the protocol in Chapter 3 to unconstrained movement can provide insight into how mental stress affects muscle recruitment and kinetics for any scenario. In addition, this information can help adapt and modify stress management strategies in workplaces and ergonomics. However, more research is needed to provide information on the target function for submaximal stress levels. Providing more data points will help refine the models and achieve higher predictive accuracy.

# 5. Discussion

To the authors' knowledge, this work is the first to describe the influence of emotional and cognitive stressors on muscle recruitment throughout the back with and without physical

loading. In addition, it is possible to use inverse kinematic simulation models to determine the corresponding physical spinal loads and divide them into kinetic component and stress-induced muscle strain.

The focus of the first study was to examine the effect of emotional and cognitve stressors, without physical stress from the sitting position. This setup reflects not only an almost undisturbed stress response, but also a sedentary scenario at office work. In this study, the trapezius muscle responded to each stressor. The mean increase during EMS is around 43%, which is within the range of other studies. The COS shows a dominant right trapezius response of 137% and 43% on the left side, which is consistent with the wide range of values reported in the literature. Chapter 1.6 briefly reviews similar studies examining the effect of stress on trapezius muscle activity, but is not exhaustive. For moderate physical work, such as dual-task writing, a similar but less pronounced trend was found in favor of the right side 67% and 8% (Leyman et al., 2004). With heavier physical exertion, the response is as high as 123%, but with associated neck and shoulder pain (Rissén et al., 2002). Overall, the large variation seems to indicate a highly individual musculoskeletal response to psychological stress. However, if studies on shoulder and neck pain are taken into account, it could be concluded that an activity-pain correlation exists (Westgaard, 1999).

Holte et.al. (Holte and Westgaard, 2002) show that pain is not necessarily associated with higher muscle activity, but that muscle relaxation during leisure time probably plays an important role. This must be especially taken into account considering that psychological stress can be a persistent situation that reduces muscle relaxation time and affects low threshold motor units (Bansevicius et al., 1997), which promotes muscle tension due to an energy crisis in muscle fibers (Chapter 1.6). For the erector spinae, this study showed a mean increase in muscle activity of 26% during COS.

In addition to the effects on the trapezius, prolonged sitting has been identified for various musculoskeletal disorders. Muscle contraction has been found to influence the development of low back pain during computer work (Schinkel-Ivy et al., 2013). Stress-induced higher muscle activity associated with a response chain similar to that described for the trapezius could promote this development. Using musculoskeletal simulation, it is possible to determine stress-induced disc loads. The stress-free sitting condition itself loads the cervical disc with 15% BW and the lumbar disc with 94% BW. This load is increased by 19% (139N) and 25% BW (189N), respectively during COS. EMS provides an additional 4% BW (25N - 28N) load in both regions.

Despite the moderate load increase, the sustained nature could contribute to the effects studied by Pape et al. (Pape et al., 2018) who linked static loading during sedentary work to disc height loss, spinal stiffness, and low back pain. To investigate the musculoskeletal response in the lumbar spine in detail, a second study was conducted. It involved a dual-task scenario that combined physical and mental loads. The basic thoracic extension-flexion movement provided a low physical load that was not intended to overload the stressor response. The experimental design provides a higher load on the m. erector spinae and allows us to split the movement into sections with and without additional loading. This design results in moderate muscle activation, superimposed on effects caused by the COS.

In contrast to the first study, only one increase above 3% in muscle activation was found in the trapezius region. However, the large standard deviation of the m. trapezius pars descendens suggests that the change is due to kinetic adaptation and requires more detailed investigation. Nevertheless, the increase is smaller compared to other studies. On the other hand, a load/motion correlated pattern is observed in the lumbar muscle groups. The load-free forward movement did not cause a significant difference in muscle activation, but extension did. It increased muscle activation by 9%. Since this muscle activation results from both kinetic and load responses, a musculoskeletal simulation is used to determine the physical response to the spinal disc loads. The models show a L4L5 47% BW difference in compression, which may be related to muscle tension due to COS itself. If the National Institute for Occupational Safety and Health (NIOSH) (Waters et al., 1994) guidelines for repetitive work of 3400 N (460% BW) in CC direction are used to estimate the stress-related increase in force, it becomes apparent that the additional load can certainly make a substantial contribution to the assessment. A study by Metha et al. (Mehta et al., 2012) found similar discrepancies for static loads like this work. They could not demonstrate an effect in the trapezius but in the multifidi and cite the absence of physical loading as the reason. After combining all results, a correlation of load/movement and mental load seems reasonable and should be further investigated. Specifically, to eliminate the overall very low EMG signal in study one and conduct a study that measures all forces on the human body. Despite studies (Dubowsky et al., 2008; Zee et al., 2007), describing a linear transfer function from surface EMG to inverse dynamic simulation models, further research should investigate this relationship for more muscle groups during different exercise and loading scenarios. The actual transfer function could differ as it depends on muscle composition and motor recruitment (Kuriki et al., 2012). To account for mental stress during different situations, a suitable tool could be the use of machine learning models as described in

chapter 4. They allow the numerical investigation of different scenarios, but rely on measurements that have to be performed in advance. They should include both minimum and maximum scenarios in load and movement and mental stress. Data collection not only provides data, but also helps to deepen the knowledge of the behavior of the stress response function.

Emotional and cognitive stress, as a prolonged situation (Bansevicius et al., 1997), lead to increased, sustained muscle tone in the trapezius. This prolonged stress can lead to higher energy expenditure as described in the energy crisis model (Simons and Travell, 1981) causing persistently higher muscle tension even when the stressful situation is no longer present. Based on the Cinderella hypothesis and its chain of reactions, this can lead to pain in the affected regions resulting from a degenerative process (Kadefors et al., 1999). Figure 5.1 represents the possible chain of action for back muscle recruitment. According to the compilation of results from this work: applied movement during the COS could reduce the effects of stress on the activity of the trapezius and help to break the chain of reaction. Furthermore, the results suggest a correlation of muscle activity affected by the COS as a function of load and movement. Increased upper body movement may reduce the stress-induced increase in activity in the trapezius, but leads to an increase in load in the lower back. However, load-free movement may counteract this. Although further studies are needed to verify this, this model would open up new possibilities for the prevention of back problems.

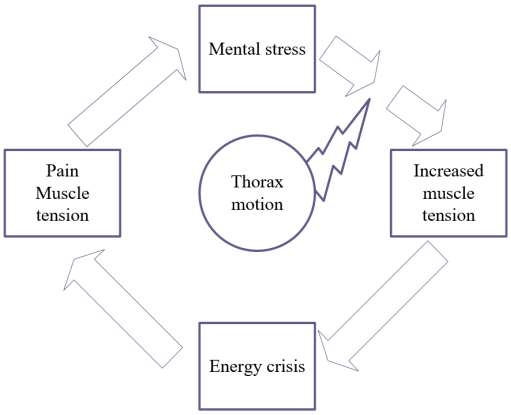


**Figure 5.1:** Reaction model describing the link of muscle pain/tension caused by mental stress in the trapezius. A possible break in the reaction chain could be the introduction of mechanical thorax load during the stressful event.

# 6. Conclusion

Many studies provide information on how psychological stress affects society and the individual himself. This work contributes to the knowledge of how psychological and cognitive stress affects the musculoskeletal system and identifies possible causes of disease development. In particular, the development of algorithms to determine stress-related disc loads can help to understand the development of back pain or disease and provide a basis for ergonomics and therapy.

In addition, the kinematic changes found during COS loading can help identify stress and allow immediate application of countermeasures. EMS and COS without kinetic loading affect the recruitment of back muscles in different ways. EMS mainly affects the trapezius, while COS alters the recruitment pattern in the upper and lower back. The second study showed that when a low/no load is applied in combination with movement, the effect of COS on the trapezius can be limited. This information can help avert long-term causes due to stress by identifying kinematic changes and applying or requesting external trunk motion to/from the seated person. For arbitrary situations, the combination of machine learning and musculoskeletal simulation tools can help investigate and prevent the effect of mental stress.

**References**

Al-Yahya, E., Dawes, H., Smith, L., Dennis, A., Howells, K., Cockburn, J., 2011. Cognitive motor interference while walking: a systematic review and meta-analysis. Neuroscience and biobehavioral reviews 35, 715–728.

Andersson, G., Hagman, J., Talianzadeh, R., Svedberg, A., Larsen, H.C., 2002. Effect of cognitive load on postural control. Brain Research Bulletin 58, 135–139.

Archetti, F., Candelieri, A., 2019. Bayesian Optimization and Data Science.

Balasubramanian, S., Melendez-Calderon, A., Burdet, E., 2012. A Robust and Sensitive Metric for Quantifying Movement Smoothness. IEEE Transactions on Biomedical Engineering 59, 2126–2136.

Balasubramanian, S., Melendez-Calderon, A., Roby-Brami, A., Burdet, E., 2015. On the analysis of movement smoothness. Journal of neuroengineering and rehabilitation 12, 112.

Bansevicius, D., Westgaard, R.H., Jensen, C., 1997. Mental stress of long duration: EMG activity, perceived tension, fatigue, and pain development in pain-free subjects. Headache 37, 499–510.

Barr, K.M., Miller, A.L., Chapin, K.B., 2010. Surface electromyography does not accurately reflect rectus femoris activity during gait: impact of speed and crouch on vasti-to-rectus crosstalk. Gait & Posture 32, 363–368.

Basmajian, J.V., 1962. Muscles Alive. Their Functions Revealed by Electromyography. Academic Medicine 37, 802.

BAUA, 2017. Beanspruchung und Stress von abhängig Beschäftigten in Deutschland nach Wirtschaftszweigen im Jahr 2012. Statista. Accessed 17. Juli 2017. Available under https://de.statista.com/statistik/daten/studie/252917/umfrage/beanspruchung-und-stress-von-arbeitnehmern-nach-wirtschaftszweigen-in-deutschland/.

Bean, J.C., Chaffin, D.B., Schultz, A.B., 1988. Biomechanical model calculation of muscle contraction forces: A double linear programming method. Functional Tissue Engineering 21, 59–66.

Bergstra, J., Bengio, Y., 2012. Random search for hyper-parameter optimization. Journal of machine learning research 13.

BIGLAND, B., LIPPOLD, O.C., 1954. The relation between force, velocity and integrated electrical activity in human muscles. The Journal of physiology 123, 214–224.

Bolgla, L.A., Uhl, T.L., 2007. Reliability of electromyographic normalization methods for evaluating the hip musculature. Journal of electromyography and kinesiology : official journal of the International Society of Electrophysiological Kinesiology 17, 102–111.

Brandes, R., Lang, F., Schmidt, R.F., 2019. Physiologie des Menschen. Mit Pathophysiologie.

Burden, A., 2010. How should we normalize electromyograms obtained from healthy participants? What we have learned from over 25 years of research. J Electromyogr Kinesiol 20, 1023–1035.

Burns, J.W., 2006. Arousal of negative emotions and symptom-specific reactivity in chronic low back pain patients. Emotion (Washington, D.C.) 6, 309–319.

Chany, A.-M., Parakkat, J., Yang, G., Burr, D.L., Marras, W.S., 2006. Changes in spine loading patterns throughout the workday as a function of experience, lift frequency, and personality. The spine journal : official journal of the North American Spine Society 6, 296–305.

Chapman, A.R., Vicenzino, B., Blanch, P., Knox, J.J., Hodges, P.W., 2010. Intramuscular fine-wire electromyography during cycling: repeatability, normalisation and a comparison to surface electromyography. J Electromyogr Kinesiol 20, 108–117.

Chen, T., Guestrin, C. Xgboost: A scalable tree boosting system. In Proceedings of the 22nd acm sigkdd international conference on knowledge discovery and data mining, pp. 785–794.

Chrousos, G.P., 2009. Stress and disorders of the stress system. Nature Reviews Endocrinology 5, 374–381.

Coan, J.A., Allen, J., 2007. Handbook of Emotion Elicitation and Assessment. Oxford University Press, Oxford.

Constantine Tsigos, Ioannis Kyrou, Eva Kassi, George P Chrousos, 2016. Stress, Endocrine Physiology and Pathophysiology. In: Tsigos, C., Kyrou, I., Kassi, E., Chrousos, G.P. (Eds.). Endotext [Internet]. MDText.com, Inc.

Cram, J.R., Kasman, G.S., Holtz, J., 1998. Introduction to surface electromyography. Aspen Publishers, Gaithersburg, Md.

Criswell, E., 2010. Cram's introduction to surface electromyography. Jones & Bartlett Publishers.

Crowninshield, R.D., Brand, R.A., 1981. A physiologically based criterion of muscle force prediction in locomotion. Functional Tissue Engineering 14, 793–801.

DAK, 2017. Anteile der zehn wichtigsten Krankheitsarten an den Arbeitsunfähigkeitstagen in Deutschland in den Jahren 2010 bis 2016. Statista. Accessed 17. Juli 2017. Available under https://de.statista.com/statistik/daten/studie/77239/umfrage/krankheit---hauptursachen-fuer-arbeitsunfaehigkeit/.

Dale Purves, George J Augustine, David Fitzpatrick, Lawrence C Katz, Anthony-Samuel LaMantia, James O McNamara, S Mark Williams, 2001. The Motor Unit. In: Purves, D., Augustine, G.J., Fitzpatrick, D., Katz, L.C., LaMantia, A.-S., McNamara, J.O., Williams, S.M. (Eds.). Neuroscience. 2nd edition. Sinauer Associates.

Damsgaard, M., Rasmussen, J., Christensen, S.T., Surma, E., de Zee, M., 2006. Analysis of musculoskeletal systems in the AnyBody Modeling System. Simulation Modelling Practice and Theory 14, 1100–1111.

Dault, M.C., Yardley, L., Frank, J.S., 2003. Does articulation contribute to modifications of postural control during dual-task paradigms? Cognitive Brain Research 16, 434–440.

Davis, K.G., Marras, W.S., 2003. Partitioning the contributing role of biomechanical, psychosocial, and individual risk factors in the development of spine loads. The spine journal : official journal of the North American Spine Society 3, 331–338.

Davis, K.G., Marras, W.S., Heaney, C.A., Waters, T.R., Gupta, P., 2002a. The impact of mental processing and pacing on spine loading: 2002 Volvo award in biomechanics. Spine 27, 2645–2653.

Davis, K.G., Marras, W.S., Heaney, C.A., Waters, T.R., Gupta, P., 2002b. The impact of mental processing and pacing on spine loading: 2002 Volvo Award in biomechanics. Spine 27, 2645–2653.

Di Fabio, R.P., 1987. Reliability of computerized surface electromyography for determining the onset of muscle activity. Physical Therapy 67, 43–48.

Dubowsky, S.R., Rasmussen, J., Sisto, S.A., Langrana, N.A., 2008. Validation of a musculoskeletal model of wheelchair propulsion and its application to minimizing shoulder joint forces. Functional Tissue Engineering 41, 2981–2988.

EBERHART, H., 1954. The principal elements in human locomotion. Human Limbs and Their Substitutes, 437–471.

Elwood Henneman, Lorne M. Mendell, 2011. Functional Organization of Motoneuron Pool and its Inputs. In: Comprehensive Physiology. American Cancer Society, pp. 423–507.

Fahrmeir, L., Kneib, T., Lang, S., 2009. Regression. Modelle, Methoden und Anwendungen. Springer-Verlag Berlin Heidelberg, Berlin, Heidelberg.

Flor, H., Turk, D.C., Birbaumer, N., 1985. Assessment of stress-related psychophysiological reactions in chronic back pain patients. Journal of Consulting and Clinical Psychology 53, 354.

Freund, H.J., 1983. Motor unit and muscle activity in voluntary motor control. Physiological reviews 63, 387–436.

Gadsby, D.C., 2009. Ion channels versus ion pumps: the principal difference, in principle. Nature reviews. Molecular cell biology 10, 344–352.

Géron, A., 2019. Hands-on machine learning with Scikit-Learn, Keras, and TensorFlow. Concepts, tools, and techniques to build intelligent systems.

Glombiewski, J.A., Tersek, J., Rief, W., 2008. Muscular reactivity and specificity in chronic back pain patients. Psychosomatic Medicine 70, 125–131.

Godin, K.W., Hansen, J.H.L., 2015. Physical task stress and speaker variability in voice quality. EURASIP Journal on Audio, Speech, and Music Processing 2015, 29.

Granata, K.P., Marras, W.S., 1993. An EMG-assisted model of loads on the lumbar spine during asymmetric trunk extensions. Functional Tissue Engineering 26, 1429–1438.

Grandey, A.A., 2000. Emotional regulation in the workplace: A new way to conceptualize emotional labor. Journal of occupational health psychology 5, 95.

2001. Greedy function approximation: a gradient boosting machine.

Gross, J.J., Levenson, R.W., 1995. Emotion elicitation using films. Cognition and Emotion 9, 87–108.

Hägg, G.M. Lack of relation between maximal force capacity and muscle disorders caused by low level static loads. A new explanation model. In IEA. Taylor and Francis Paris, pp. 9–11. Taylor and Francis Paris.

Hald, R.D., Bottjen, E.J., 1987. Effect of Visual Feedback on Maximal and Submaximal lsokinetic Test Measurements of Normal Quadricem - and Hamstrings. The Journal of orthopaedic and sports physical therapy 9, 86–93.

Hamacher, D., Hamacher, D., Müller, R., Schega, L., Zech, A., 2017. Exploring phase dependent functional gait variability. Human Movement Science 52, 191–196.

Hart, S.G., Staveland, L.E., 1988. Development of NASA-TLX (Task Load Index). Results of Empirical and Theoretical Research. In: Hancock, P.A., Meshkati, N. (Eds.). Advances in Psychology : Human Mental Workload. North-Holland, pp. 139–183.

Hatze, H., 1981. Estimation of myodynamic parameter values from observations on isometrically contracting muscle groups. European journal of applied physiology and occupational physiology 46, 325–338.

Heller, B.W., Veltink, P.H., Rijkhoff, N.J., Rutten, W.L., Andrews, B.J., 1993. Reconstructing muscle activation during normal walking: a comparison of symbolic and connectionist machine learning techniques. Biological Cybernetics 69, 327–335.

Henneman, E., Somjen, G., Carpenter, D.O., 1965. Excitability and inhibitability of motoneurons of different sizes. Journal of Neurophysiology 28, 599–620.

Henriksson, KG, 1988. Muscle pain in neuromuscular disorders and primary fibromyalgia. European journal of applied physiology and occupational physiology 57, 348–352.
Herzog, W., 1987. Individual muscle force estimations using a non-linear optimal design. Journal of Neuroscience Methods 21, 167–179.
Hodges, P.W., Richardson, C.A., 1996. Inefficient Muscular Stabilization of the Lumbar Spine Associated With Low Back Pain: A Motor Control Evaluation of Transversus Abdominis. Spine 21, 2640–2650.
Hof, A.L., 1984. EMG and muscle force: An introduction. Human Movement Science 3, 119–153.
Hof, A.L., van den Berg, J., 1981. EMG to force processing II: Estimation of parameters of the Hill muscle model for the human triceps surae by means of a calfergometer. Functional Tissue Engineering 14, 759–770.
Hogan, N. (Ed.), 1982. Control and Coordination of Voluntary Arm Movements. 1982 American Control Conference.
Hogan, N., 1984. An organizing principle for a class of voluntary movements. The Journal of Neuroscience 4, 2745.
Hogan, N., Sternad, D., 2007. On rhythmic and discrete movements. Reflections, definitions and implications for motor control. Experimental brain research 181, 13–30.
Hogan, N., Sternad, D., 2009. Sensitivity of Smoothness Measures to Movement Duration, Amplitude, and Arrests. Journal of motor behavior 41, 529–534.
Holte, K.A., Westgaard, R.H., 2002. Daytime trapezius muscle activity and shoulder-neck pain of service workers with work stress and low biomechanical exposure. American journal of industrial medicine 41, 393–405.
Hopkins, P.M., 2006. Skeletal muscle physiology. Continuing Education in Anaesthesia Critical Care & Pain 6, 1–6.
Hoy, D., Brooks, P., Blyth, F., Buchbinder, R., 2010a. The Epidemiology of low back pain. Best Practice & Research Clinical Rheumatology 24, 769–781.
Hoy, D., Protani, M., De, R., Buchbinder, R., 2010b. The epidemiology of neck pain. Best Practice & Research Clinical Rheumatology 24, 783–792.
HUXLEY, A.F., NIEDERGERKE, R., 1954. Structural changes in muscle during contraction; interference microscopy of living muscle fibres. Nature 173, 971–973.
Kadefors, R., Forsman, M., Zoéga, B., Herberts, P., 1999. Recruitment of low threshold motor-units in the trapezius muscle in different static arm positions. Ergonomics 42, 359–375.
Knowles, J.R., 1980. Enzyme-catalyzed phosphoryl transfer reactions. Annual review of biochemistry 49, 877–919.
Knudson, D.V., 2003. Fundamentals of biomechanics. Kluwer Academic / Plenum Publ, New York.
Knutson, L.M., Soderberg, G.L., Ballantyne, B.T., Clarke, W.R., 1994. A study of various normalization procedures for within day electromyographic data. Journal of Electromyography and Kinesiology 4, 47–59.
Kolotylova, T., Koschke, M., Bär, K.-J., Ebner-Priemer, U., Kleindienst, N., Bohus, M., Schmahl, C., 2010. Development of the" Mannheim Multicomponent Stress Test"(MMST). Psychotherapie, Psychosomatik, Medizinische Psychologie 60, 64–72.
Konrad, P., 2005. The ABC of EMG. A Practical Introduction to Kinesiological Electromyography. Noraxon INC., USA.

Kuriki, H.U., Mello, E.M., Azevedo, F.M. de, Takahashi, L.S.O., Alves, N., de Faria Negrão Filho, Rúben, 2012. The relationship between electromyography and muscle force. INTECH Open Access Publisher, London.

Landis, C., 1930. Walter B. Cannon. Bodily Changes in Pain, Hunger, Fear and Rage. (2nd ed., revised and enlarged.) New York: Appleton, 1929. Pp. xvi+404. The Pedagogical Seminary and Journal of Genetic Psychology 38, 527–531.

Larsson, S.E., Larsson, R., Zhang, Q., Cai, H., Oberg, P.A., 1995. Effects of psychophysiological stress on trapezius muscles blood flow and electromyography during static load. European journal of applied physiology and occupational physiology 71, 493–498.

Lazarus, R.S., Folkman, S., 1984. Stress, appraisal, and coping. Springer publishing company.

Lejuez, C.W., Kahler, C.W., Brown, R.A., 2003. A modified computer version of the Paced Auditory Serial Addition Task (PASAT) as a laboratory-based stressor. The Behavior Therapist.

Leyman, E., Mirka, G., Kaber, D., Sommerich, C., 2004. Cervicobrachial muscle response to cognitive load in a dual-task scenario. Ergonomics 47, 625–645.

Leyman, E.L.C., Mirka, G.A., Kaber, D.B., Sommerich, C.M., 2001. Assessing the Relationship between Cognitive Load and Cervicobrachial Muscle Response during a Typing Task. Proceedings of the Human Factors and Ergonomics Society Annual Meeting 45, 1092–1096.

Liu, M.M., Herzog, W., Savelberg, H.H., 1999. Dynamic muscle force predictions from EMG: an artificial neural network approach. Journal of Electromyography and Kinesiology 9, 391–400.

Lloyd, D.G., Besier, T.F., 2003. An EMG-driven musculoskeletal model to estimate muscle forces and knee joint moments in vivo. Journal of Biomechanics 36, 765–776.

Lovallo, W.R., Thomas, T.L., 2000. Stress hormones in psychophysiological research: Emotional, behavioral, and cognitive implications. 05216263.

Luca, C.J. de, 1997. The Use of Surface Electromyography in Biomechanics. Journal of Applied Biomechanics 13, 135–163.

Luca, C.J. de, Gilmore, L.D., Kuznetsov, M., Roy, S.H., 2010. Filtering the surface EMG signal: Movement artifact and baseline noise contamination. Journal of Biomechanics 43, 1573–1579.

Luca, C.J. de, Kuznetsov, M., Gilmore, L.D., Roy, S.H., 2012. Inter-electrode spacing of surface EMG sensors: reduction of crosstalk contamination during voluntary contractions. Journal of Biomechanics 45, 555–561.

Luca, C.J. de, Merletti, R., 1988. Surface myoelectric signal cross-talk among muscles of the leg. Electroencephalography and Clinical Neurophysiology 69, 568–575.

Luca, C.J. de, van Dyk, E.J., 1975. Derivation of some parameters of myoelectric signals recorded during sustained constant force isometric contractions. Biophysical journal 15, 1167–1180.

Luh, J.-J., Chang, G.-C., Cheng, C.-K., Lai, J.-S., Kuo, T.-S., 1999. Isokinetic elbow joint torques estimation from surface EMG and joint kinematic data: using an artificial neural network model. Journal of electromyography and kinesiology : official journal of the International Society of Electrophysiological Kinesiology 9, 173–183.

Lundberg, U., 2002. Psychophysiology of work: Stress, gender, endocrine response, and work-related upper extremity disorders*. American journal of industrial medicine 41, 383–392.

Lundberg, U., Dohns, I.E., Melin, B., Sandsjö, L., Palmerud, G., Kadefors, R., Ekström, M., Parr, D., 1999. Psychophysiological stress responses, muscle tension, and neck and shoulder pain among supermarket cashiers. Journal of occupational health psychology 4, 245.

Lundberg, U., Forsman, M., Zachau, G., Eklöf, M., Palmerud, G., Melin, B., Kadefors, R., 2002. Effects of experimentally induced mental and physical stress on motor unit recruitment in the trapezius muscle. Work & stress 16, 166–178.

Lymn, R.W., Taylor, E.W., 1971. Mechanism of adenosine triphosphate hydrolysis by actomyosin. Biochemistry 10, 4617–4624.

M. Wærsted, T. Eken, R. Westgaard, 1996. Activity of single motor units in attention-demanding tasks: firing pattern in the human trapezius muscle. undefined.

Mason, L., Baxter, J., Bartlett, P.L., Frean, M.R. Boosting algorithms as gradient descent. In Advances in neural information processing systems, pp. 512–518.

McGill, S.M., 1992. A myoelectrically based dynamic three-dimensional model to predict loads on lumbar spine tissues during lateral bending. Functional Tissue Engineering 25, 395–414.

McGill, S.M., Norman, R.W., 1986. Partitioning of the L4-L5 dynamic moment into disc, ligamentous, and muscular components during lifting. Spine 11, 666–678.

Mehta, R.K., Nussbaum, M.A., Agnew, M.J., 2012. Muscle- and task-dependent responses to concurrent physical and mental workload during intermittent static work. Ergonomics 55, 1166–1179.

Mesin, L., Merletti, R., Rainoldi, A., 2009. Surface EMG: the issue of electrode location. J Electromyogr Kinesiol 19, 719–726.

Miller, R.H., 2018. Hill-Based Muscle Modeling. In: Handbook of Human Motion. Springer International Publishing, Cham, pp. 373–394.

Montavon, G., Orr, G.B., Müller, K.-R., 2012. Neural networks: tricks of the trade. Springer, Berlin.

Mork, P.J., Westgaard, R.H., 2007. The influence of body posture, arm movement, and work stress on trapezius activity during computer work. European journal of applied physiology 101, 445–456.

Moroney, S.P., Schultz, A.B., Miller, J.A.A., 1988. Analysis and measurement of neck loads. Journal of Orthopaedic Research 6, 713–720.

Morris, A.D., Kemp, G.J., Lees, A., Frostick, S.P., 1998. A study of the reproducibility of three different normalisation methods in intramuscular dual fine wire electromyography of the shoulder. Journal of electromyography and kinesiology : official journal of the International Society of Electrophysiological Kinesiology 8, 317–322.

1989. Muscle and tendon: properties, models, scaling, and application to biomechanics and motor control.

Nimbarte, A.D., 2014. Risk of neck musculoskeletal disorders among males and females in lifting exertions. International Journal of Industrial Ergonomics 44, 253–259.

Nussbaum, M.A., Chaffin, D.B., 1998. Lumbar muscle force estimation using a subject-invariant 5-parameter EMG-based model. Functional Tissue Engineering 31, 667–672.

Nussbaum, M.A., Chaffin, D.B., Martin, B.J., 1995. A back-propagation neural network model of lumbar muscle recruitment during moderate static exertions. Functional Tissue Engineering 28, 1015–1024.

Nussbaum, M.A., Martin, B.J., Chaffin, D.B., 1997. A neural network model for simulation of torso muscle coordination. Functional Tissue Engineering 30, 251–258.

2014 Oct. Occupational Exposures and Back Disorders, Stockholm.

Oh, S.E., Choi, A., Mun, J.H., 2013. Prediction of ground reaction forces during gait based on kinematics and a neural network model. Journal of Biomechanics 46, 2372–2380.

Pandy, M.G., 2001. Computer modeling and simulation of human movement. Annual review of biomedical engineering 3, 245–273.

Pape, J.L., Brismée, J.-M., Sizer, P.S., Matthijs, O.C., Browne, K.L., Dewan, B.M., Sobczak, S., 2018. Increased spinal height using propped slouched sitting postures: Innovative ways to rehydrate intervertebral discs. Applied Ergonomics 66, 9–17.

Peacock, B., Westers, T., Walsh, S., Nicholson, K., 1981. Feedback and maximum voluntary contraction. Ergonomics 24, 223–228.

Pedotti, A., Krishnan, V.V., Stark, L., 1978. Optimization of muscle-force sequencing in human locomotion. Mathematical Biosciences 38, 57–76.

Piazza, S.J., 2006. Muscle-driven forward dynamic simulations for the study of normal and pathological gait. Journal of neuroengineering and rehabilitation 3, 5.

Piazza, S.J., Delp, S.L., 1996. The influence of muscles on knee flexion during the swing phase of gait. Functional Tissue Engineering 29, 723–733.

Putzer, M. A numerical study to determine the effect of ligament stiffness on kinematics of the lumbar spine during flexion.

Rainoldi, A., Nazzaro, M., Merletti, R., Farina, D., Caruso, I., Gaudenti, S., 2000. Geometrical factors in surface EMG of the vastus medialis and lateralis muscles. Journal of electromyography and kinesiology : official journal of the International Society of Electrophysiological Kinesiology 10, 327–336.

Rao, A.S.R.S., Rao, C.R., 2020. Principles and methods for data science. Elsevier, Amsterdam.

Rasmussen, C.E., Williams, C.K.I., 2008. Gaussian processes for machine learning. MIT Press, Cambridge, Mass.

Rasmussen, J., Damsgaard, M., Voigt, M., 2001. Muscle recruitment by the min/max criterion — a comparative numerical study. Functional Tissue Engineering 34, 409–415.

Reinhardt, T., Schmahl, C., Wüst, S., Bohus, M., 2012. Salivary cortisol, heart rate, electrodermal activity and subjective stress responses to the Mannheim Multicomponent Stress Test (MMST). Psychiatry Research 198, 106–111.

Riley, M.A., Baker, A.A., Schmit, J.M., 2003. Inverse relation between postural variability and difficulty of a concurrent short-term memory task. Brain Research Bulletin 62, 191–195.

Rissén, D., Melin, B., Sandsjö, L., Dohns, I., Lundberg, U., 2002. Psychophysiological stress reactions, trapezius muscle activity, and neck and shoulder pain among female cashiers before and after introduction of job rotation. Work & stress 16, 127–137.

Röhrle, H., Scholten, R., Sigolotto, C., Sollbach, W., Kellner, H., 1984. Joint forces in the human pelvis-leg skeleton during walking. Functional Tissue Engineering 17, 409–424.

Roman-Liu, D., Grabarek, I., Bartuzi, P., Choromanski, W., 2013. The influence of mental load on muscle tension. Ergonomics 56, 1125–1133.

Roy, S.H., Luca, G. de, Cheng, M.S., Johansson, A., Gilmore, L.D., Luca, C.J. de, 2007. Electro-mechanical stability of surface EMG sensors. Medical and Biological Engineering and Computing 45, 447–457.

Ruffieux, J., Keller, M., Lauber, B., Taube, W., 2015. Changes in Standing and Walking Performance Under Dual-Task Conditions Across the Lifespan. Sports Medicine 45, 1739–1758.

Russel, J.A., Weiss, A., Mendelsohn, G.A., 1989. Affect grid. A single-item scale of pleasure and arousal. Journal of Personality and Social Psychology 57, 493–502.

SAGE (Ed.), 2015. How high is high? A meta-analysis of NASA-TLX global workload scores. SAGE Publications Inc, Los Angeles, CA.

Savelberg, H.H., Herzog, W., 1997. Prediction of dynamic tendon forces from electromyographic signals: An artificial neural network approach. Journal of Neuroscience Methods 78, 65–74.

SBU Yellow Report no 227, 2014. Occupational exposures and back disorders. http://www.sbu.se/en.

Schinkel-Ivy, A., Nairn, B.C., Drake, J.D.M., 2013. Investigation of trunk muscle co-contraction and its association with low back pain development during prolonged sitting. J Electromyogr Kinesiol 23, 778–786.

Schmidt, R.F., Schaible, H.-G., Birbaumer, N.-P., 2006. Neuro- und Sinnesphysiologie. Springer Medizin Verlag Heidelberg, Berlin, Heidelberg.

Schneider, S., Lipinski, S., Schiltenwolf, M., 2006. Occupations associated with a high risk of self-reported back pain. Representative outcomes of a back pain prevalence study in the Federal Republic of Germany. European Spine Journal 15, 821–833.

2020a. scikit-optimize: sequential model-based optimization in Python — scikit-optimize 0.7.4 documentation. https://scikit-optimize.github.io/stable/ (Jul 21, 2020).

Scovil, C.Y., Ronsky, J.L., 2006. Sensitivity of a Hill-based muscle model to perturbations in model parameters. Functional Tissue Engineering 39, 2055–2063.

Selye, H., 1956. Endocrine reactions during stress. Anesthesia & Analgesia 35, 182–193.

Selye, H., 1975. Confusion and controversy in the stress field. Journal of human stress 1, 37–44.

Shahidi, B., Haight, A., Maluf, K., 2013. Differential effects of mental concentration and acute psychosocial stress on cervical muscle activity and posture. Journal of Electromyography and Kinesiology 23, 1082–1089.

Shankar, S., Gander, R.E., Brandell, B.R., 1989. Changes in the myoelectric signal (MES) power spectra during dynamic contractions. Electroencephalography and Clinical Neurophysiology 73, 142–150.

Sharma, N., Gedeon, T., 2012. Objective measures, sensors and computational techniques for stress recognition and classification. A survey. Computer methods and programs in biomedicine 108, 1287–1301.

Simons, D.G., Travell, J., 1981. Myofascial trigger points, a possible explanation. Biennial Review of Pain 10, 106–109.

Solomonow, M., Baratta, R., Bernardi, M., Zhou, B., Lu, Y., Zhu, M., Acierno, S., 1994. Surface and wire EMG crosstalk in neighbouring muscles. Journal of electromyography and kinesiology : official journal of the International Society of Electrophysiological Kinesiology 4, 131–142.

Taib, M.F., Bahn, S., Yun, M.H., 2016. The effect of psychosocial stress on muscle activity during computer work: Comparative study between desktop computer and mobile computing products. Work 54, 543–555.

Taib, M.F., Yun, M.H., 2014. The effect of psychosocial stress on trapezius muscle activity during computer work: A review. In: IEEE International Conference on Industrial Engineering and Engineering Management, pp. 485–490.

Taulli, T., 2019. Artificial Intelligence Basics. A Non-Technical Introduction. Apress.

Taylor, M.R., Sutton, E.E., Diestelkamp, W.S., Bigelow, K.E., 2015. Subtle Differences During Posturography Testing Can Influence Postural Sway Results: The Effects of Talking, Time Before Data Acquisition, and Visual Fixation. Journal of Applied Biomechanics 31, 324–329.

2020b. TensorFlow. https://www.tensorflow.org/ (Jul 20, 2020).

Teufel, E., 2018. Risk Factors for Cardiovascular Disease. In: Encyclopedia of Cardiovascular Research and Medicine, pp. 307–314.

1938. The heat of shortening and the dynamic constants of muscle. Proceedings of the Royal Society of London. Series B - Biological Sciences 126, 136–195.

Toyoshima, C., 2007. Ion Pumping by Calcium ATPase of Sarcoplasmic Reticulum. In Regulatory Mechanisms of Striated Muscle Contraction. Springer, Berlin, Heidelberg, pp. 295–303. Symposium Entitled Regulatory Proteins of Striated Muscle - Structure, Function and Disorder; Symposium "Regulatory Proteins of Striated Muscle - Structure, Function and Disorder; NIPS Conference. Springer, Berlin, Heidelberg.

Trevithick, B.A., Ginn, K.A., Halaki, M., Balnave, R., 2007. Shoulder muscle recruitment patterns during a kayak stroke performed on a paddling ergometer. Journal of electromyography and kinesiology : official journal of the International Society of Electrophysiological Kinesiology 17, 74–79.

Umberger, B.R., Gerritsen, K.G.M., Martin, P.E., 2003. A model of human muscle energy expenditure. Computer methods in biomechanics and biomedical engineering 6, 99–111.

Wang, L., Buchanan, T.S., 2002. Prediction of joint moments using a neural network model of muscle activations from EMG signals. IEEE transactions on neural systems and rehabilitation engineering : a publication of the IEEE Engineering in Medicine and Biology Society 10, 30–37.

Waters, T.R., Putz-Anderson, V., Garg, A., 1994. Applications manual for the revised NIOSH lifting equation.

2004. Welcome to SENIAM. http://www.seniam.org/ (Feb 10, 2017).

Westgaard, R.H., 1999. Effects of physical and mental stressors on muscle pain. Scandinavian Journal of Work, Environment & Health 25 Suppl 4, 19–24.

Wickens, C.D., 1991. Processing resources and attention. Multiple-task performance 1991, 3–34.

Winter, D.A., Yack, H.J., 1987. EMG profiles during normal human walking: stride-to-stride and inter-subject variability. Electroencephalography and Clinical Neurophysiology 67, 402–411.

Woittiez, R.D., Huijing, P.A., Rozendal, R.H., 1983. Influence of muscle architecture on the length-force diagram. A model and its verification. Pflugers Archiv : European journal of physiology 397, 73–74.

Woollacott, M., Shumway-Cook, A., 2002. Attention and the control of posture and gait. A review of an emerging area of research. Gait & Posture 16, 1–14.

Wrightson, J.G., Ross, E.Z., Smeeton, N.J., 2016. The Effect of Cognitive-Task Type and Walking Speed on Dual-Task Gait in Healthy Adults. Motor control 20, 109–121.

2020c. XGBoost Documentation — xgboost 1.2.0-SNAPSHOT documentation. https://xgboost.readthedocs.io/en/latest/index.html (Jul 08, 2020).

2020d. XGBoost Documentation — xgboost 1.2.0-SNAPSHOT documentation. https://xgboost.readthedocs.io/en/latest/# (Jul 20, 2020).

Yang, J.F., Winter, D.A., 1984. Electromyographic amplitude normalization methods: improving their sensitivity as diagnostic tools in gait analysis. Archives of Physical Medicine and Rehabilitation 65, 517–521.

Zee, M. de, Dalstra, M., Cattaneo, P.M., Rasmussen, J., Svensson, P., Melsen, B., 2007. Validation of a musculo-skeletal model of the mandible and its application to mandibular distraction osteogenesis. Functional Tissue Engineering 40, 1192–1201.

# Acknowledgements

I would like to thank Sebastian for the support, discussion and critical thinking.

The whole LBM team

and of course

Anna and Ute.

# SELBSTÄNDIGKEITSERKLÄRUNG

Ich, Franz Süß geboren am 15.11.1976 in Zwiesel erkläre hiermit, dass ich die vorliegende Arbeit ohne unzulässige Hilfe Dritter und ohne Benutzung anderer als der angegebenen Hilfsmittel angefertigt habe.
Die aus anderen Quellen direkt oder indirekt übernommenen Daten und Konzepte sind unter Angabe der Quelle gekennzeichnet. Insbesondere habe ich nicht die entgeltliche Hilfe von Vermittlungs- bzw. Beratungsdiensten (Promotionsberater oder andere Personen) in Anspruch genommen.
Die Arbeit wurde bisher weder im In- noch im Ausland in gleicher oder ähnlicher Form einer anderen Prüfungsbehörde vorgelegt.

Ort, Datum Unterschrift